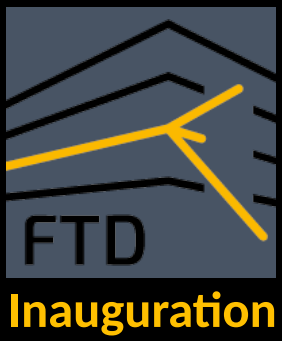


# Low Temperature Quantum Sensors



NI

Loredana Gastaldo

Kirchhoff Institute for Physics  
Heidelberg University

NII

MII

MI

E



UNIVERSITÄT  
HEIDELBERG  
ZUKUNFT  
SEIT 1386

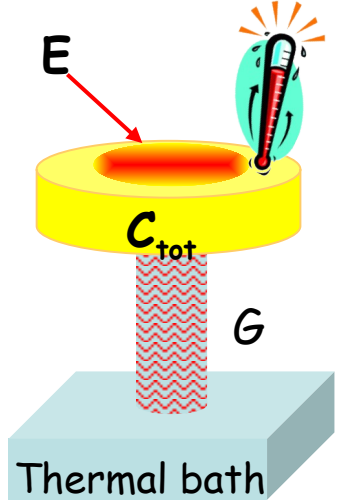
# Outline

- Metallic magnetic calorimeters
  - Thermodynamical properties
  - Readout
  - Fabrication
- MMC applications and performance
  - x-ray
  - Molecular fragments
  - Neutrino mass - ECHo
- Conclusions

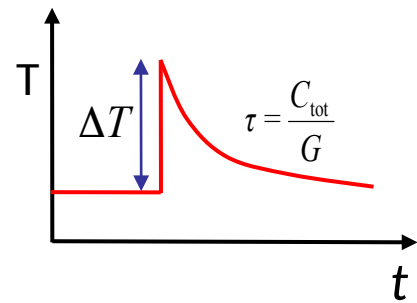
# Low Temperature Calorimeters

Near equilibrium detectors

Energy deposition induces increase of temperature



$$\Delta T \cong \frac{E}{C_{\text{tot}}}$$

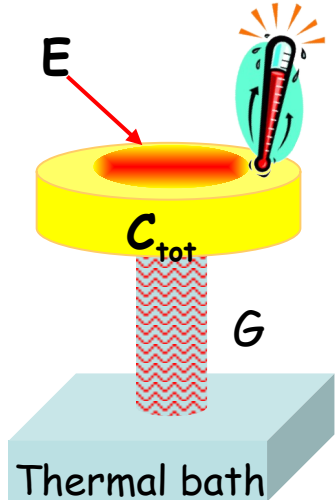


- Very small volume
- Working temperature below 100 mK
  - small specific heat
  - small thermal noise
- Very sensitive temperature sensors

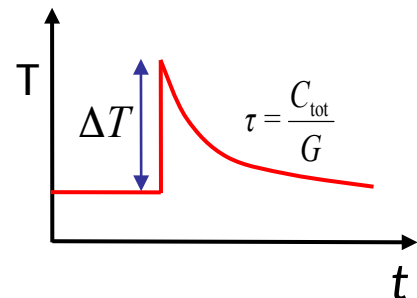
# Low Temperature Calorimeters

Near equilibrium detectors

Energy deposition induces increase of temperature

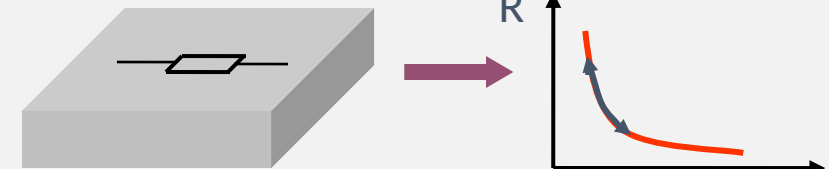


$$\Delta T \cong \frac{E}{C_{\text{tot}}}$$

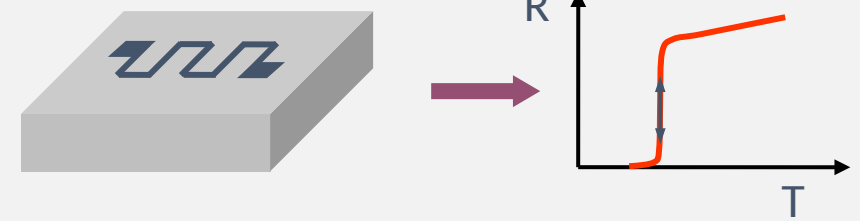


- Very small volume
- Working temperature below 100 mK  
small specific heat  
small thermal noise
- Very sensitive temperature sensors

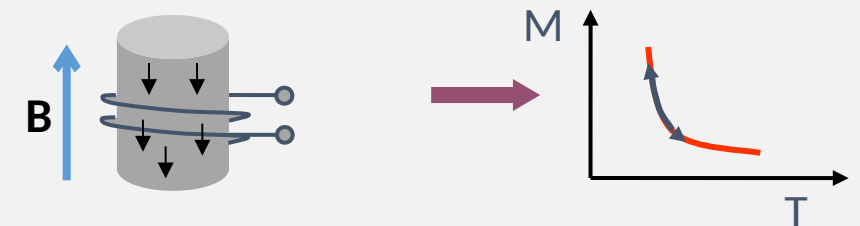
Resistance of highly doped semiconductors



Resistance at superconducting transition, TES



Magnetization of paramagnetic material, MMC



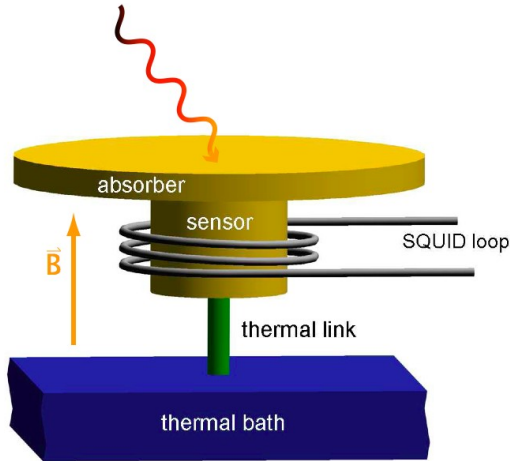
# Metallic Magnetic Calorimeters

A.Fleischmann, C. Enss and G. M. Seidel,  
Topics in Applied Physics **99** (2005) 63

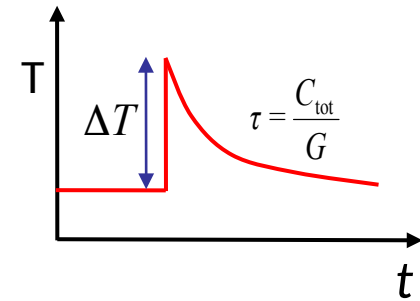
A.Fleischmann et al.,  
AIP Conf. Proc. **1185** (2009) 571

## Paramagnetic temperature sensor

Dilute alloy Au:Er or Ag:Er (Er concentration: a few hundred ppm)



$$\Delta T \cong \frac{E}{C_{\text{tot}}}$$



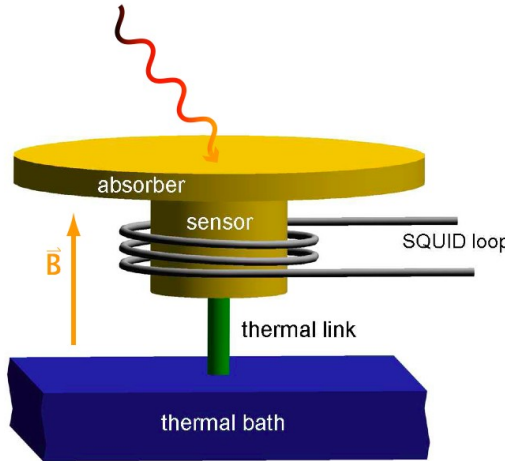
# Metallic Magnetic Calorimeters

A.Fleischmann, C. Enss and G. M. Seidel,  
Topics in Applied Physics **99** (2005) 63

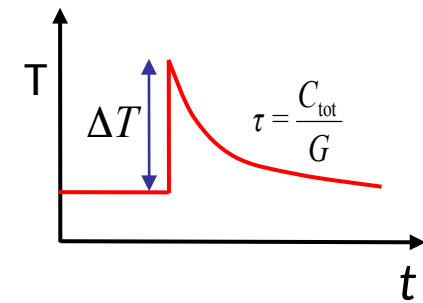
A.Fleischmann et al.,  
AIP Conf. Proc. **1185** (2009) 571

## Paramagnetic temperature sensor

Dilute alloy Au:Er or Ag:Er (Er concentration: a few hundred ppm)



$$\Delta T \cong \frac{E}{C_{\text{tot}}} \xrightarrow{\text{MMC}} \Delta \Phi_s \propto \frac{\partial M}{\partial T} \Delta T \rightarrow \Delta \Phi_s \propto \frac{\partial M}{\partial T} \frac{E}{C_{\text{tot}}}$$



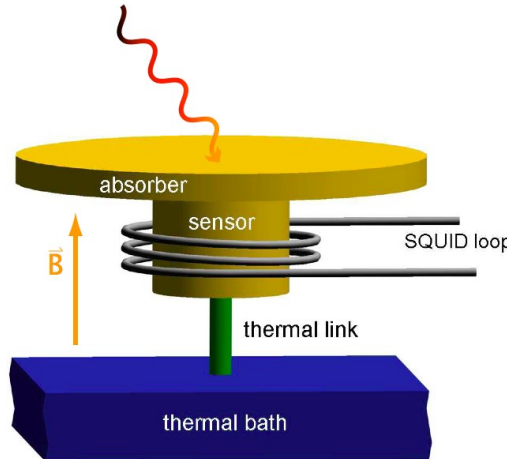
# Metallic Magnetic Calorimeters

A.Fleischmann, C. Enss and G. M. Seidel,  
Topics in Applied Physics **99** (2005) 63

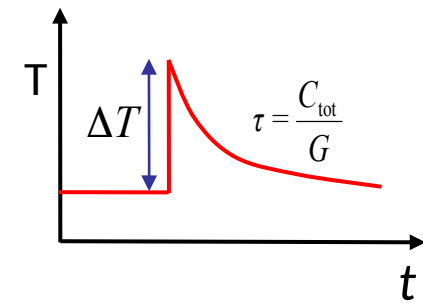
A.Fleischmann et al.,  
AIP Conf. Proc. **1185** (2009) 571

## Paramagnetic temperature sensor

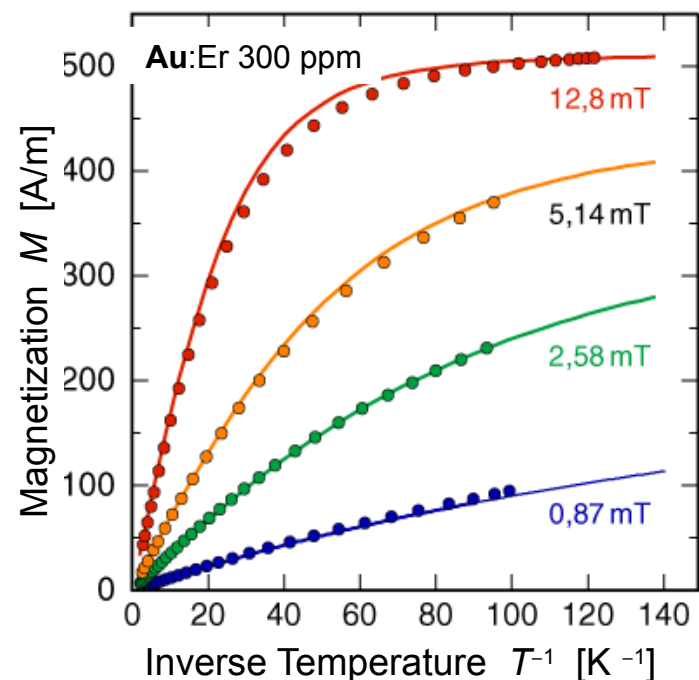
Dilute alloy Au:Er or Ag:Er (Er concentration: a few hundred ppm)



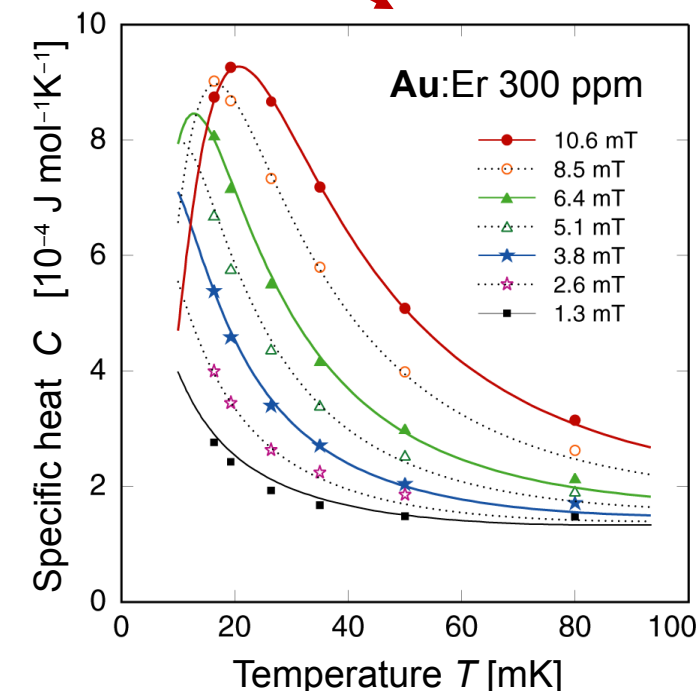
$$\Delta T \cong \frac{E}{C_{\text{tot}}} \xrightarrow{\text{MMC}}$$



$$\Delta \Phi_s \propto \frac{\partial M}{\partial T} \Delta T \rightarrow \Delta \Phi_s \propto \frac{\partial M}{\partial T} \frac{E}{C_{\text{tot}}}$$



Very good agreement between data and theoretical expectation for interacting spin system



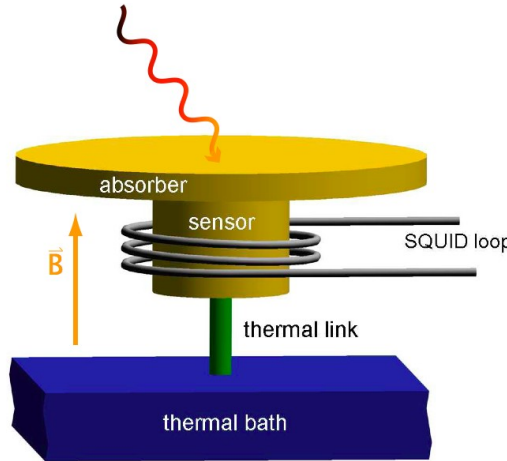
# Metallic Magnetic Calorimeters

A.Fleischmann, C. Enss and G. M. Seidel,  
Topics in Applied Physics **99** (2005) 63

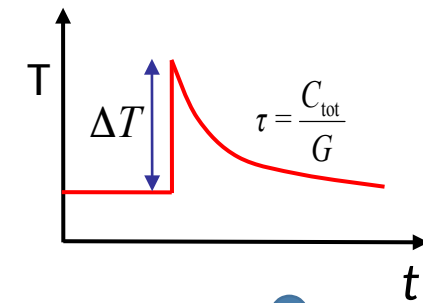
A.Fleischmann et al.,  
AIP Conf. Proc. **1185** (2009) 571

## Paramagnetic temperature sensor

Dilute alloy Au:Er or Ag:Er (Er concentration: a few hundred ppm)



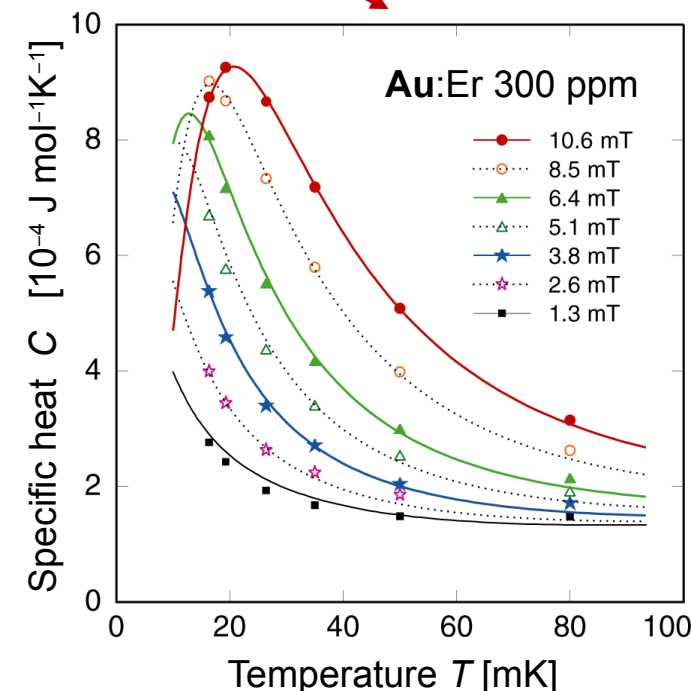
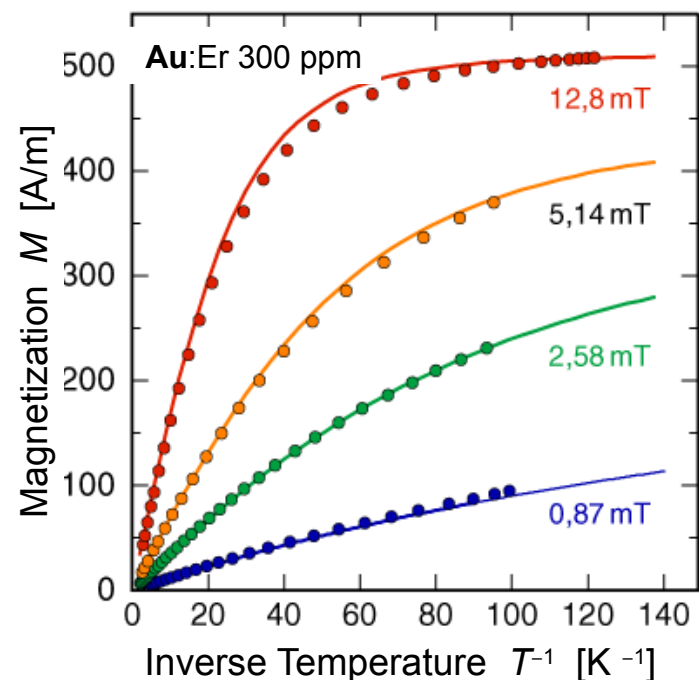
$$\Delta T \cong \frac{E}{C_{\text{tot}}} \xrightarrow{\text{MMC}}$$



Optimization of detector geometries for applications

Very good agreement between data and theoretical expectation for interacting spin system

$$\Delta \Phi_s \propto \frac{\partial M}{\partial T} \Delta T \rightarrow \Delta \Phi_s \propto \frac{\partial M}{\partial T} \frac{E}{C_{\text{tot}}}$$

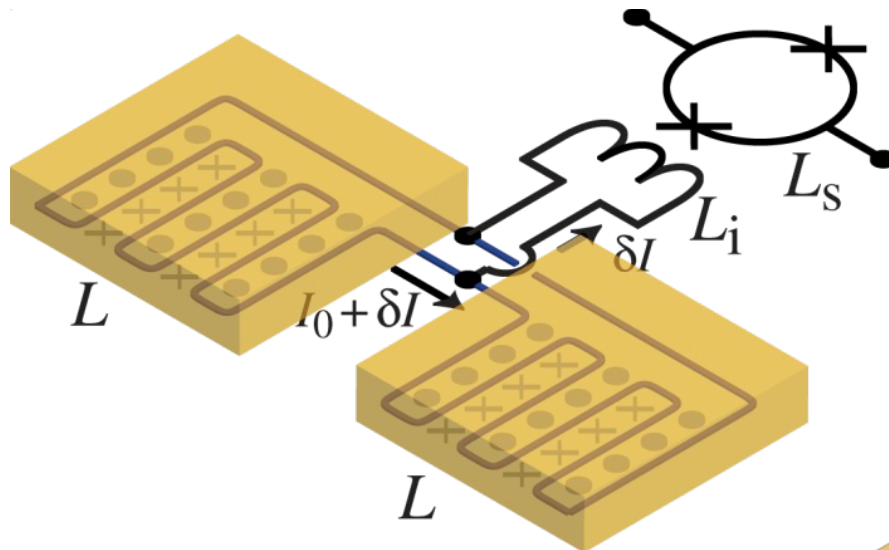


# Detector geometries

- planar paramagnetic sensor
- superconducting coil
- transformed coupled to a dc SQUID

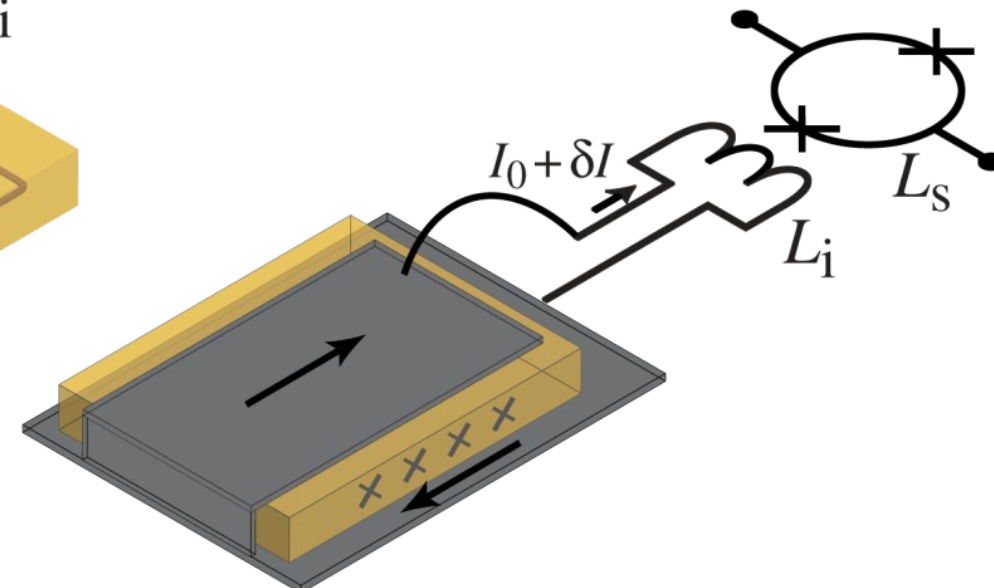
## Well established:

- superconducting meander shaped pickup loop
- planar sensor on top of meander-shaped coil
- gradiometric design



## Sandwich geometry:

- planar sensor sandwiched between stripline
- best magnetic flux coupling

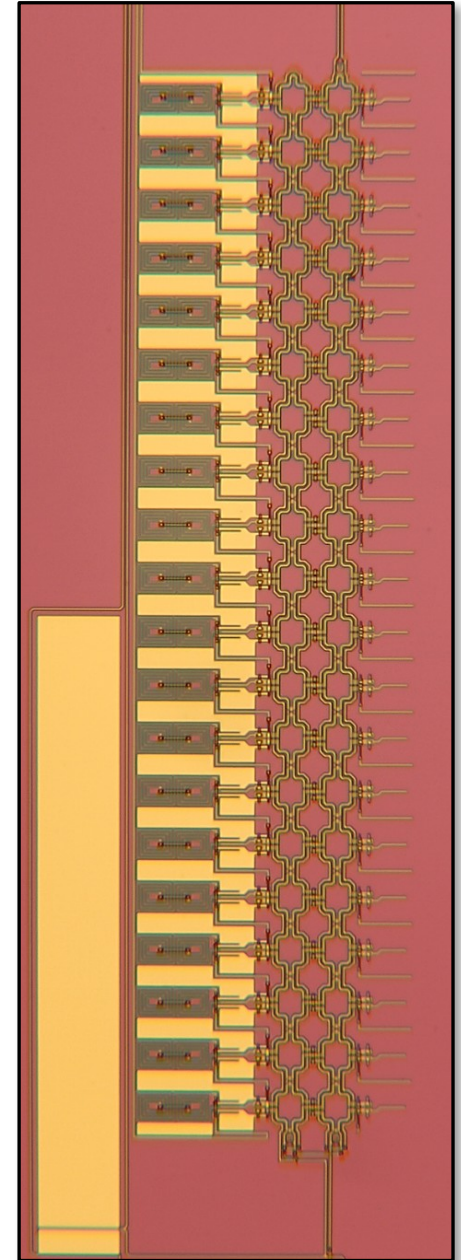
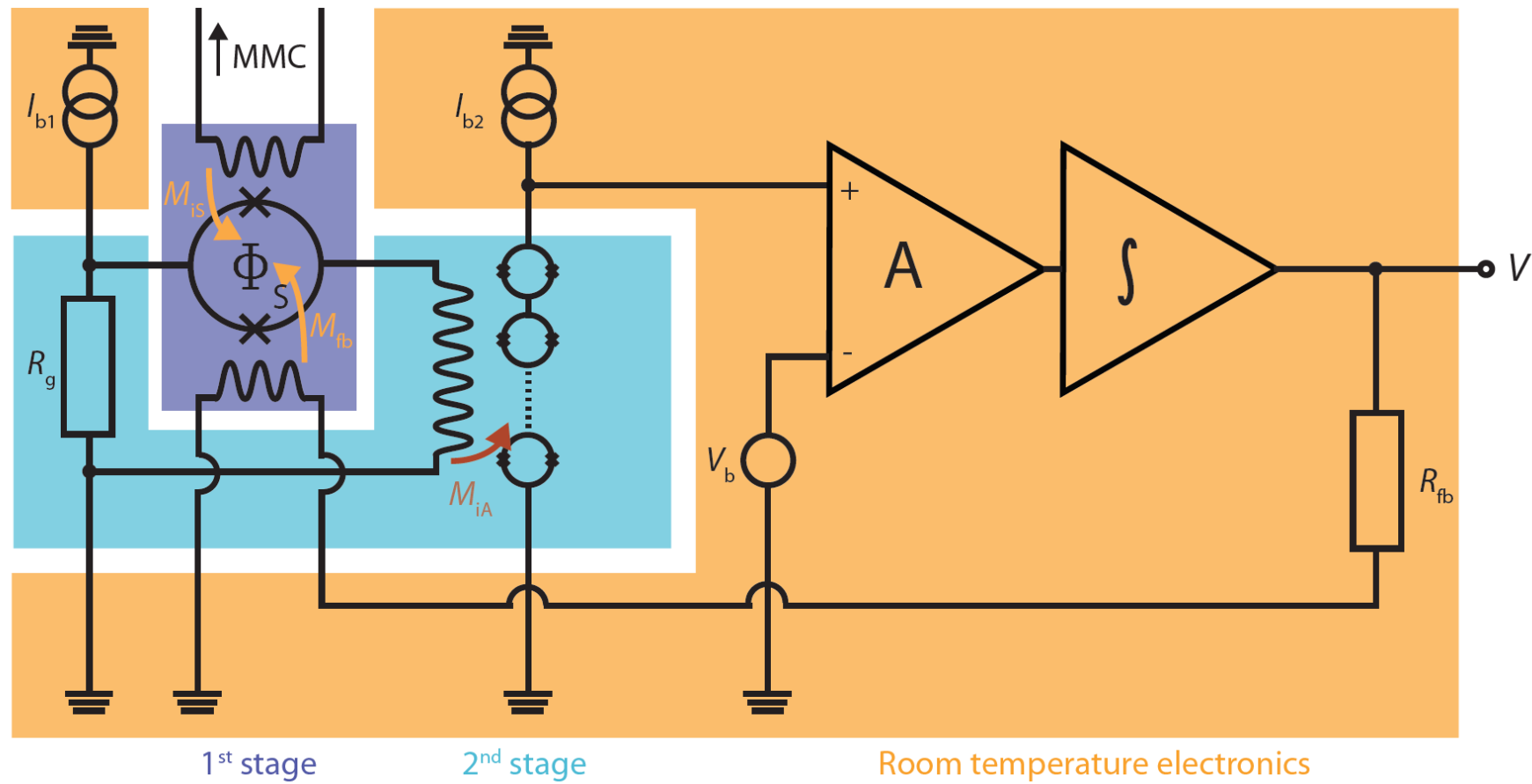


# MMC readout

Two-stage dc-SQUID readout with flux-locked loop

low noise

small power dissipation on detector SQUID chip (voltage bias 1<sup>st</sup> stage)

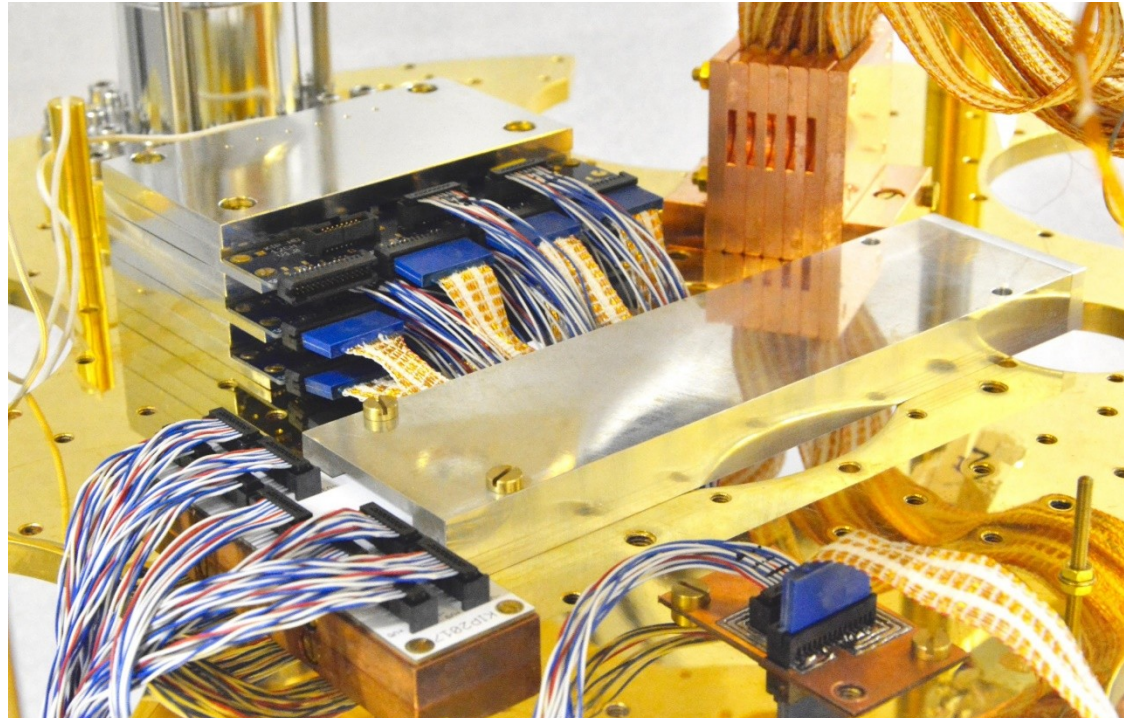
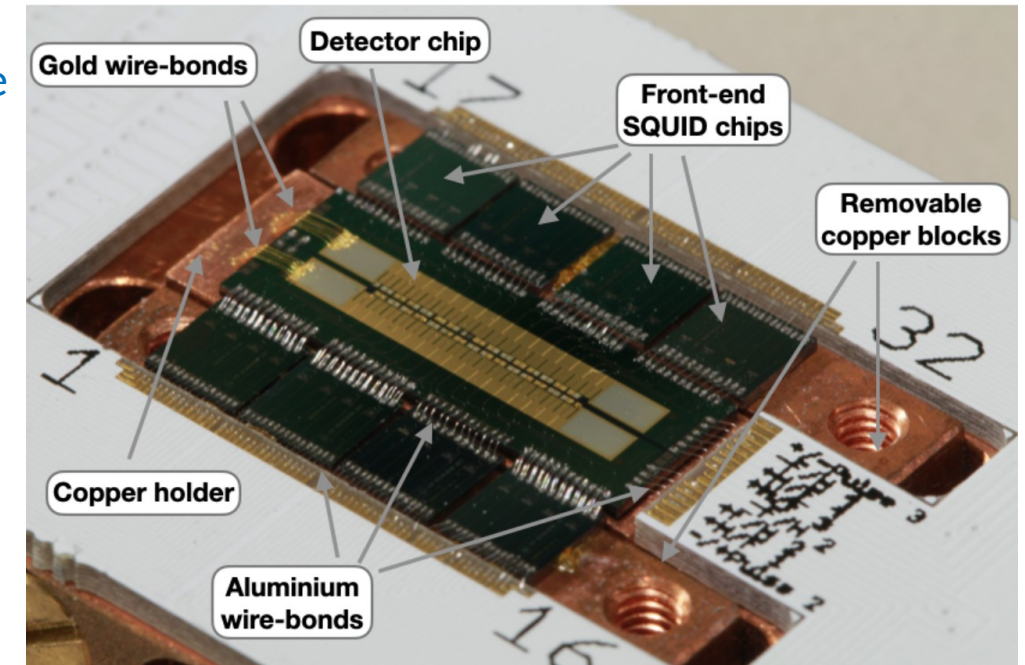


In house produced SQUID array

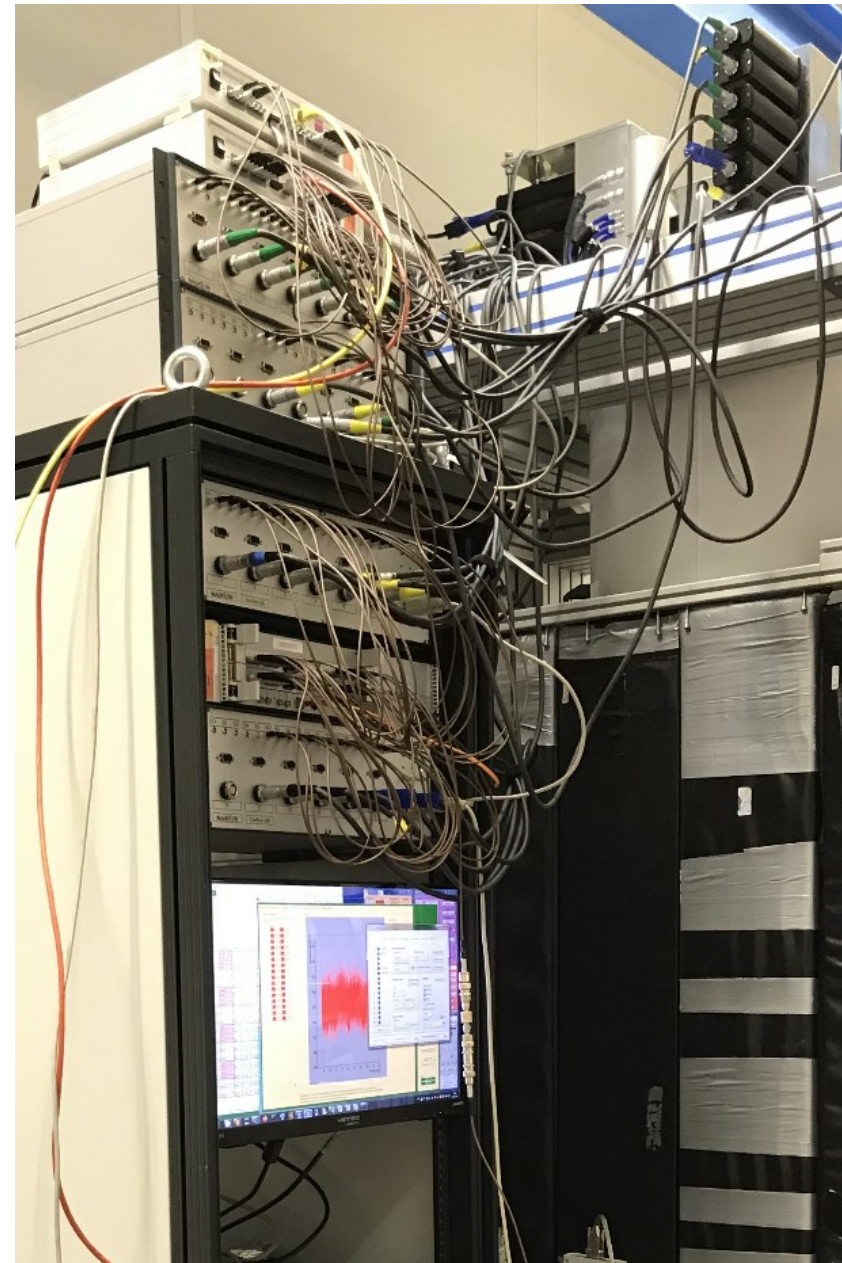
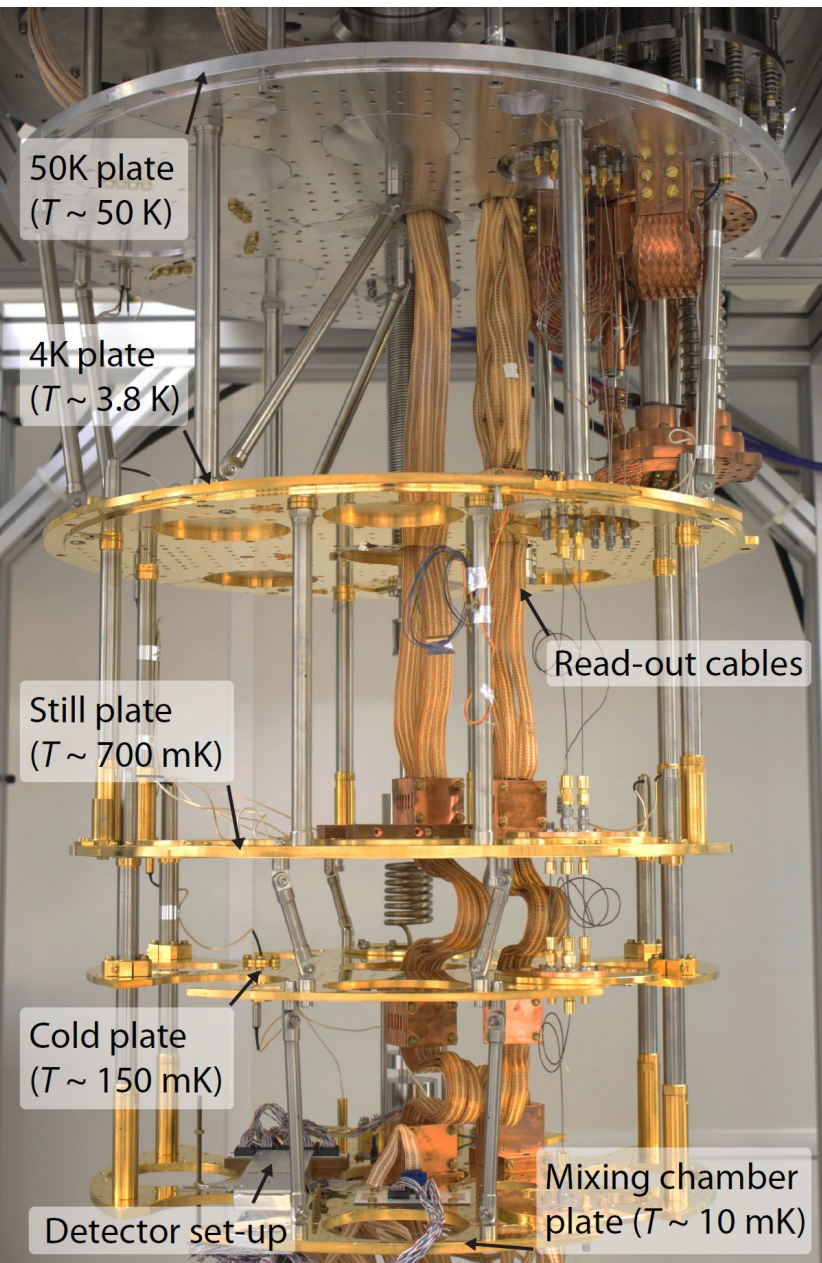
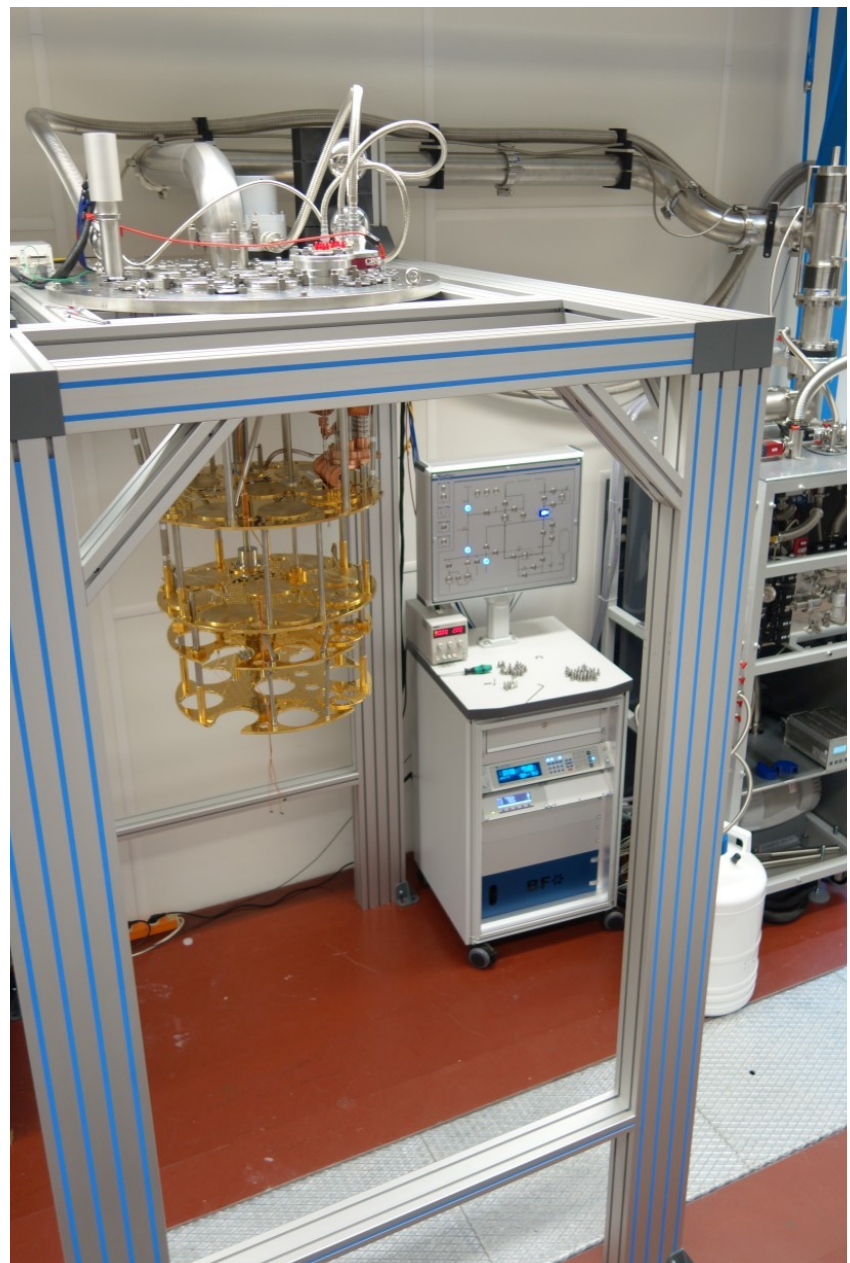
# MMC readout



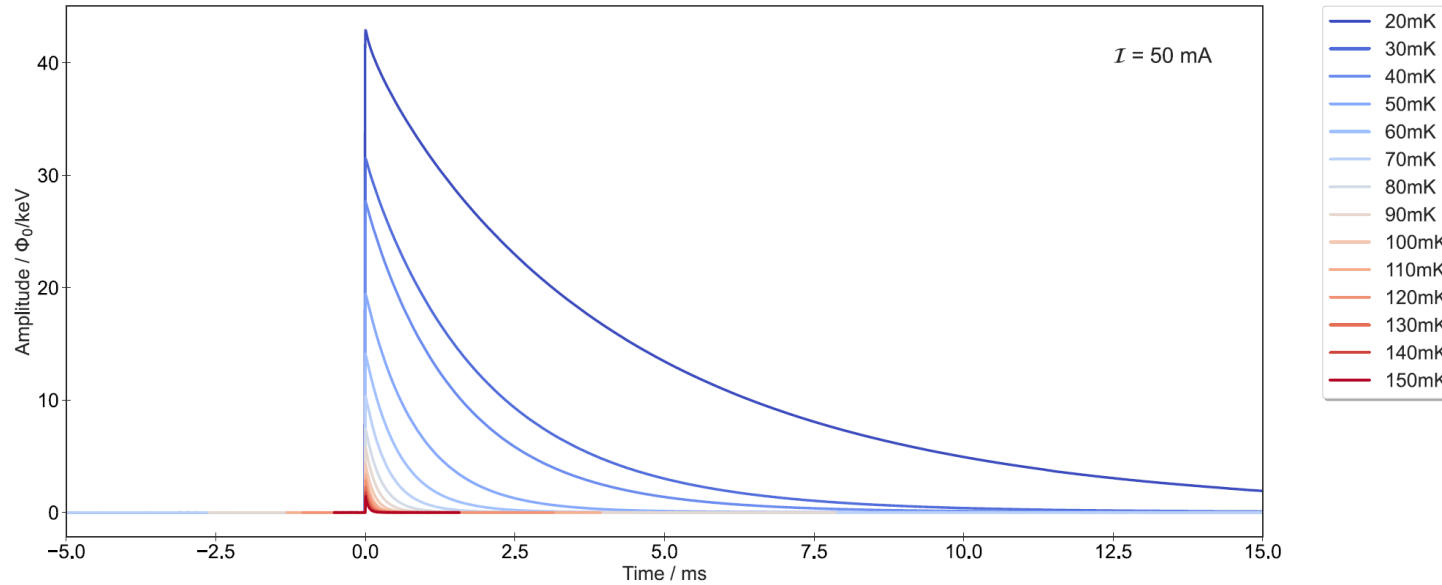
Detector module



# MMC readout



# Performance

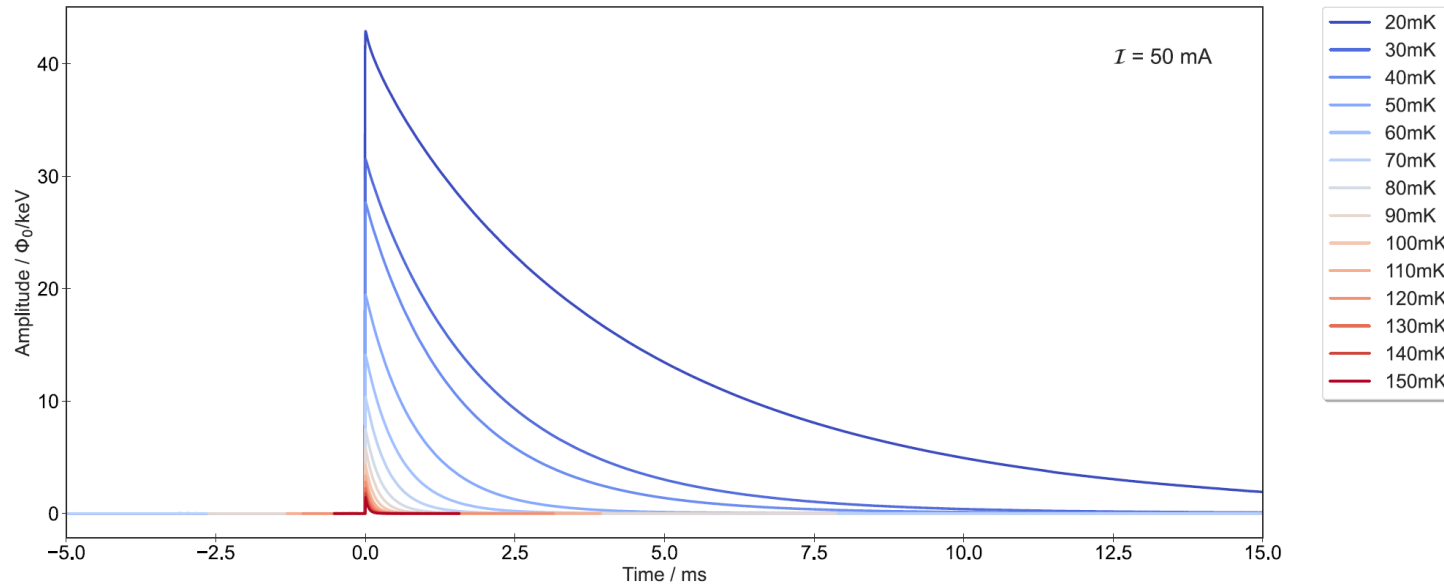


Operation over a large temperature range  
→ operation of large arrays

Large dynamic range  
→ no saturation of the signal

Design defined decay constant  
→ thermal link optimized for  
detector heat capacity at operating  
temperature

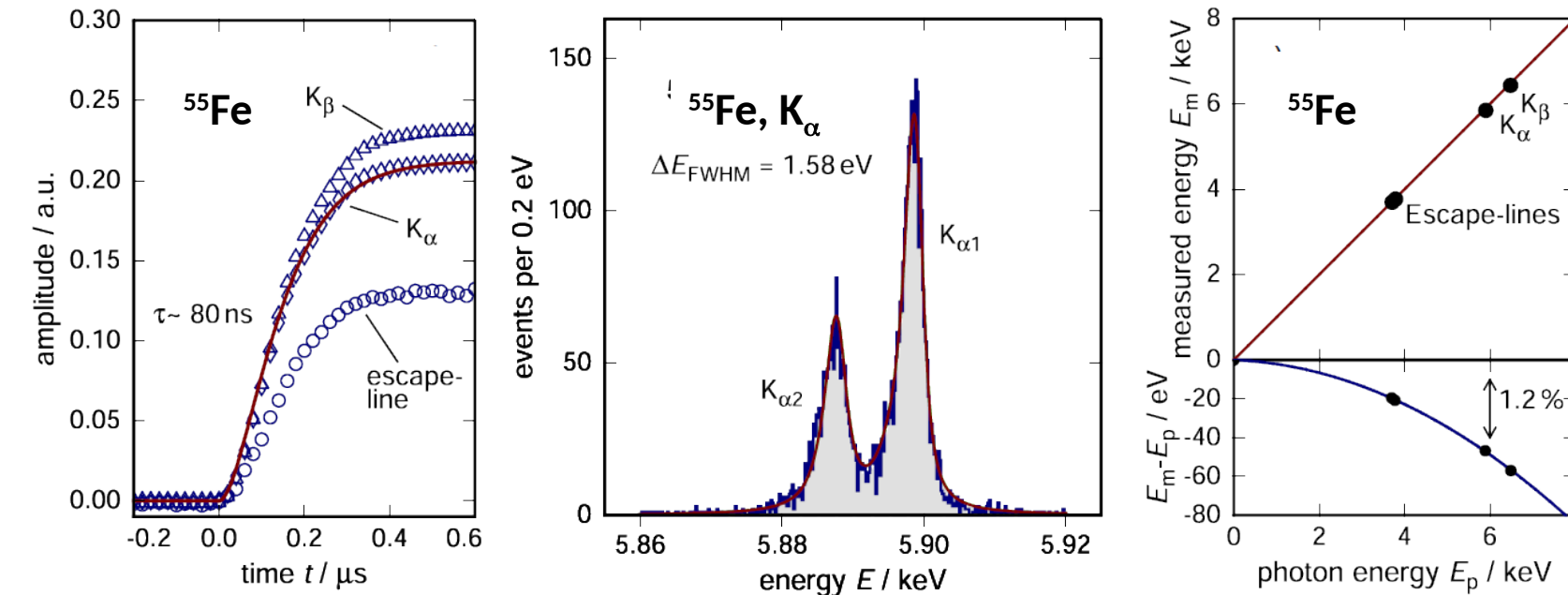
# Performance



Operation over a large temperature range  
→ operation of large arrays

Large dynamic range  
→ no saturation of the signal

Design defined decay constant  
→ thermal link optimized for  
detector heat capacity at operating  
temperature



Fast risetime  
→ Reduction un-resolved pile-up

Extremely good energy resolution  
→ identification of small structures

Excellent linearity  
→ precise definition of the energy scale

# MMC fabrication

40 m<sup>2</sup> Cleanroom class 100  
at Kirchhoff Institute for Physics

Wet bench  
Chemistry bench  
Maskless aligner  
UHV sputtering system  
Dry etching system

- Flexibility in design and fabrication
- Reliable processes for thin films
- Production of MMC array and superconducting electronics



# MMC fabrication

40 m<sup>2</sup> Cleanroom class 100  
at Kirchhoff Institute for Physics

Wet bench  
Chemistry bench  
Maskless aligner  
UHV sputtering system  
Dry etching system

- Flexibility in design and fabrication
- Reliable processes for thin films
- Production of MMC array and superconducting electronics

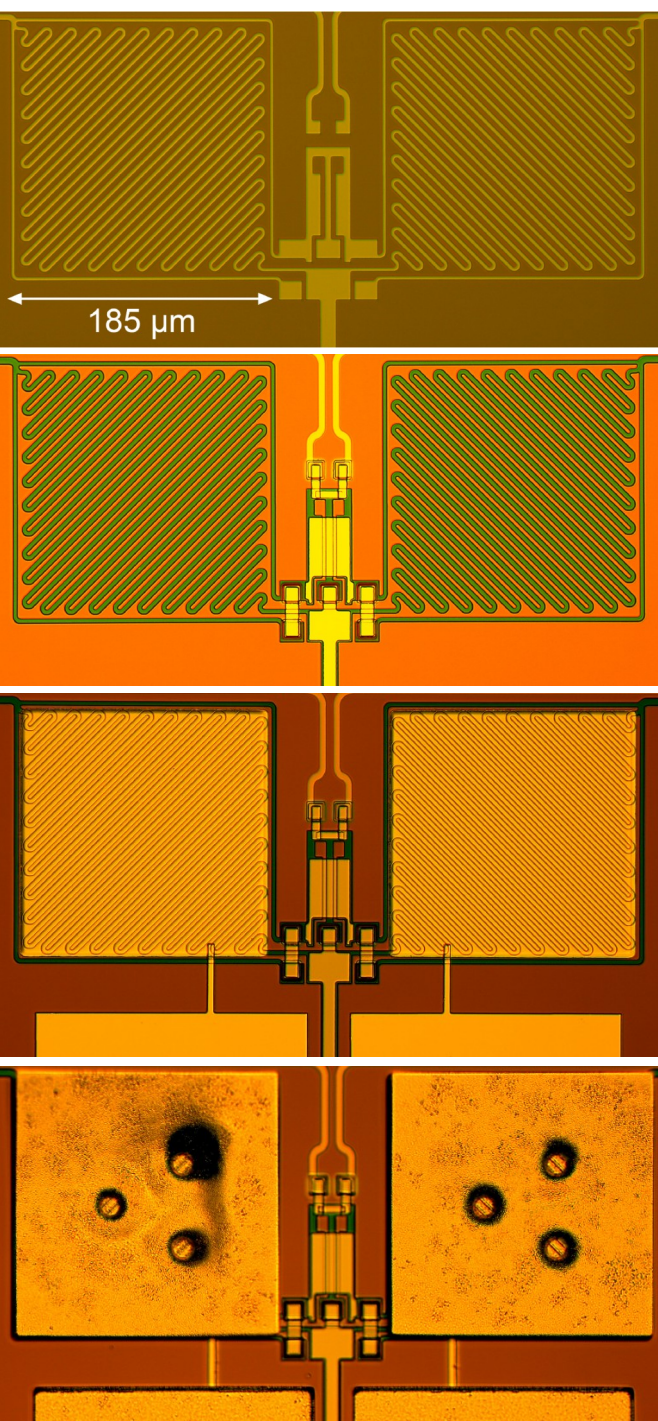
In-house fabrication facility for innovative detectors



# MMC fabrication

ECHO-100k wafer

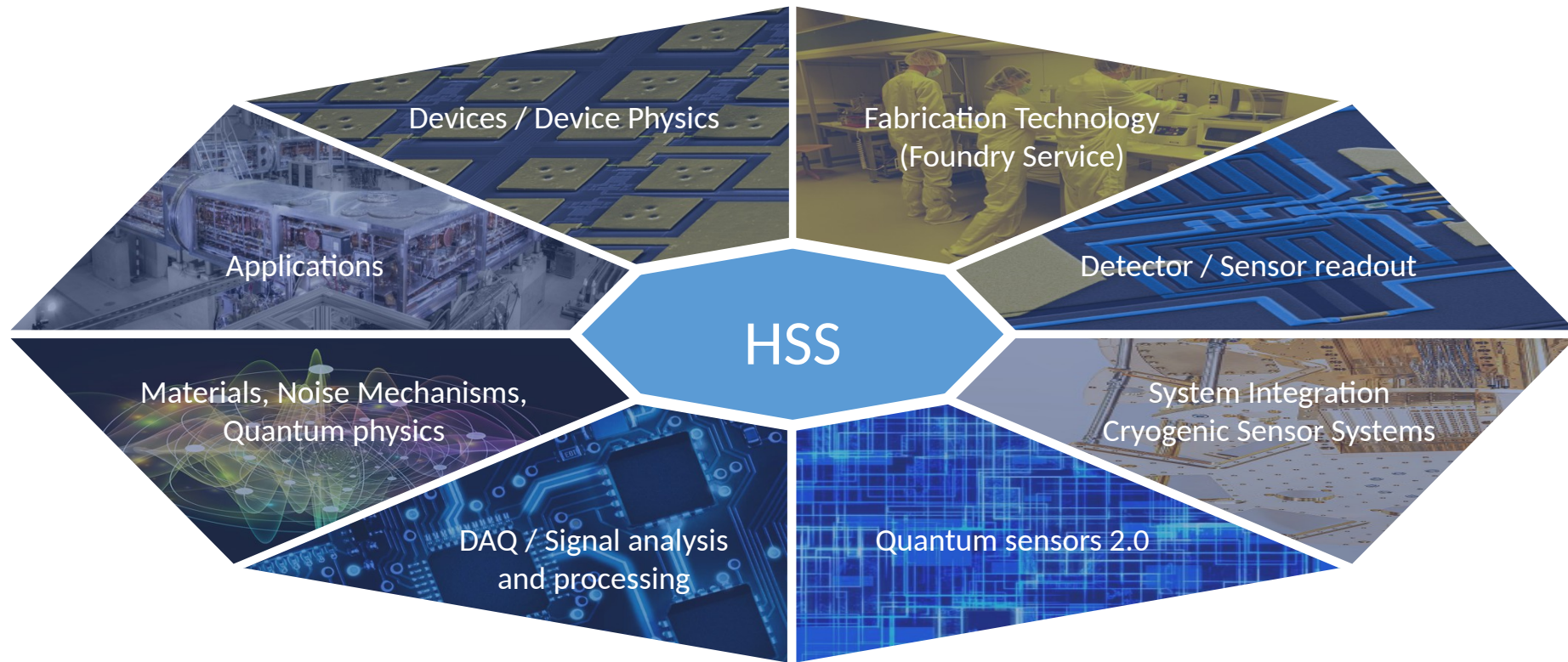
Fabrication steps				
#	Layer	Material	Thickness	Deposition technique
1	Pick-up coils, SQUID lines (layer 1)	Nb	250 nm	Sputtering + etching
2	Isolation	$\text{Nb}_2\text{O}_5$	-	Anodisation
3	Isolation	$\text{SiO}_2$	175 nm	Sputtering + lift-off
4	Isolation	$\text{SiO}_2$	175 nm	Sputtering + lift-off
5	Heaters	AuPd	150 nm	Sputtering + lift-off
6	SQUID lines (layer 2)	Nb	600 nm	Sputtering + lift-off
7	Sensor	AgEr	480 nm	Sputtering + lift-off
8	Thermalisation	Au	300 nm	Sputtering + lift-off
9	Stems	Au	100 nm	Sputtering
10	Absorber - 1st layer	Au	3 $\mu\text{m}$	Electroplating + lift-off
11	$^{163}\text{Ho}$ host material	Ag	100 nm	Sputtering
12	$^{163}\text{Ho}$ implantation	$^{163}\text{Ho}$	-	Ion-implantation
13	$^{163}\text{Ho}$ host material	Ag	100 nm	Sputtering + lift-off
14	Absorber - 2nd layer	Au	3 $\mu\text{m}$	Sputtering + lift-off



# Helmholtz-foundry for MMCs and superconducting electronics



= Center for High-Resolution Superconducting Sensors  
joint effort by IPE (KIT), IMS (KIT), and KIP (Heidelberg University)



S. Kempf (IMS, scientific director)

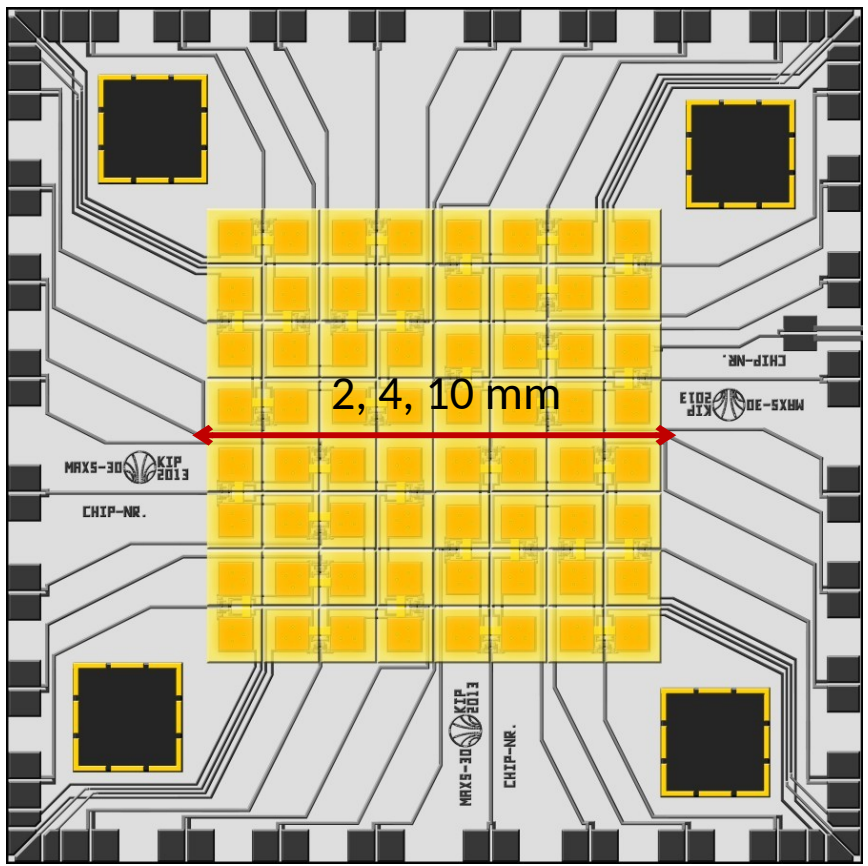
F. Simon, A. Kopmann, M. Kleifges, M. Wegner (IPE)

C. Enss (IPE+KIP)



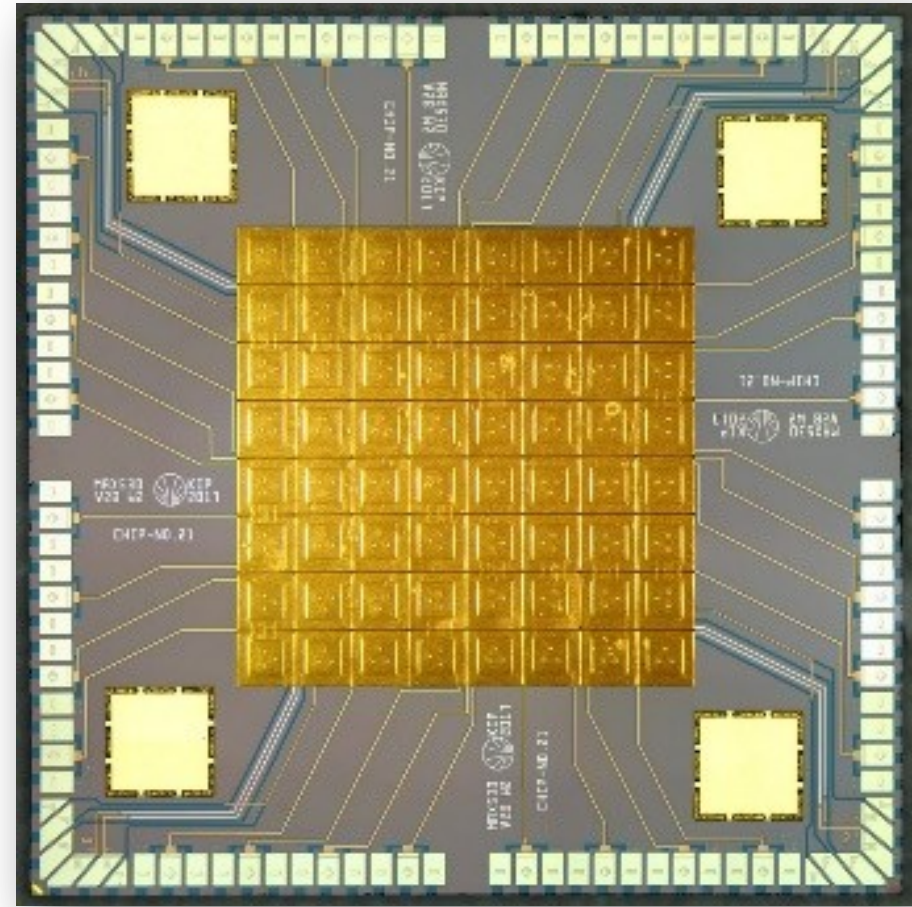
# Application s and Performan

# Microcalorimeter arrays for X-rays spectroscopy - maXs



maXs-20/30/100:

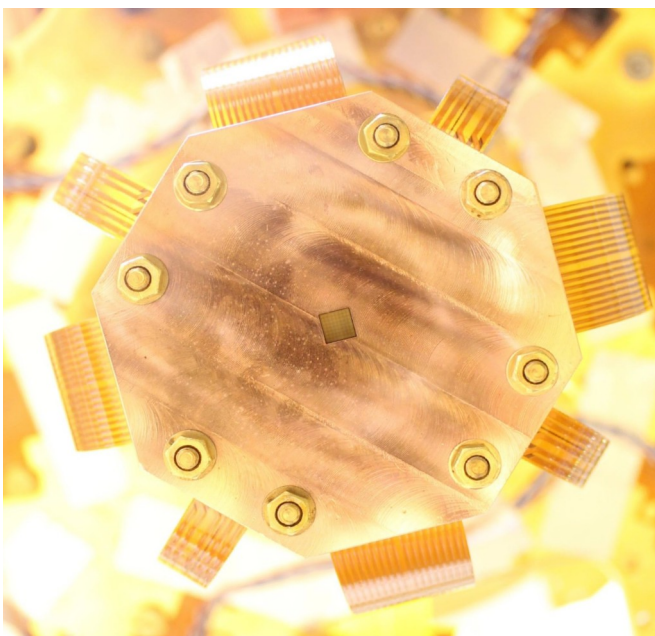
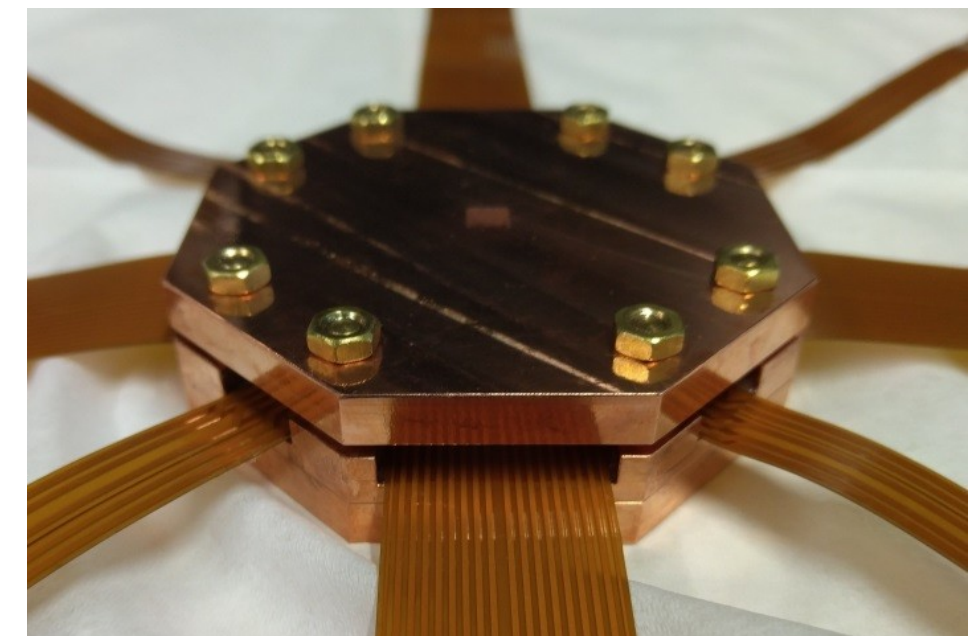
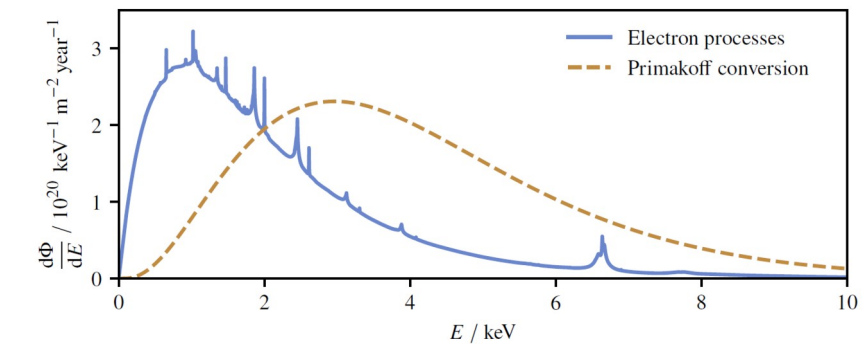
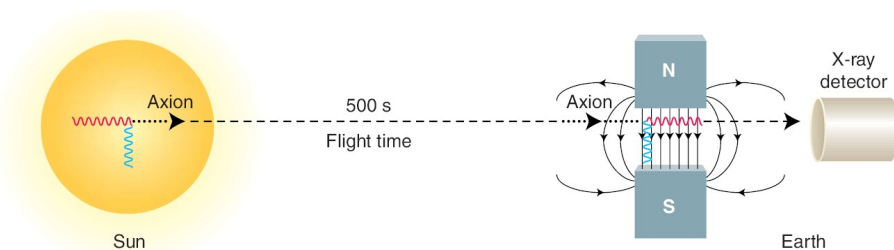
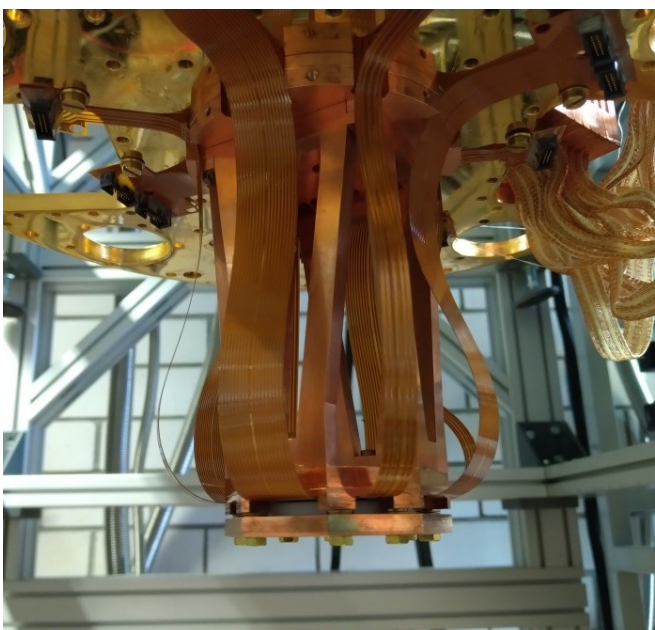
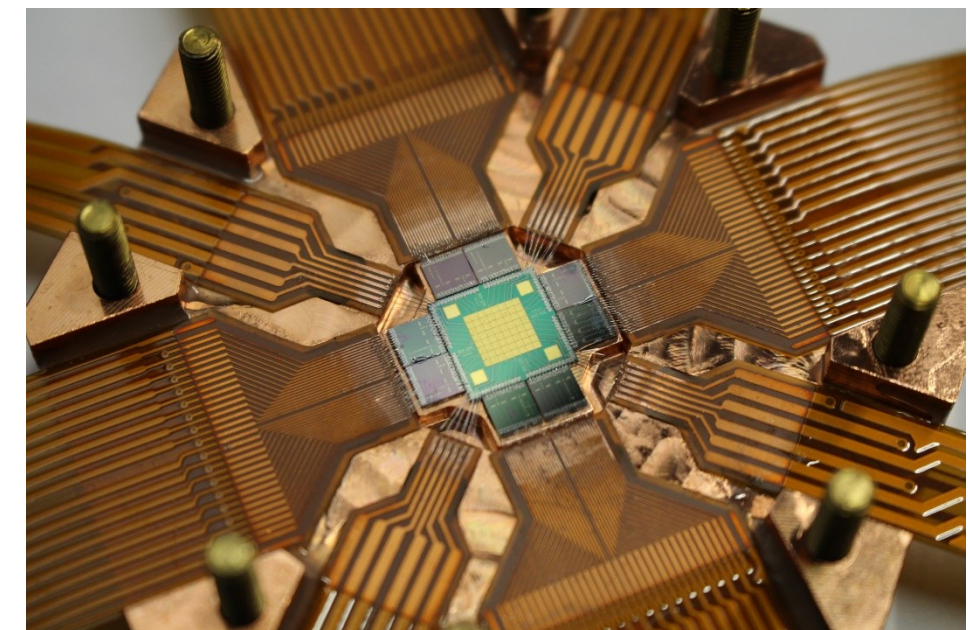
- 8x8 pixels for photons up to 20/30/100 keV
- with  $\Delta E_{FWHM} = 2/5/30$  eV
- 32 two-stage dc-SQUIDs



maXs-30

Absorber size:  $500 \times 500 \times 30 \mu\text{m}^3$

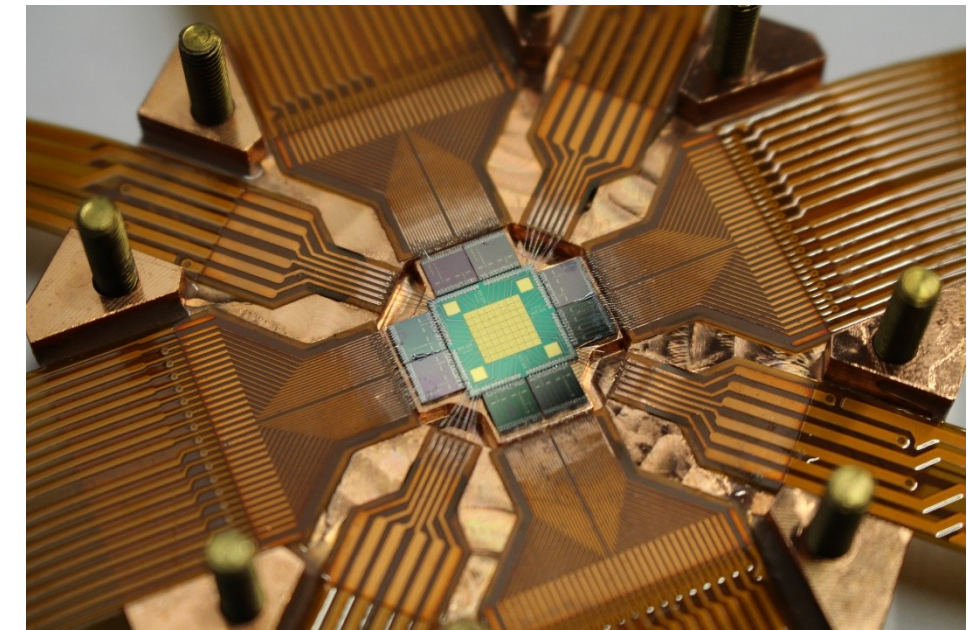
# maXs-30 set-up for IAXO



Design suitable for IAXO telescope

High purity materials for background reduction

# maXs-30 set-up for IAXO

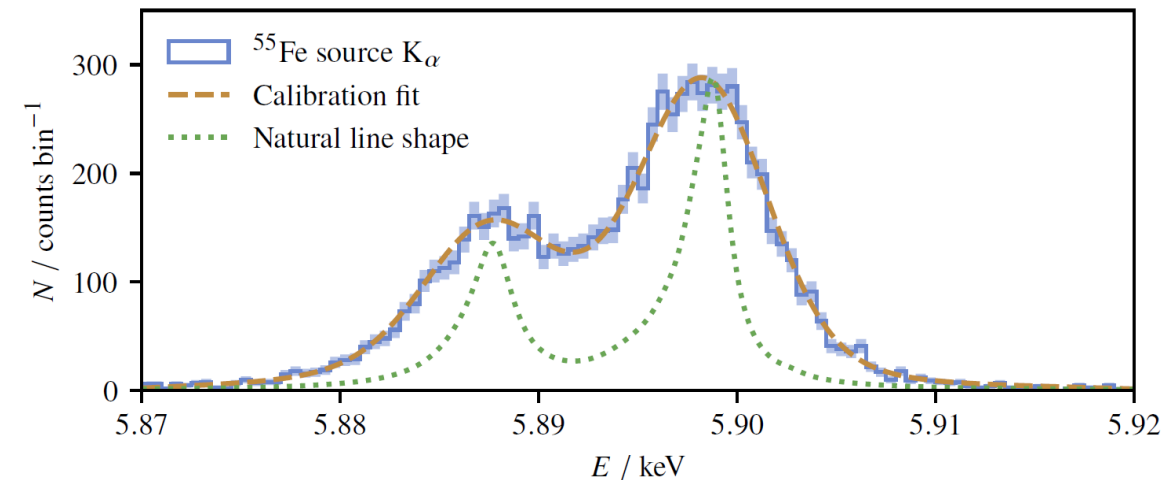
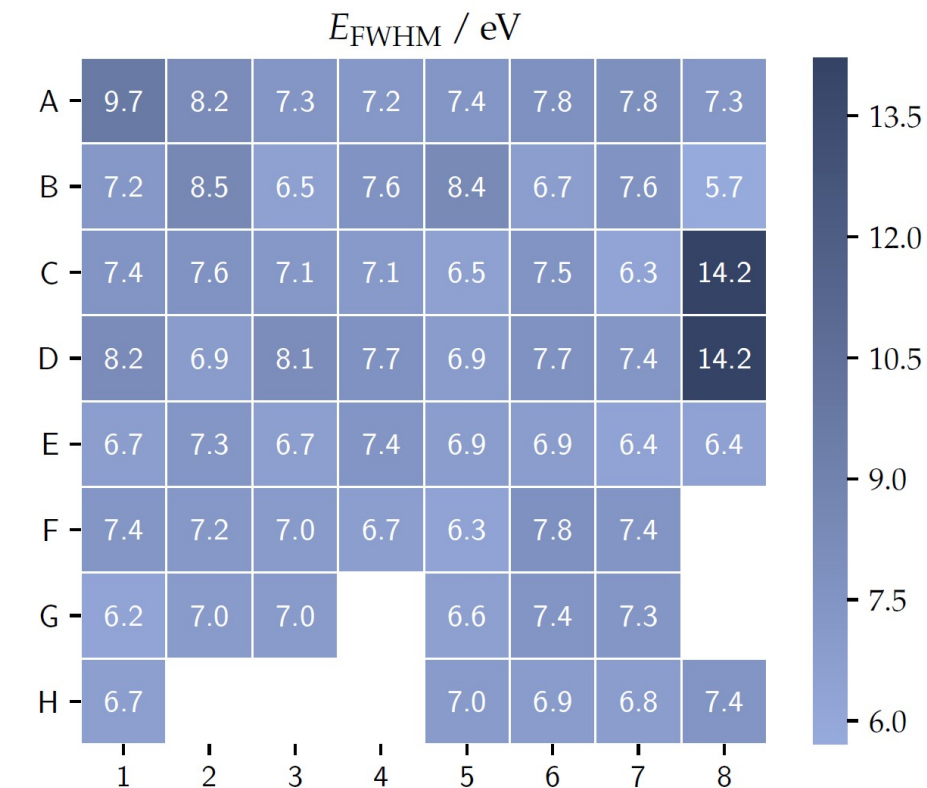


$^{55}\text{Fe}$  calibration source

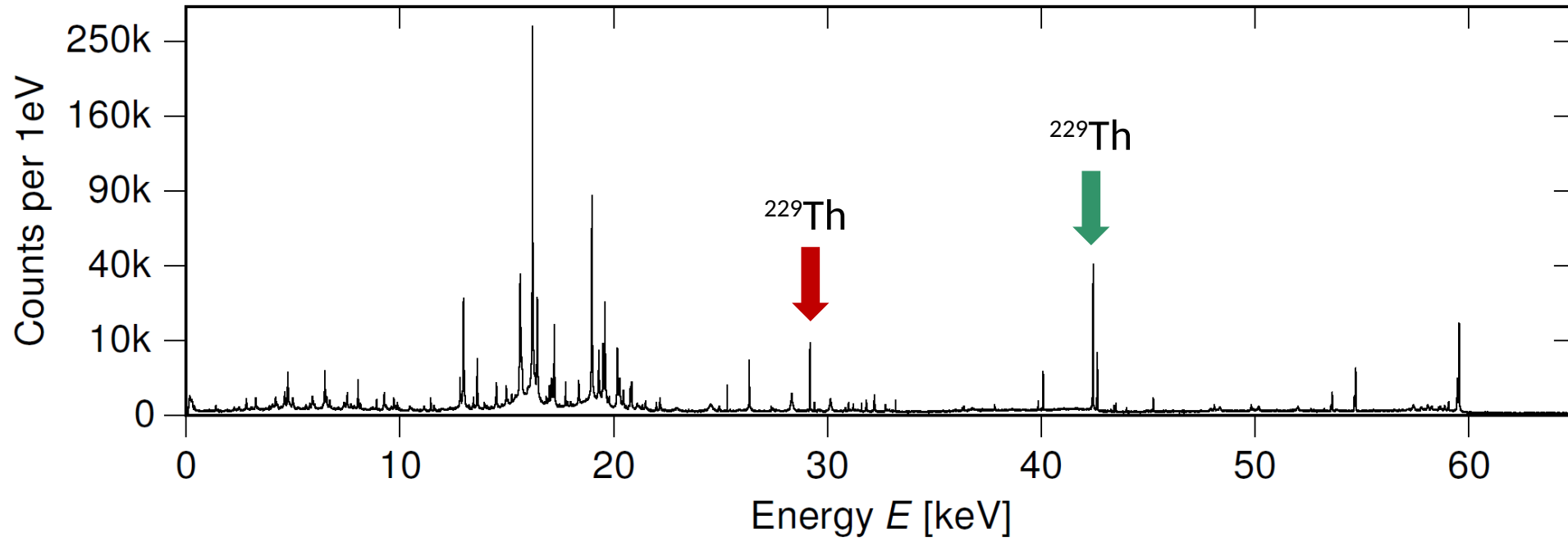
Stopping power @10 keV ~100%

- Homogeneous performance over the array
- Stable operation over 1 month

D. Unger et al., *JINST* **16** (2021) P06006, [arXiv:2010.15348](#) [physics.ins-det]

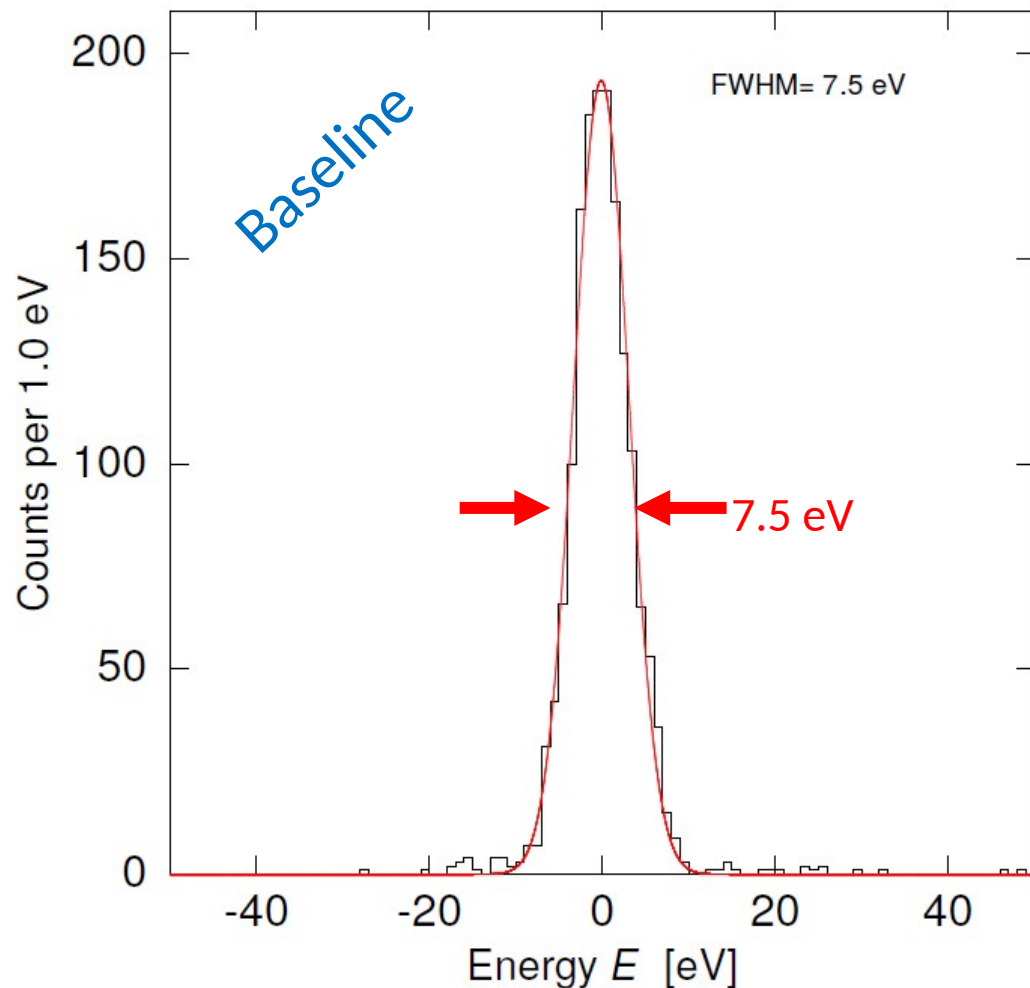


# maXs-30 with $^{241}\text{Am} + ^{233}\text{U}$ external sources

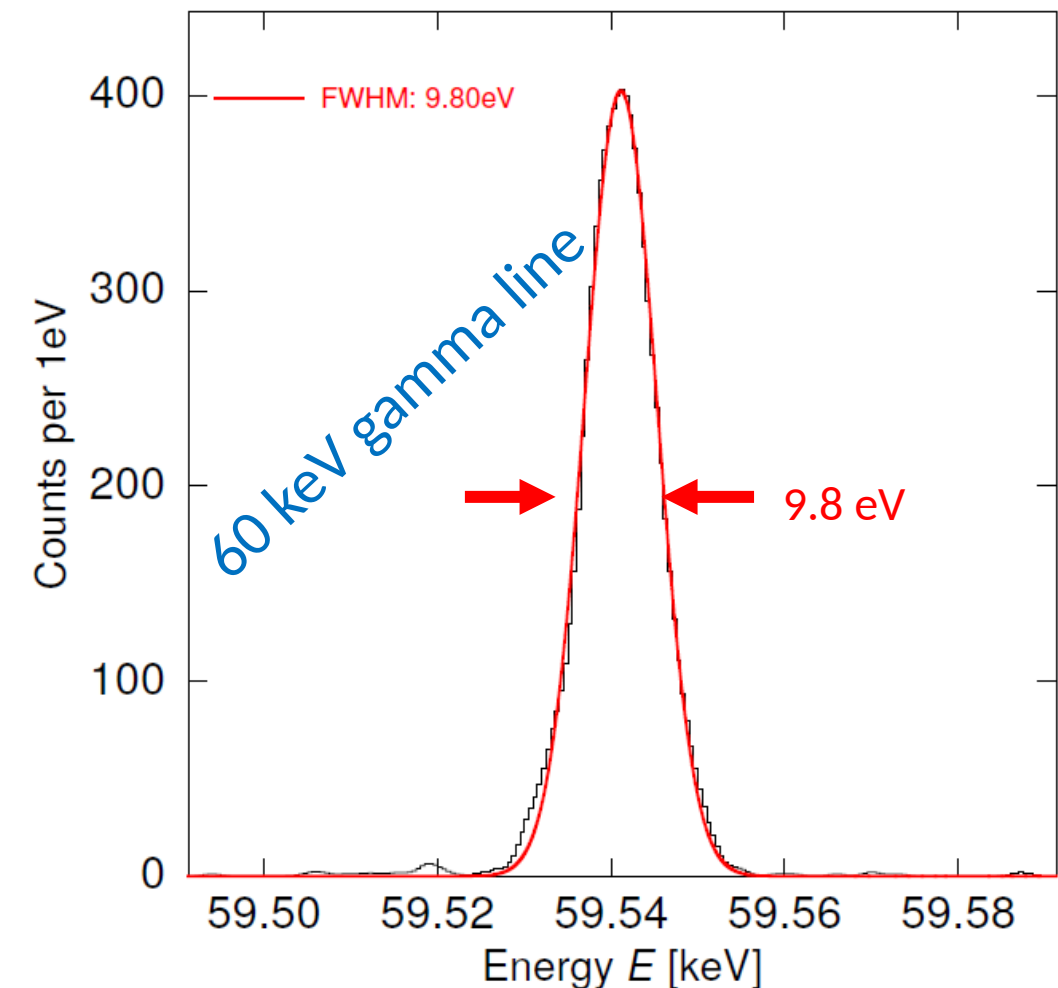


Co-added 20 channels, several weeks

# maXs-30 with $^{241}\text{Am} + ^{233}\text{U}$ external sources



Very close to design value

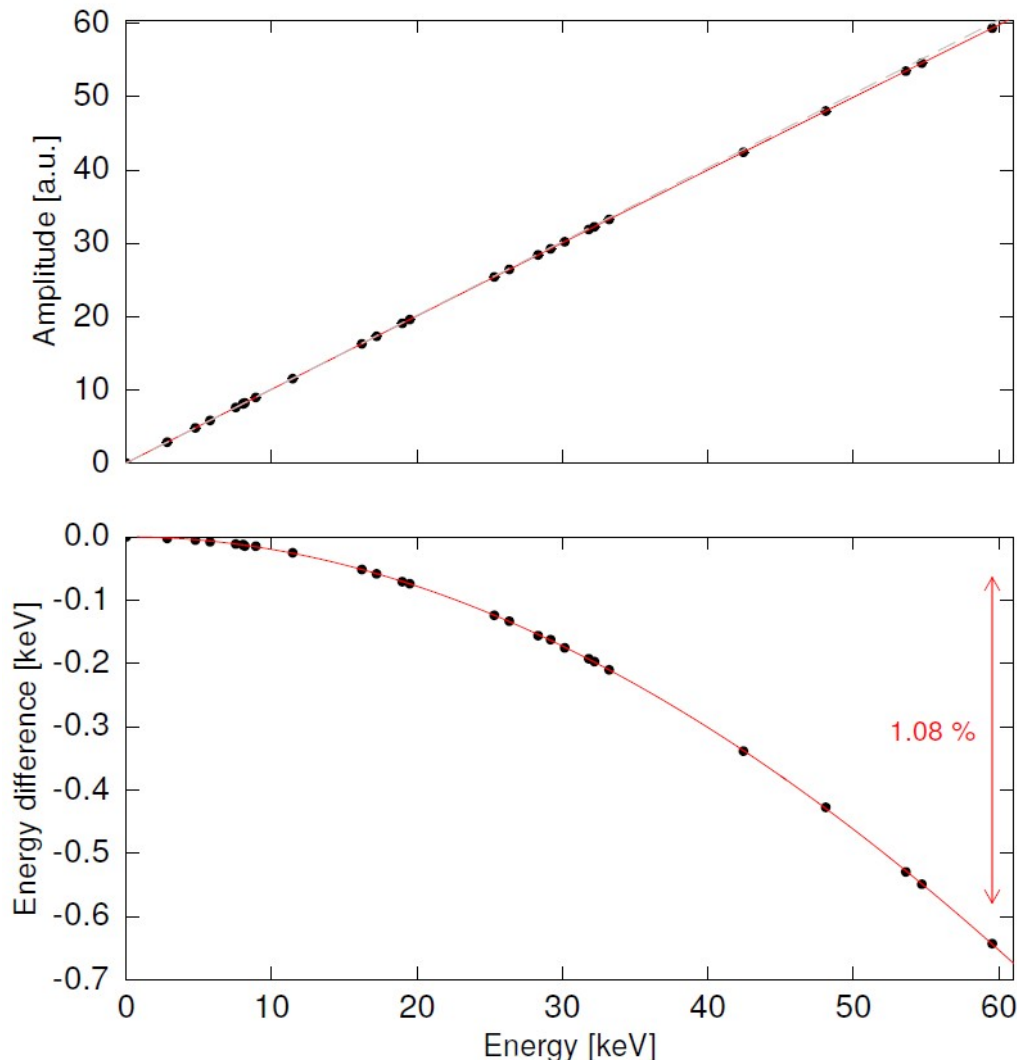


Energy resolution  $\Delta E_{\text{FWHM}} = 9.8 \text{ eV} @ 59 \text{ keV}$

World record resolving power: 6000

T. Sikorsky et al., *Phys. Rev. Lett.* **125** (2020) 142503

# maXs-30 set-up - $^{241}\text{Am}$ + $^{233}\text{U}$ external sources

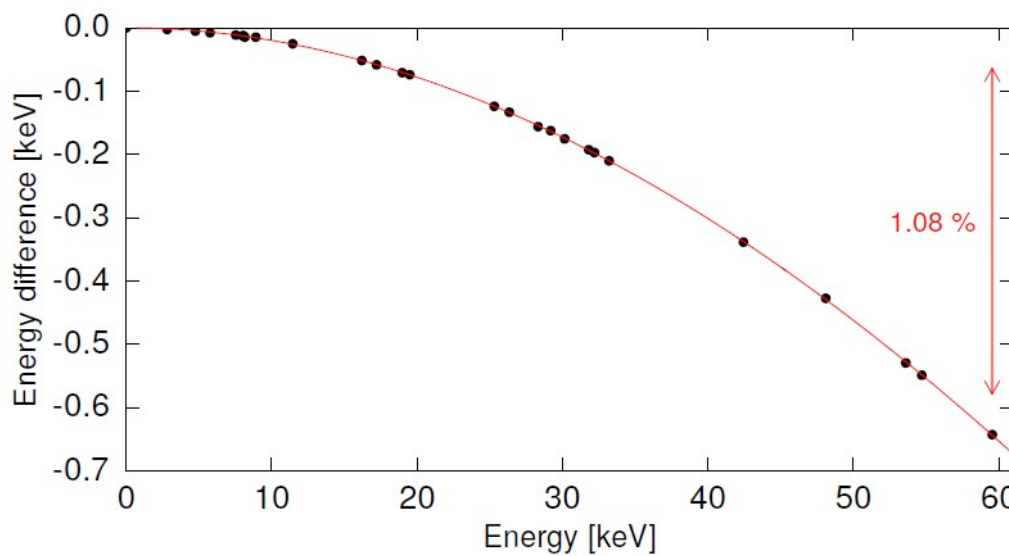
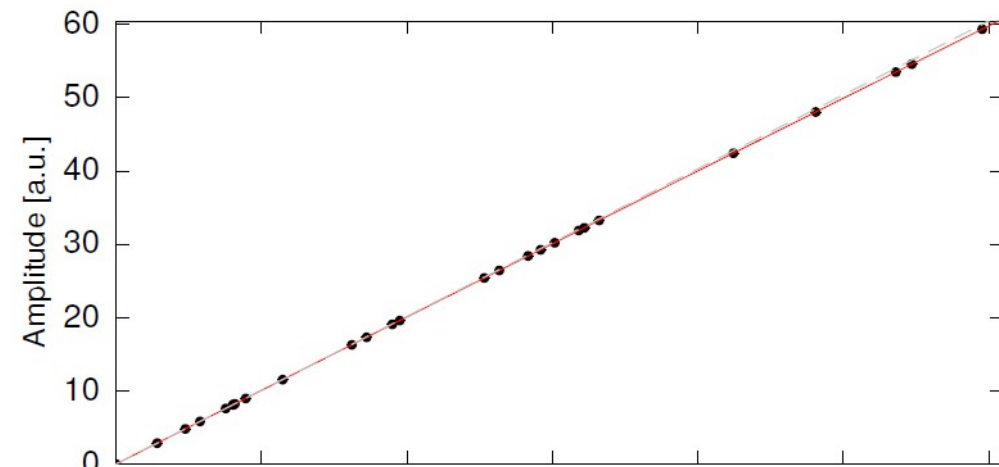


## Energy calibration

- Polynomial function 2<sup>nd</sup> to 4<sup>th</sup> order
- Stable over long measuring time

non-linearity as expected from thermodynamics!

# maXs-30 set-up - $^{241}\text{Am}$ + $^{233}\text{U}$ external sources

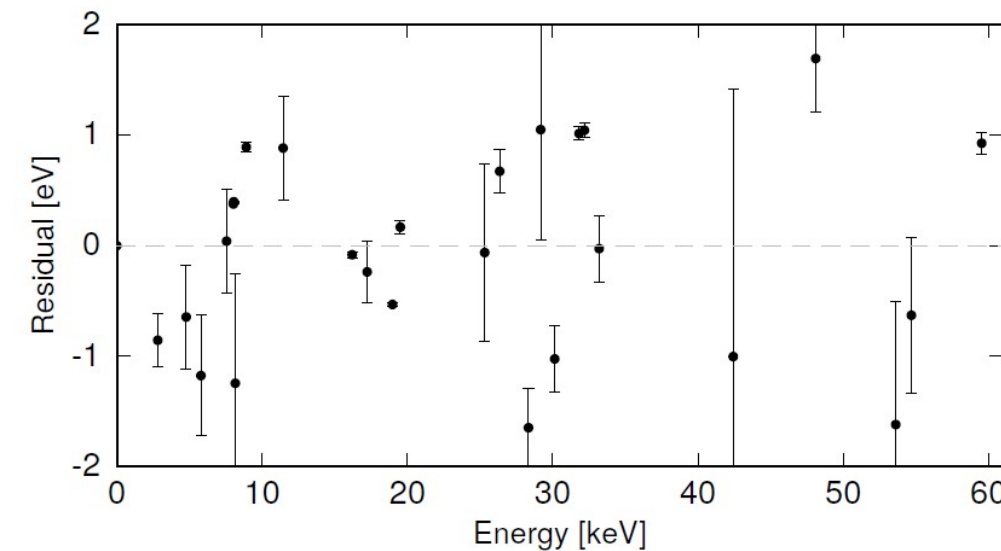


non-linearity as expected from thermodynamics!

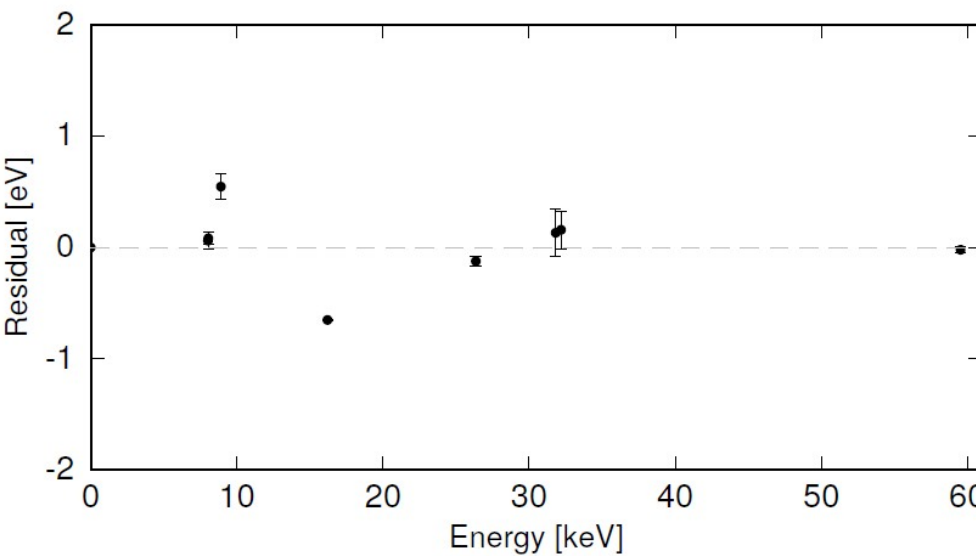
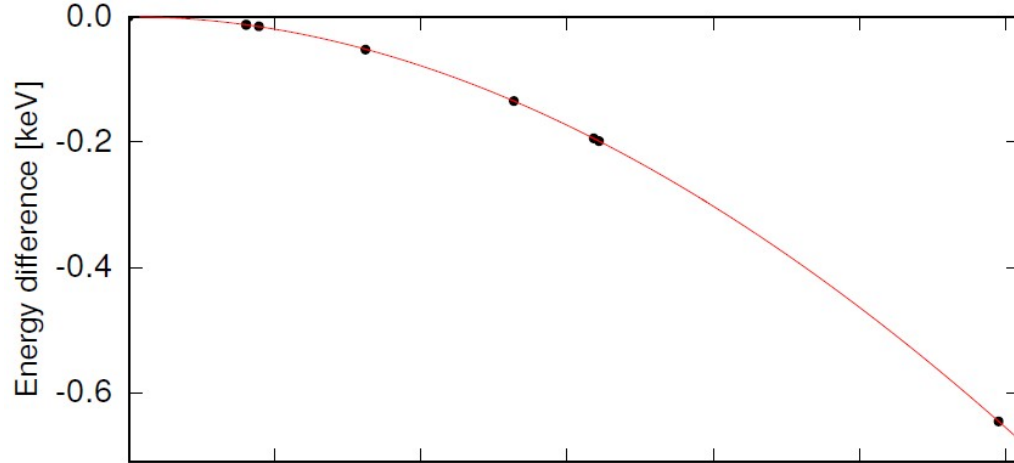
## Energy calibration

- Polynomial function 2<sup>nd</sup> to 4<sup>th</sup> order
- Stable over long measuring time

Most lines from literature have too large uncertainty!



# maXs-30 set-up - $^{241}\text{Am}$ + $^{233}\text{U}$ external sources



## Energy calibration

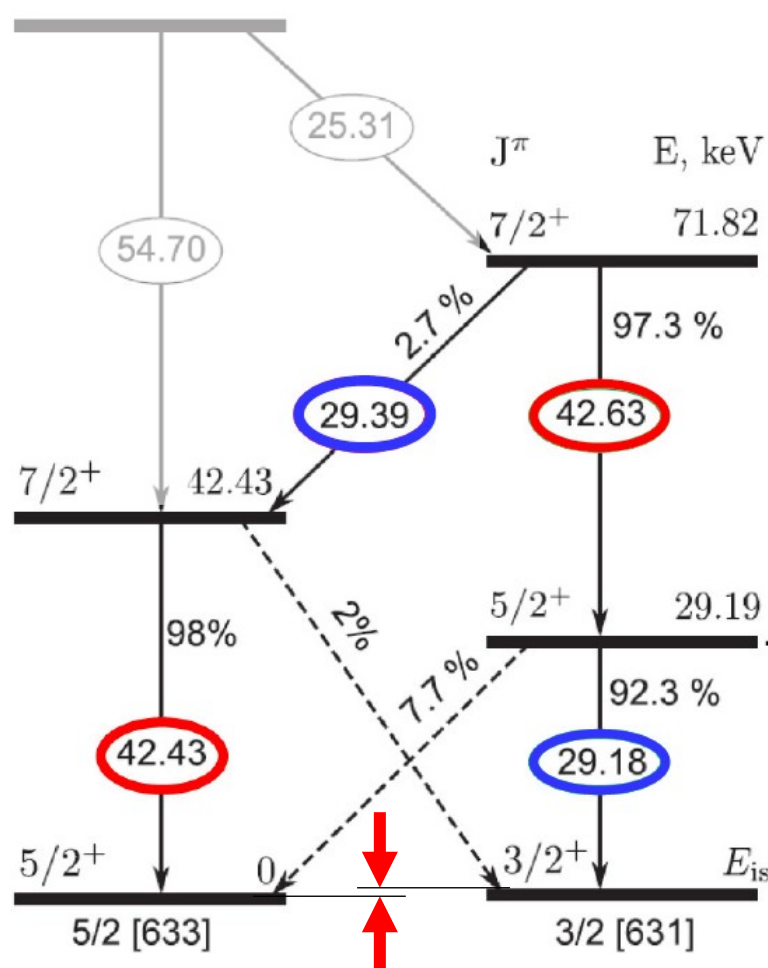
- Polynomial function 2<sup>nd</sup> to 4<sup>th</sup> order
- Stable over long measuring time

Sub-eV agreement for carefully selected calibration lines.

# maXs-30 set-up - $^{241}\text{Am}$ + $^{233}\text{U}$ external sources

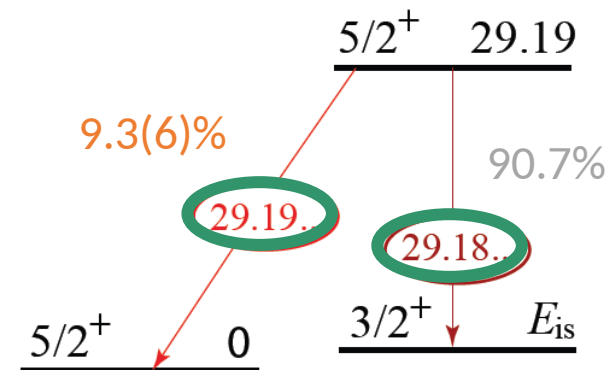
## i) from transitions within lowest 5 states

B.R. Beck et al, PRL 98, 142501 (2007)



$$\begin{aligned} E_{\text{iso}} &= E_{29.39 \text{ keV}} - E_{29.18 \text{ keV}} - (E_{42.63 \text{ keV}} - E_{42.43 \text{ keV}}) \\ &= \Delta E_{29 \text{ keV}} - \Delta E_{42 \text{ keV}} \end{aligned}$$

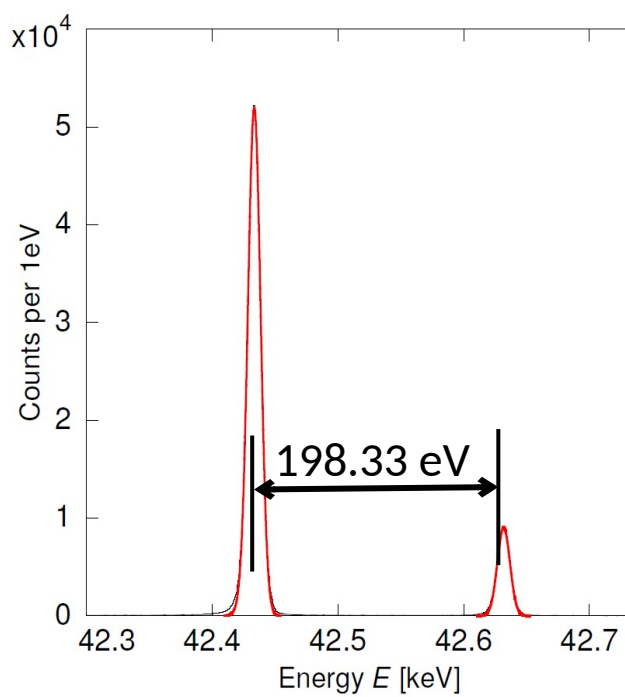
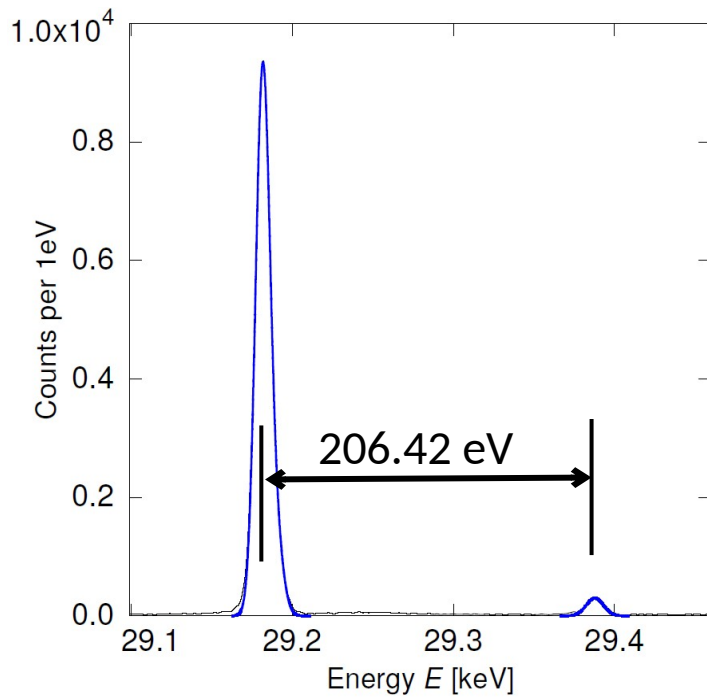
## ii) resolving the 29.2keV doublet



T. Sikorsky et al., Phys. Rev. Lett. **125** (2020) 142503

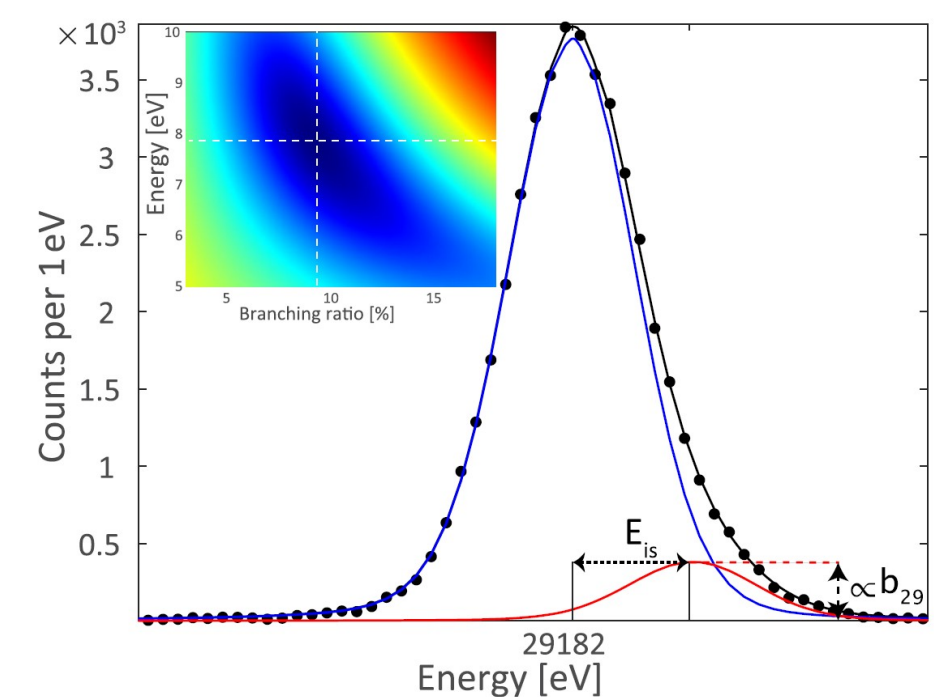
# maXs-30 set-up - $^{241}\text{Am}$ + $^{233}\text{U}$ external sources

i) from transitions within lowest 5 states



Isomer energy:  $\Delta E_{\text{iso}} = 8.10 \text{ eV} \pm 0.17 \text{ eV}$

ii) resolving the 29.2keV doublet

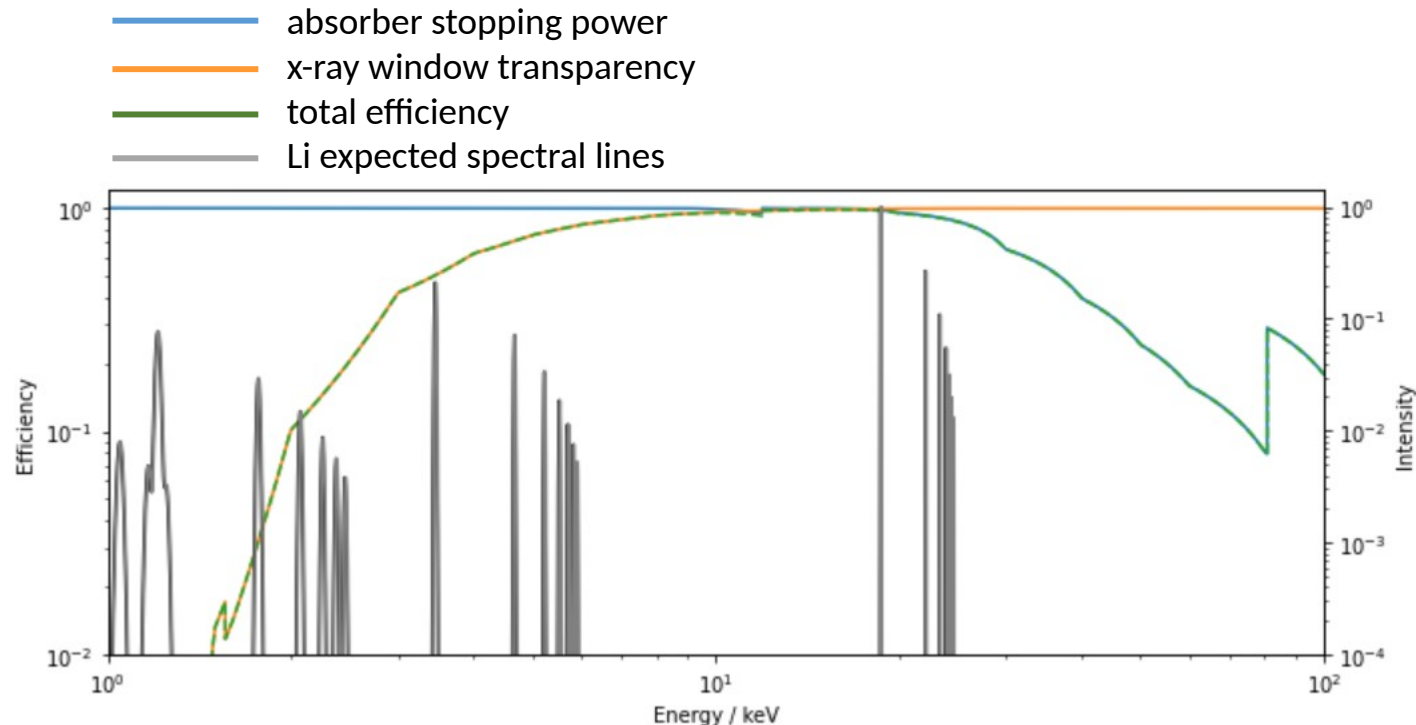
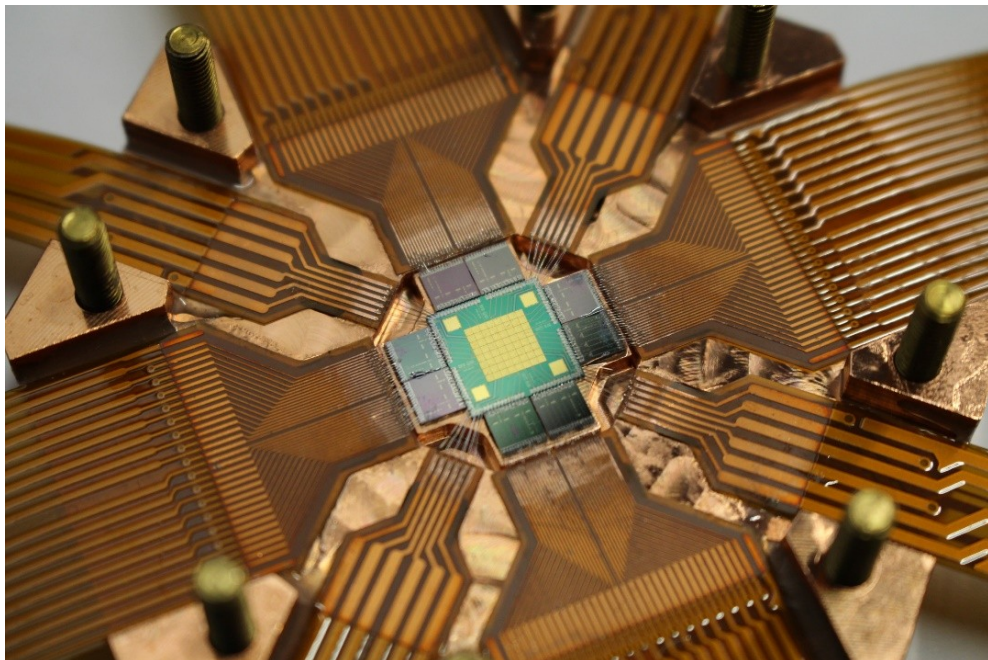


Isomer energy:  $E_{\text{iso}} = 7.8 \text{ eV} \pm 0.3 \text{ eV}$

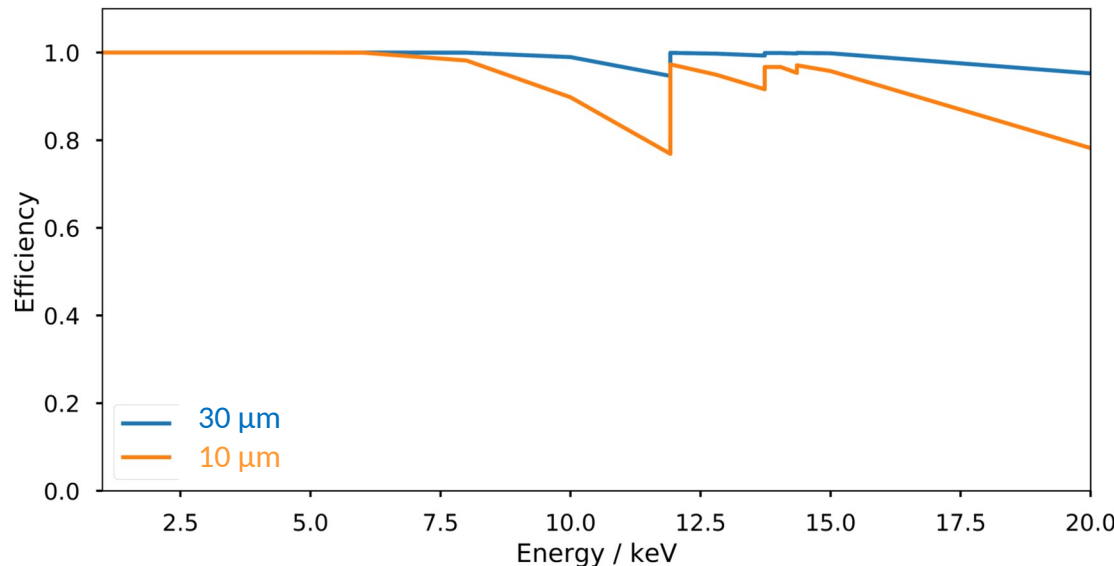
# Muonic atoms – QUARTET Collaboration

High energy resolution spectroscopy of muonic atoms for charge radii determination

- Proof of concept experiment with muonic atoms (as Lithium)  
→ PSI measurements scheduled October 2023
- Next future goal: study the nuclei in the range  $2 < Z < 11$



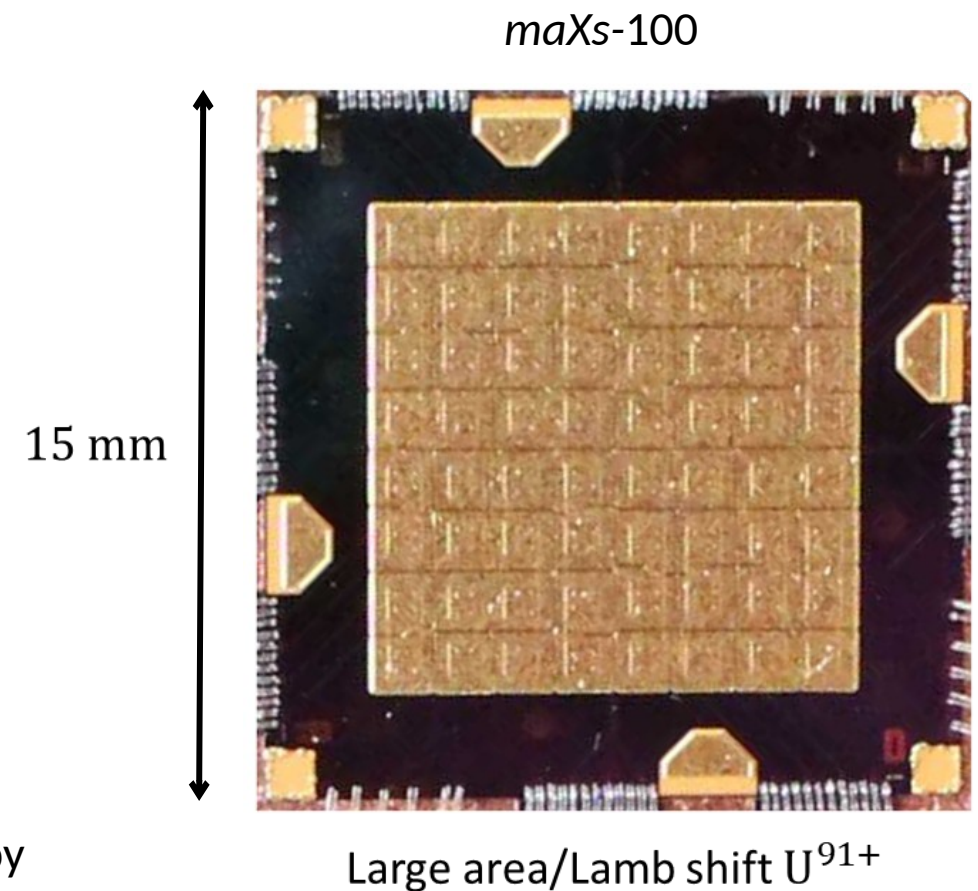
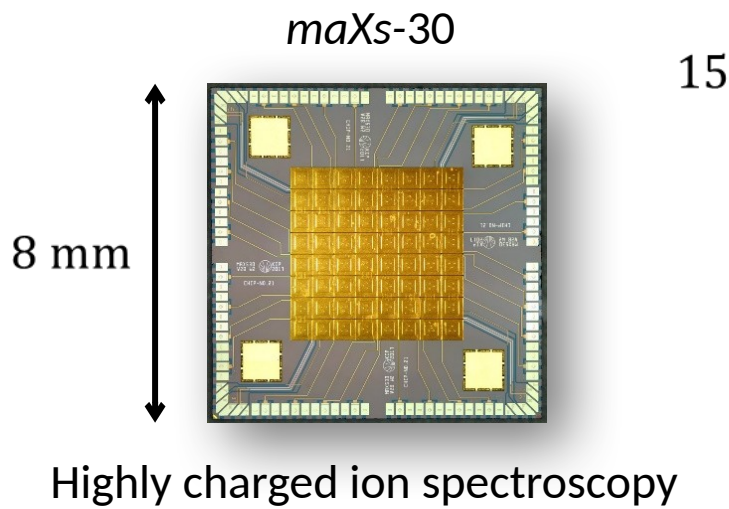
# From maXs-30 to maXs-100



Absorber volume can be adjusted for the particles to be detected

Sensor volume is optimized to match the heat capacity of the absorber at the working temperature

Same design, but scaled up!



# Highly ionized heavy ions

Study of **heavy, highly-charged** ions allows  
**high precision QED measurements in extreme E-fields**  
→ spectroscopy of **H-like** and **He-like Uranium** ions

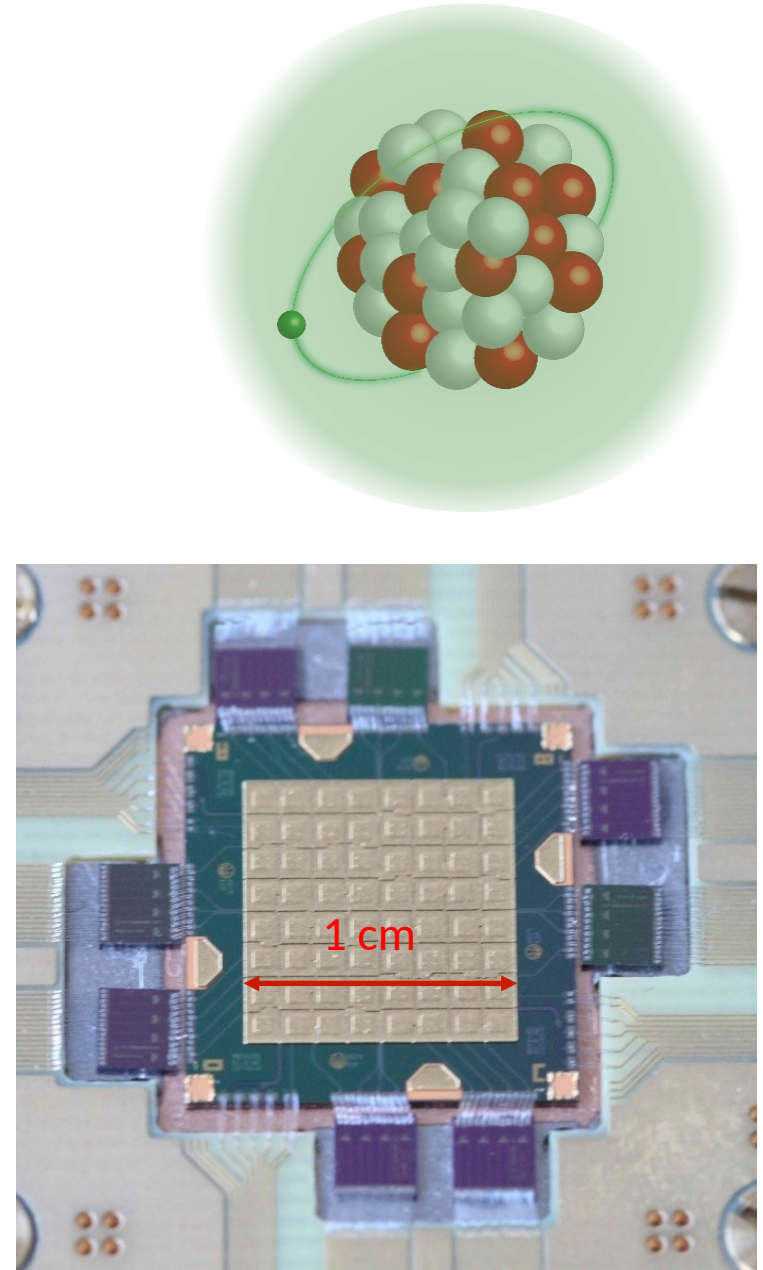
With:

**maXs-100 detector**

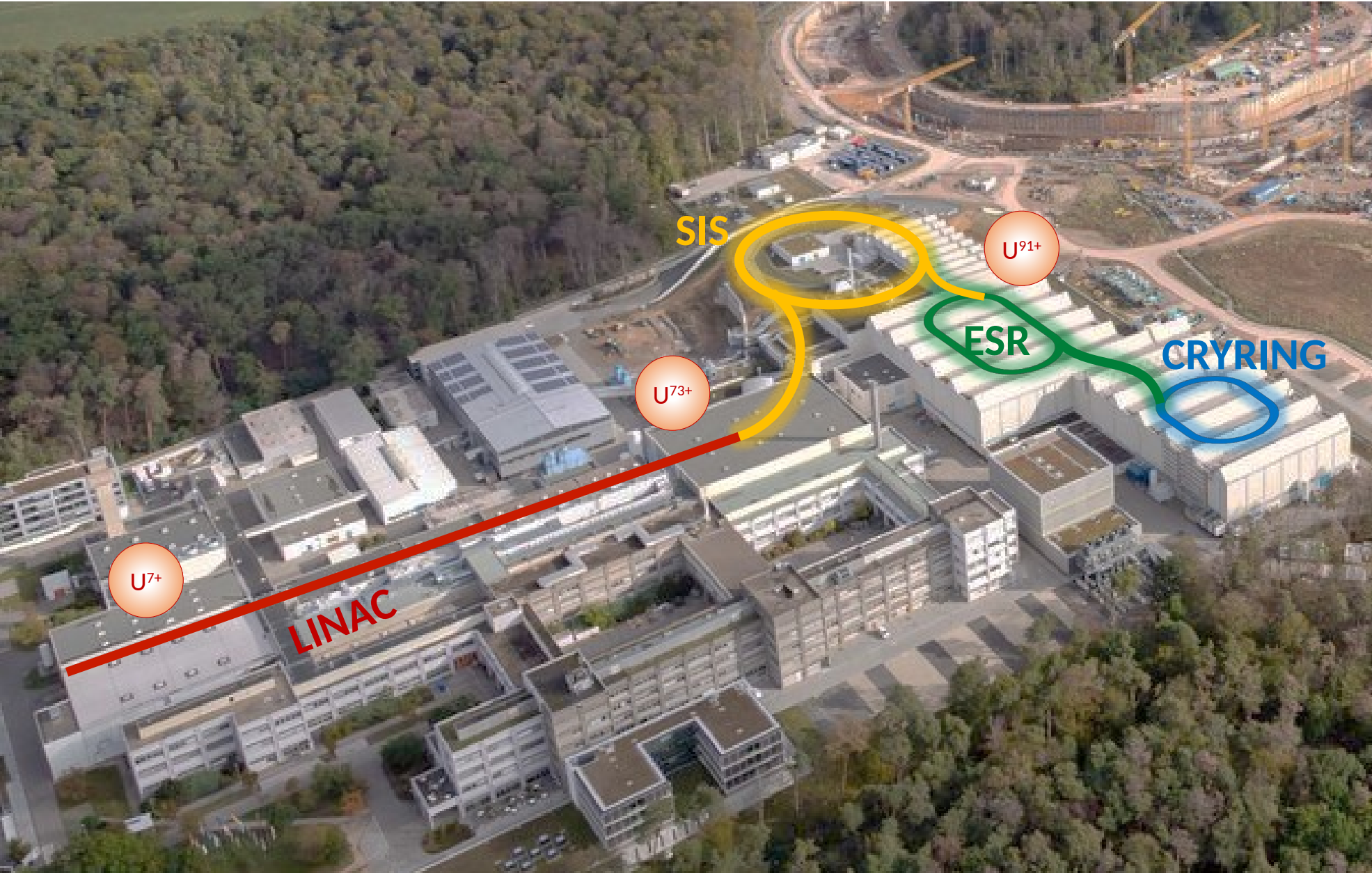
- 1 cm<sup>2</sup> effective area
- $\Delta E_{FWHM} = 40 \text{ eV} @ 60 \text{ keV}$
- Non-linearity ~ 0.2 % @ 136 keV
- 300 ns coincidence capability

Where:

**GSI cryring**



# GSI - Darmstadt: 2 weeks beamtime



**LINAC**

Accelerate to 11.4 MeV/u

**SIS**

Accelerate to 400 MeV/u

Stripper foil:

remove all but one electron

**ESR**

Decelerate to 10 MeV/u

**CRYRING**

Stored ion beam

# Experimental configuration

## Electron cooler

- Superimpose electron and ion beam
- Reduce momentum spread
- $U^{91+} + e^- \rightarrow U^{90+} + \gamma$

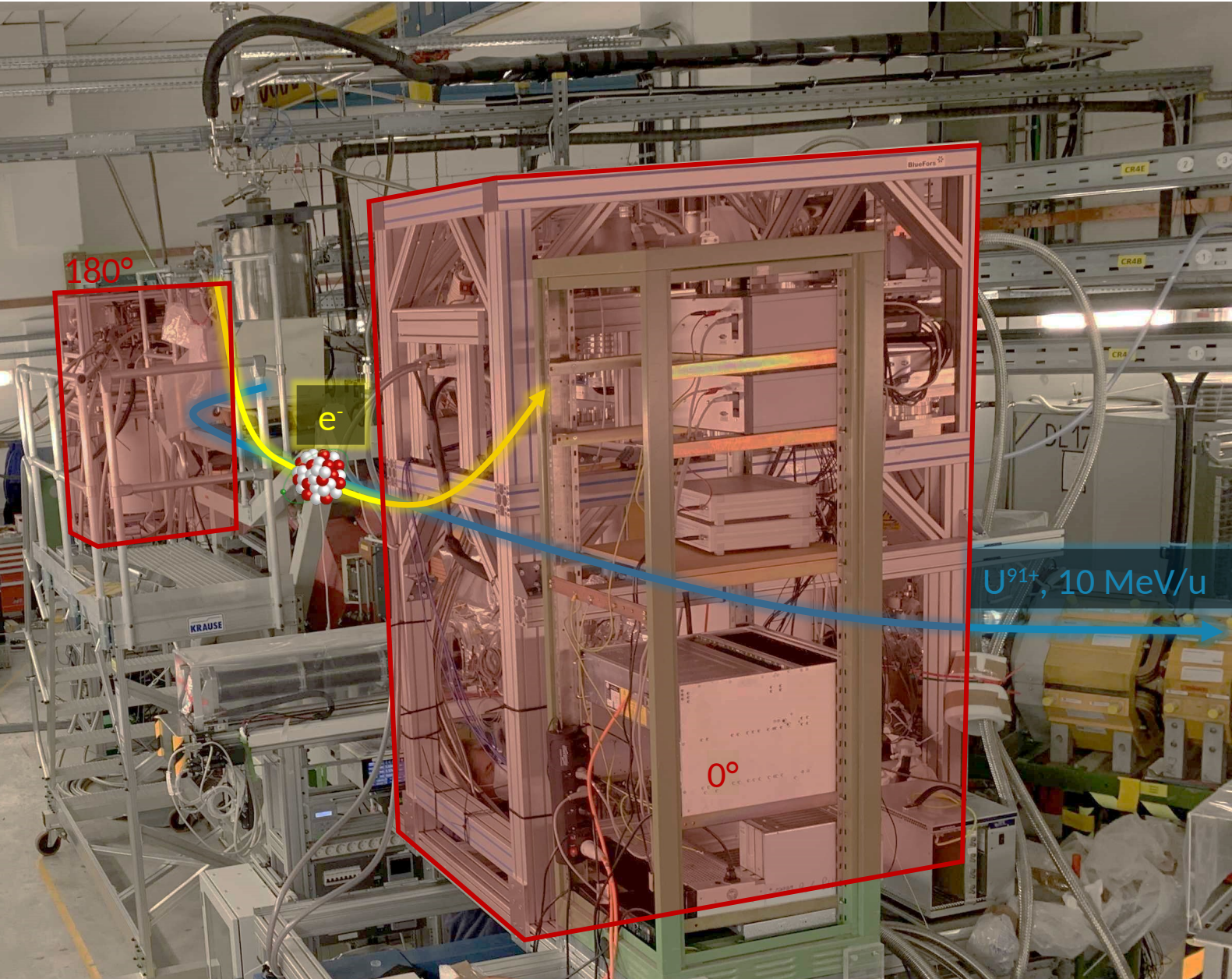
## 2 detector systems

- At  $0^\circ$  and  $180^\circ$  scattering angle
- 13 keV red shift @  $180^\circ$
- 15 keV blue shift @  $0^\circ$
- intrinsic Doppler shift correction

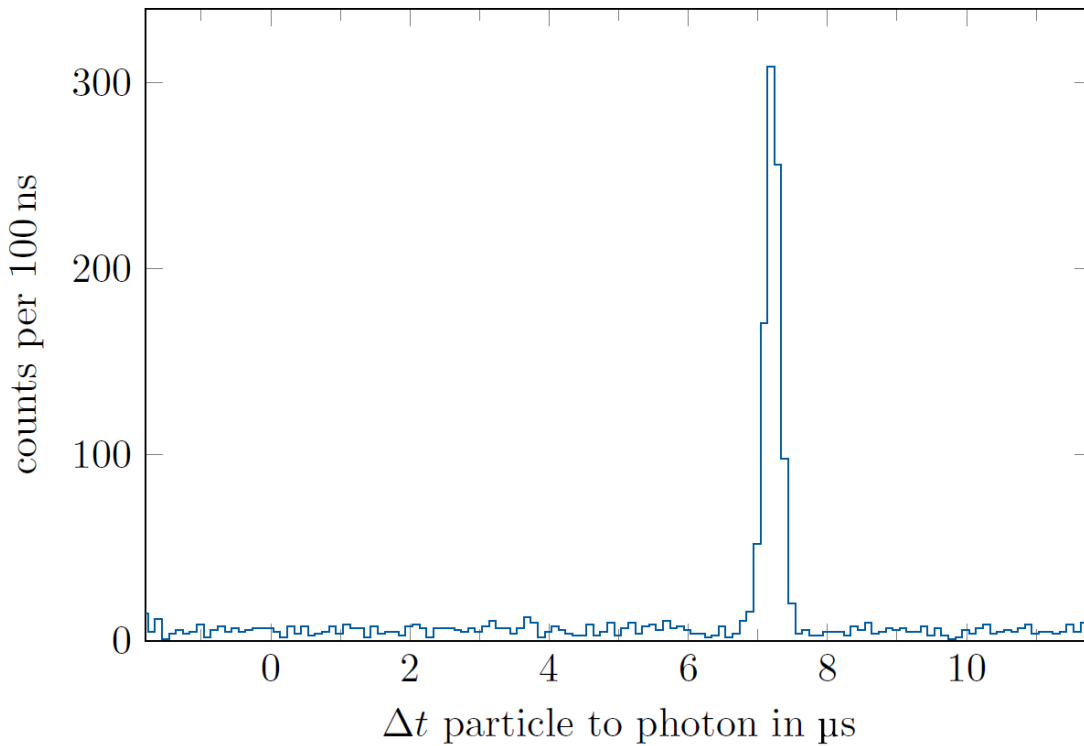
## 2x maXs100

- In total 102/128 pixels operated
- Energy resolution
  - 80 eV FWHM @ 122 keV
  - 60 eV FWHM @ 122 keV

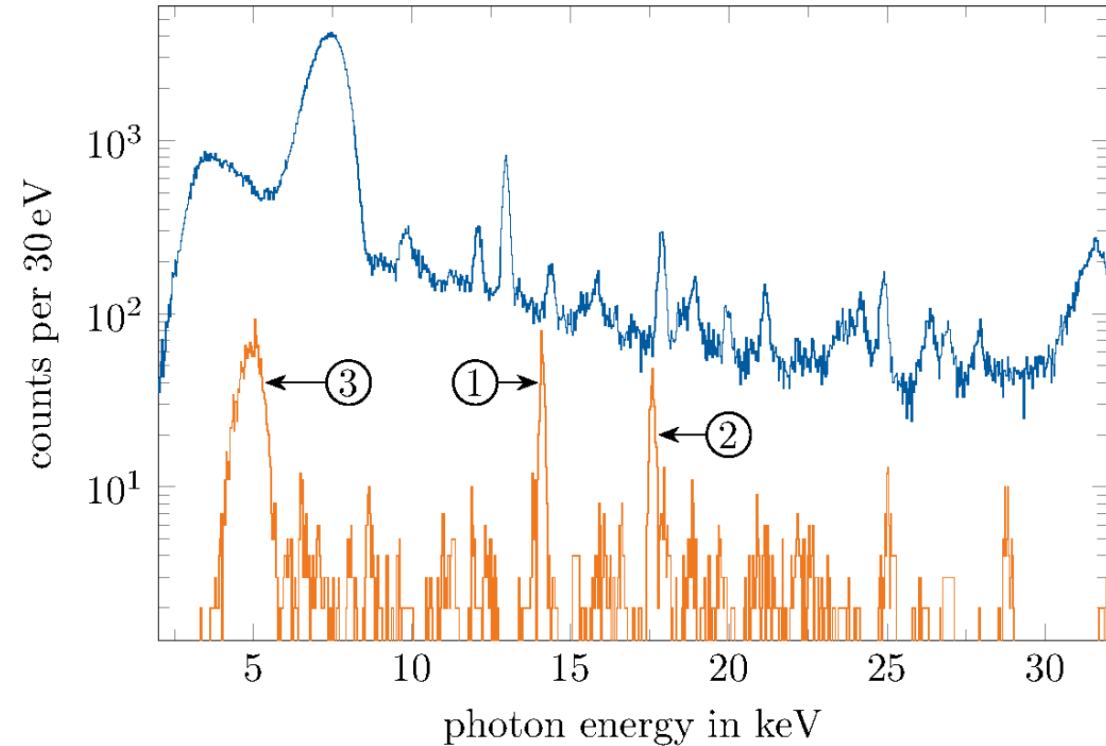
## Composite calibration source



# Highly ionized heavy ions - U<sup>90+</sup>



Photons emitted by ions undergoing radiative recombination with the cooler electrons show a **fixed time delay** wrt the signal due to the ions detection

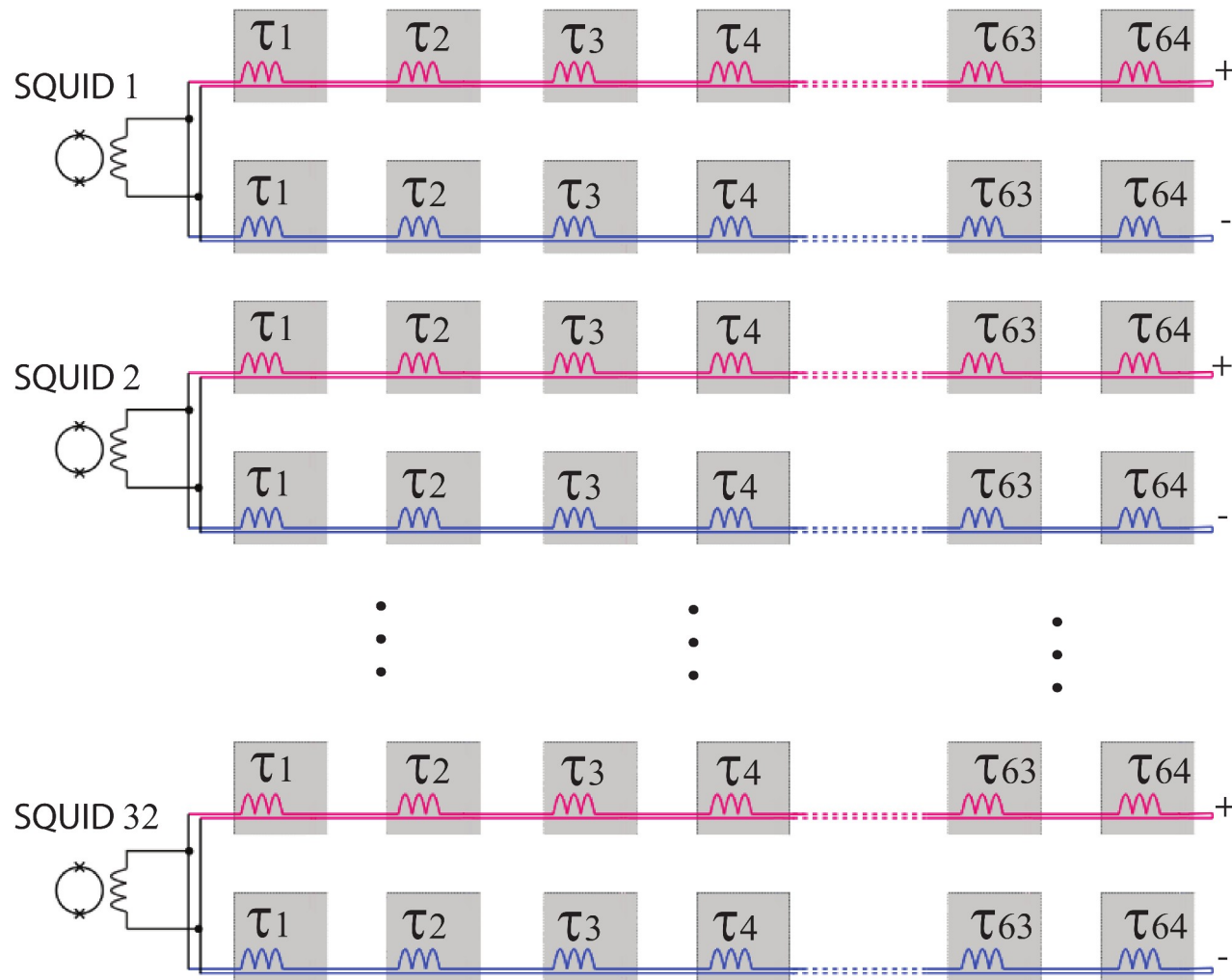


Transitions can be clearly observed/identified

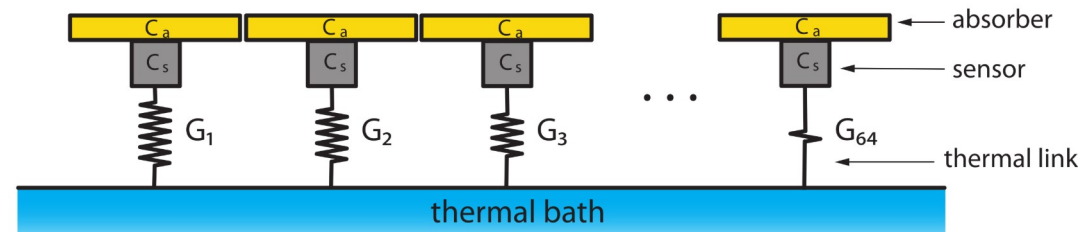
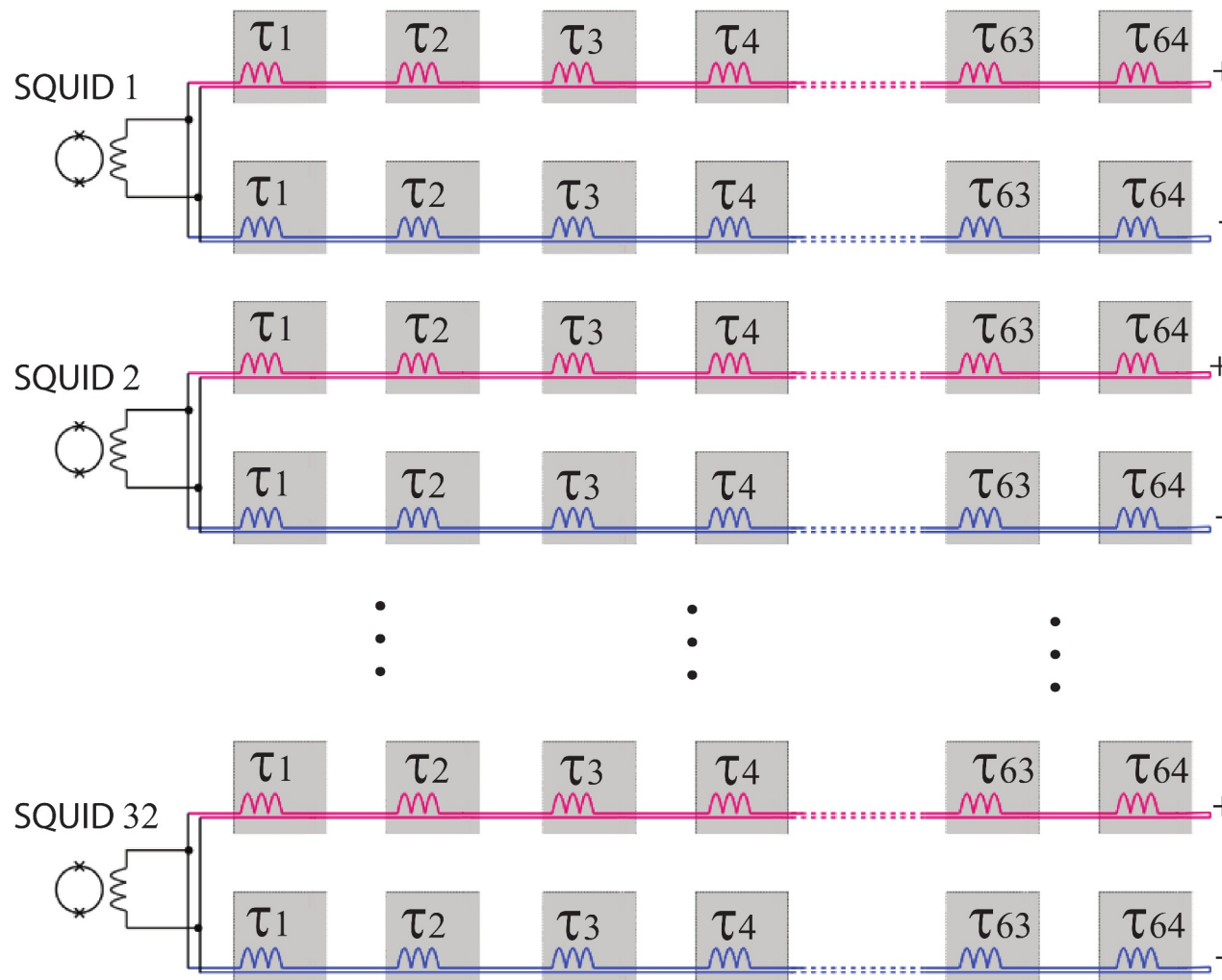
Analysis still on-going

32 readout channels for 4000 pixels

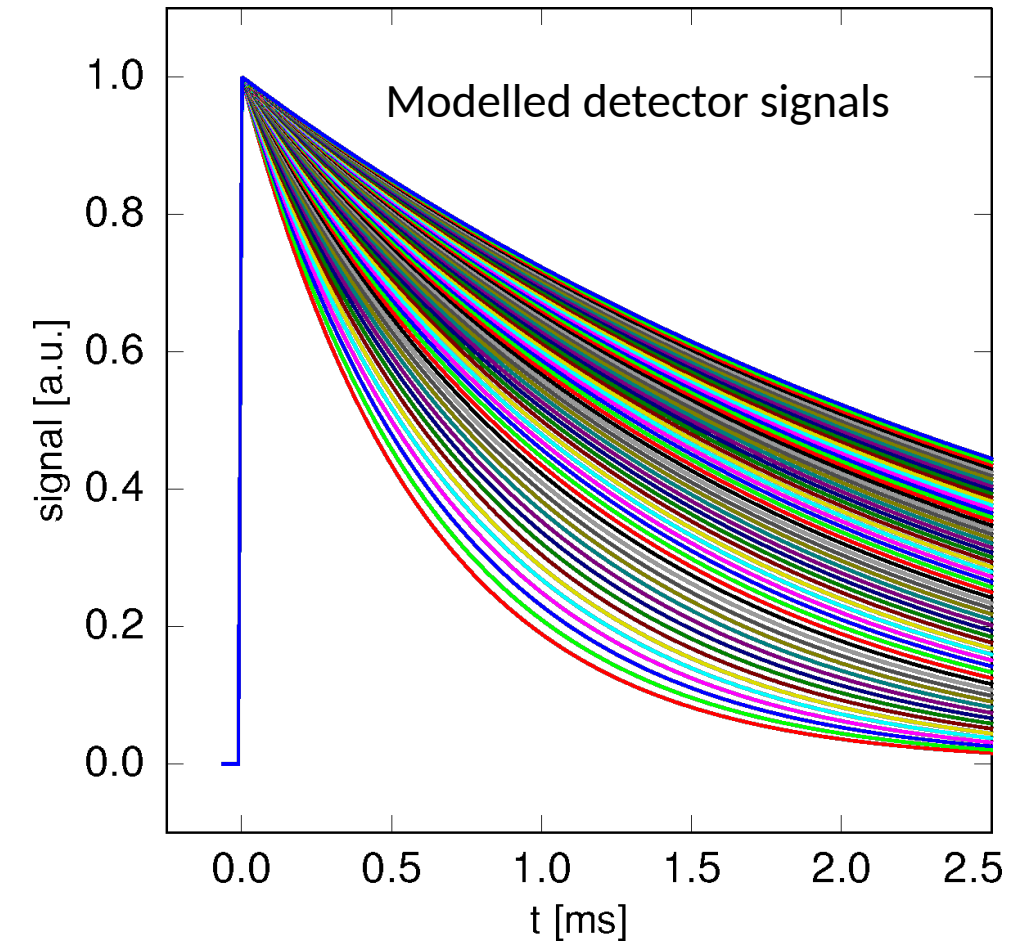
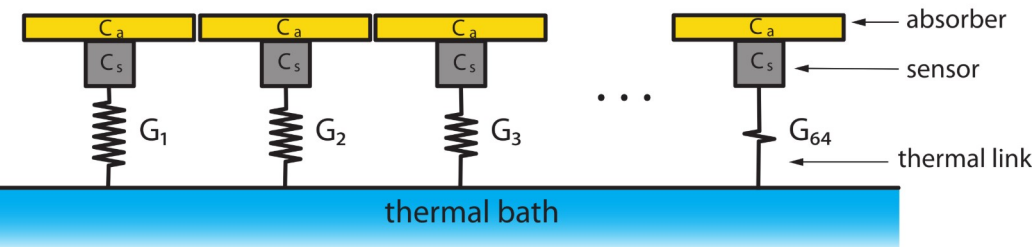
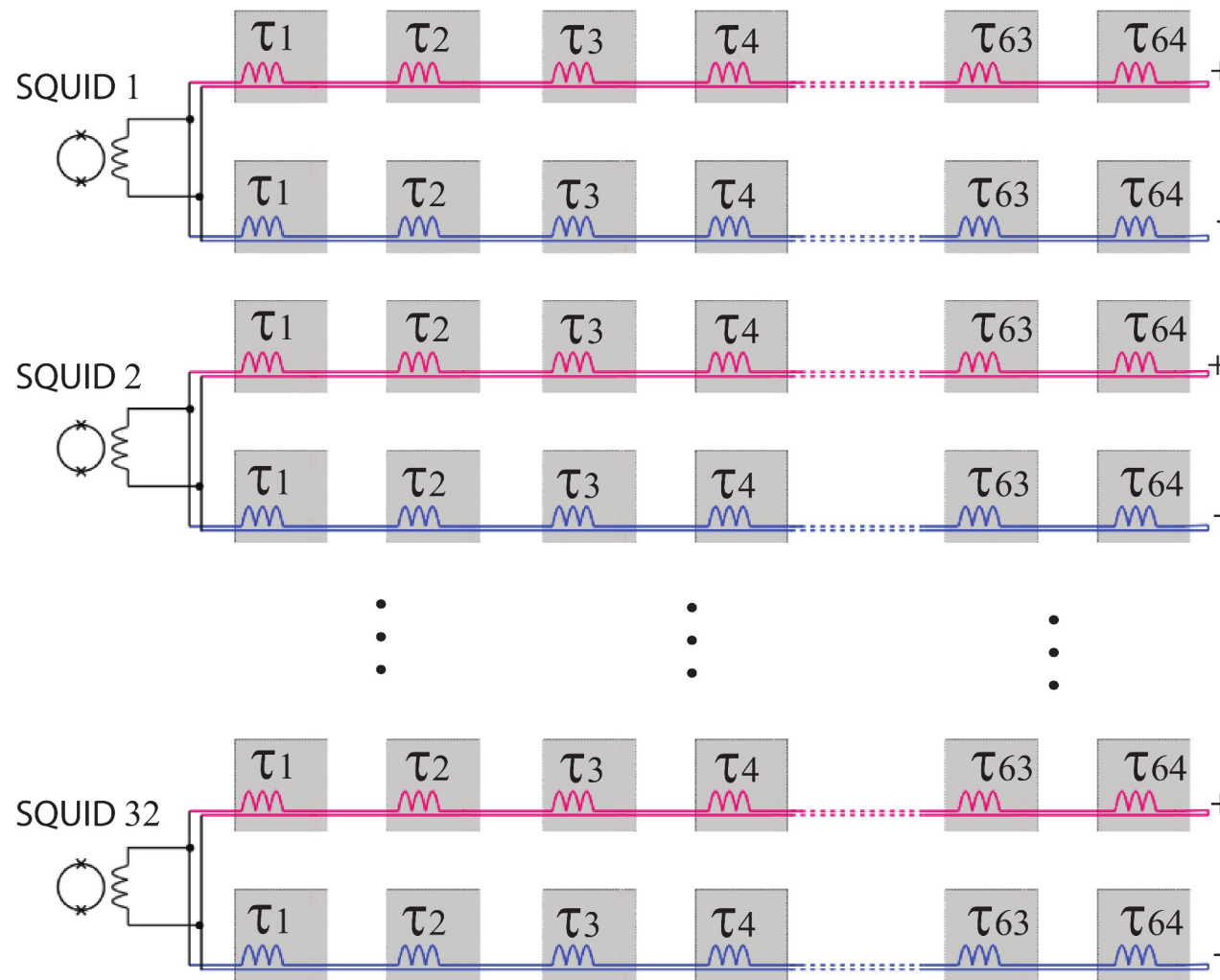
# MOCCA - readout scheme



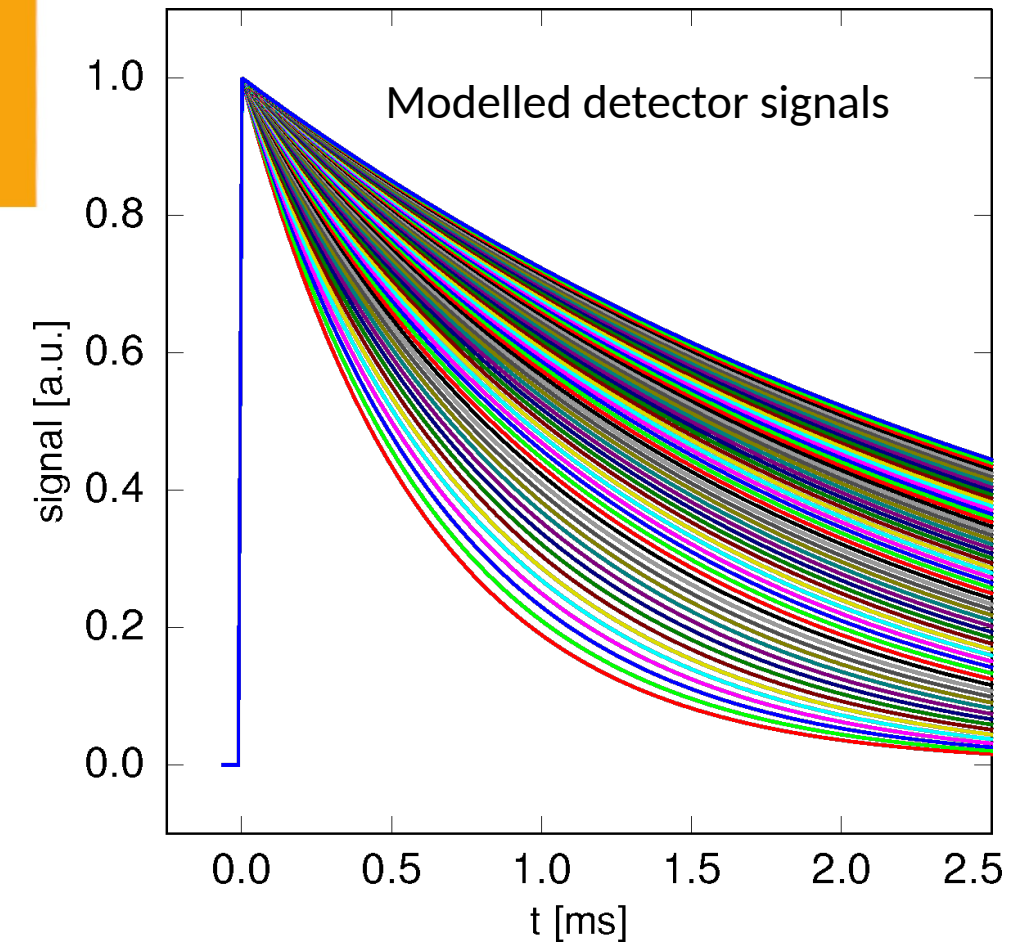
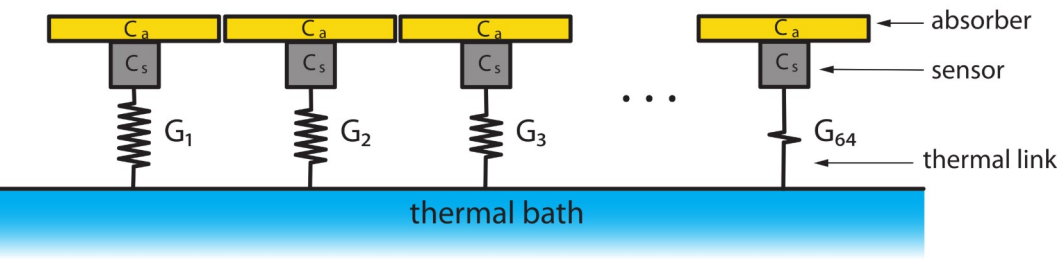
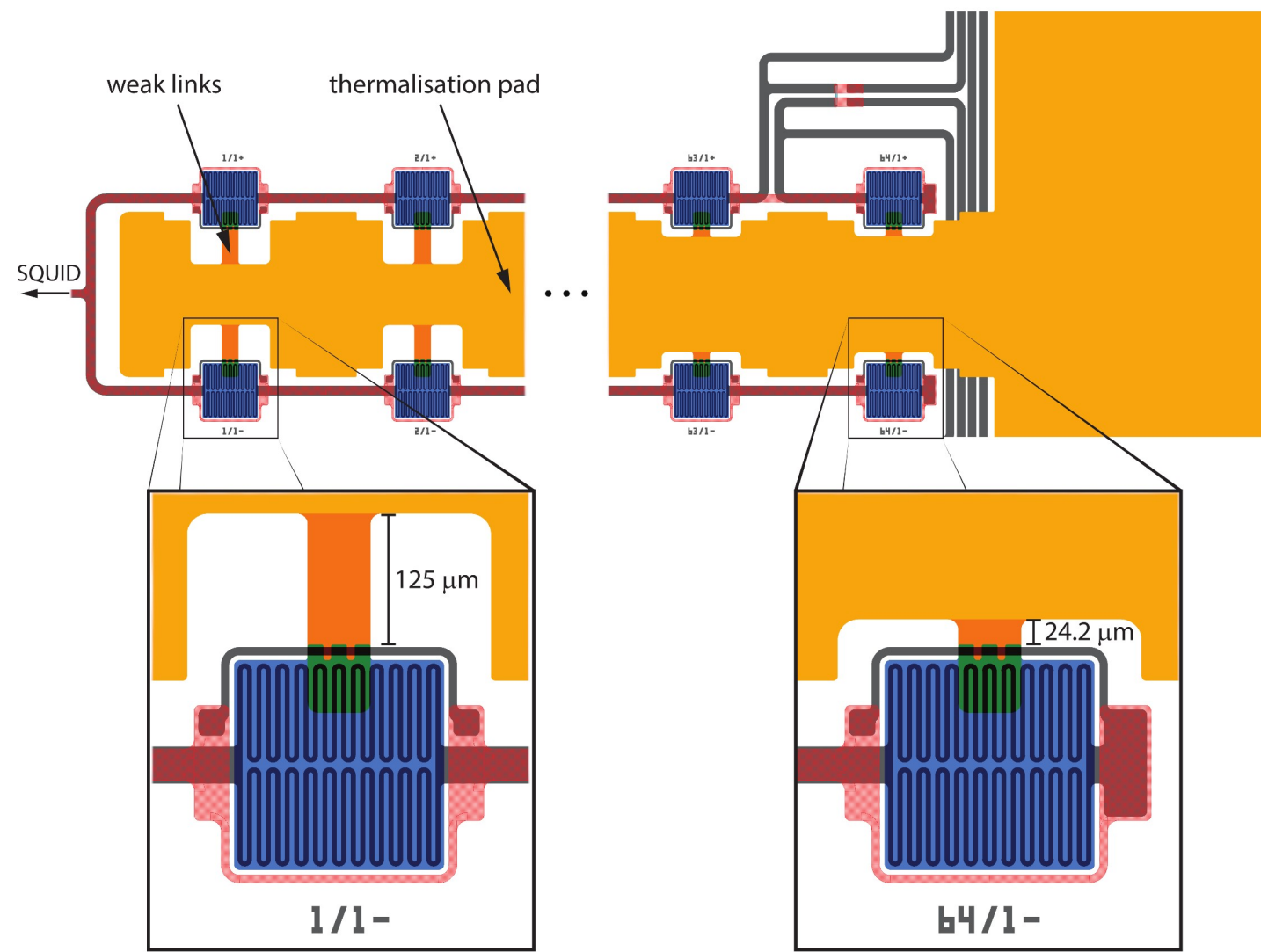
# MOCCA - readout scheme



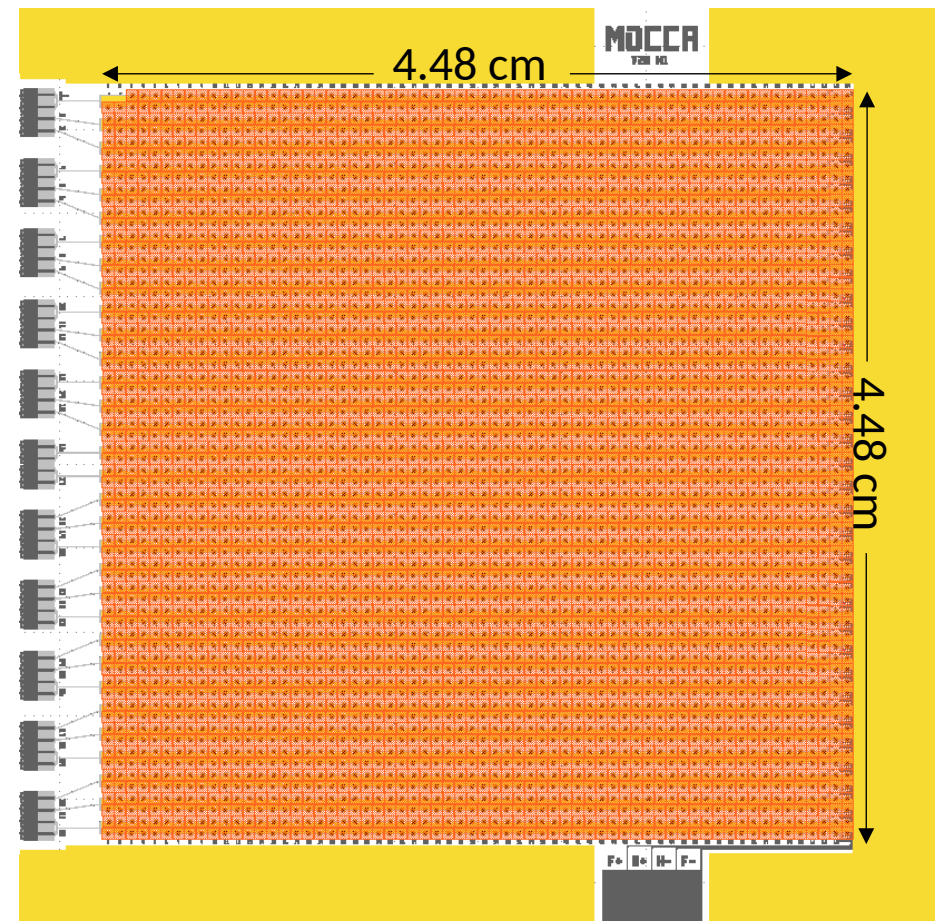
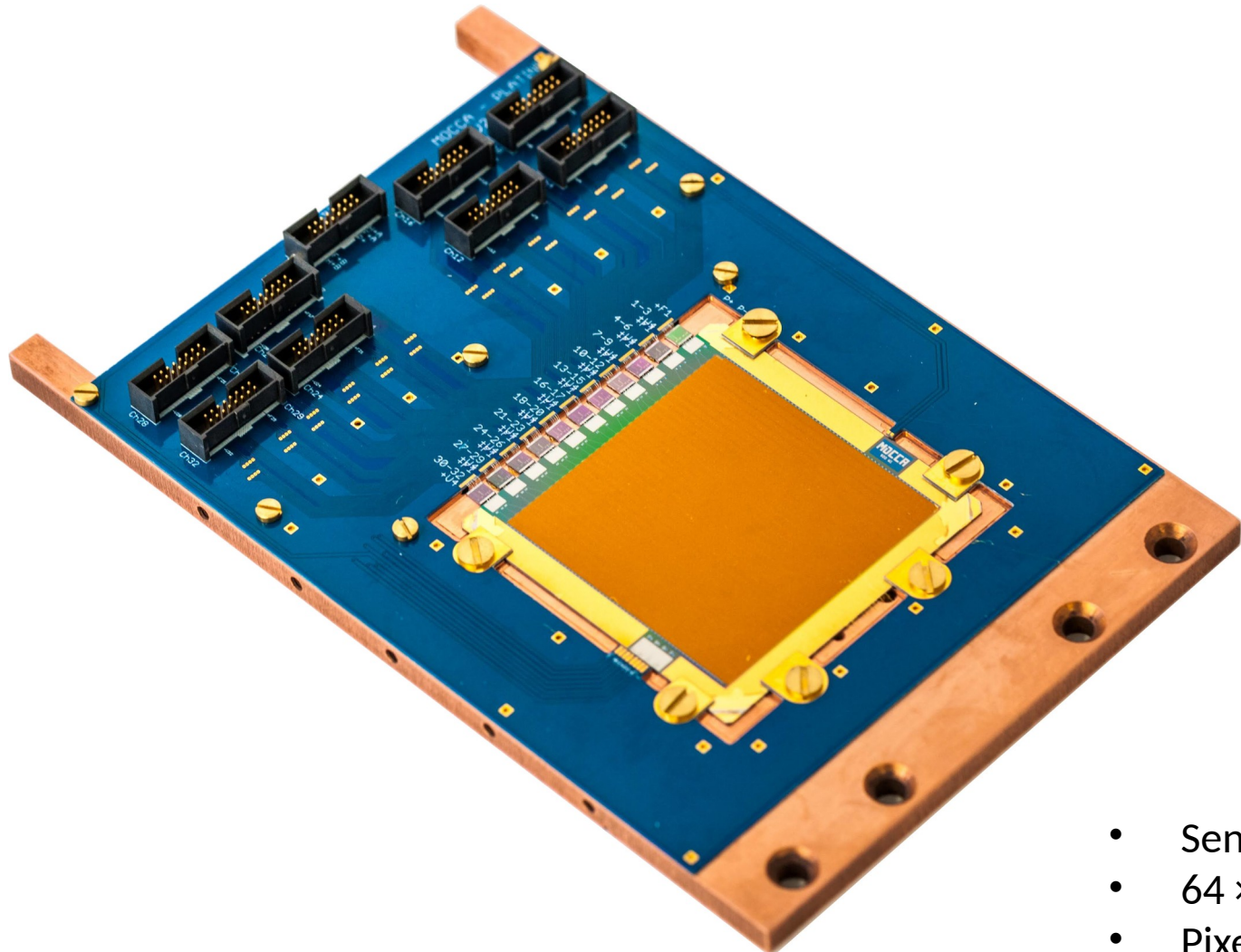
# MOCCA - readout scheme



# MOCCA - readout scheme



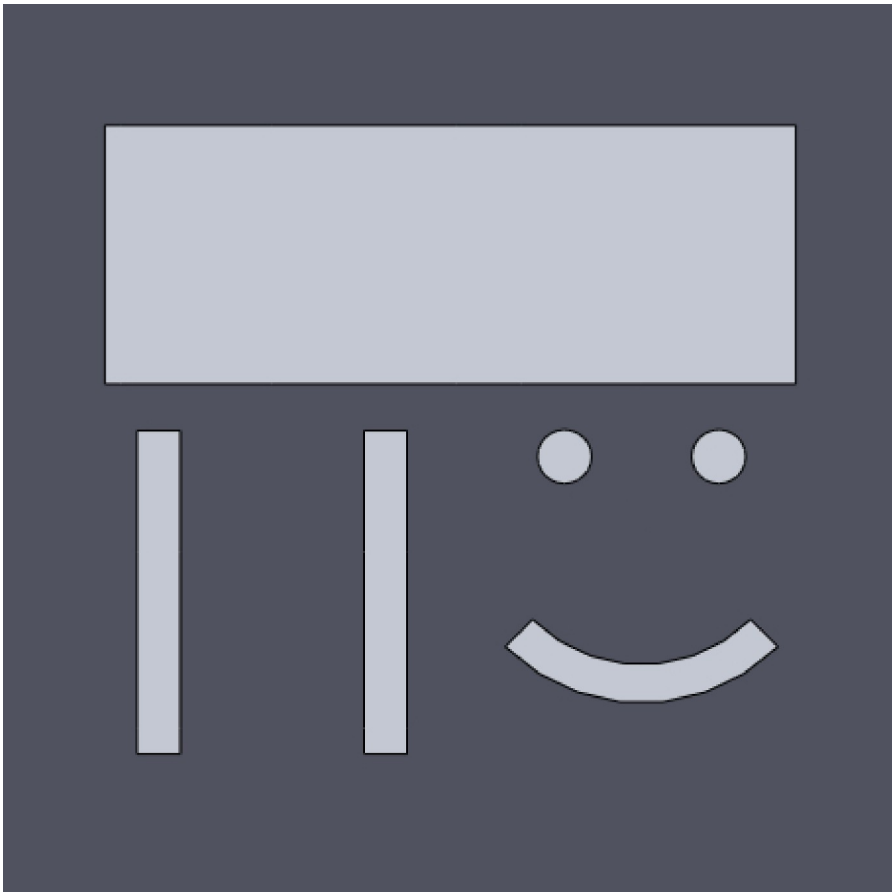
# MOCCA - a 4k-Pixel Molecular Camera



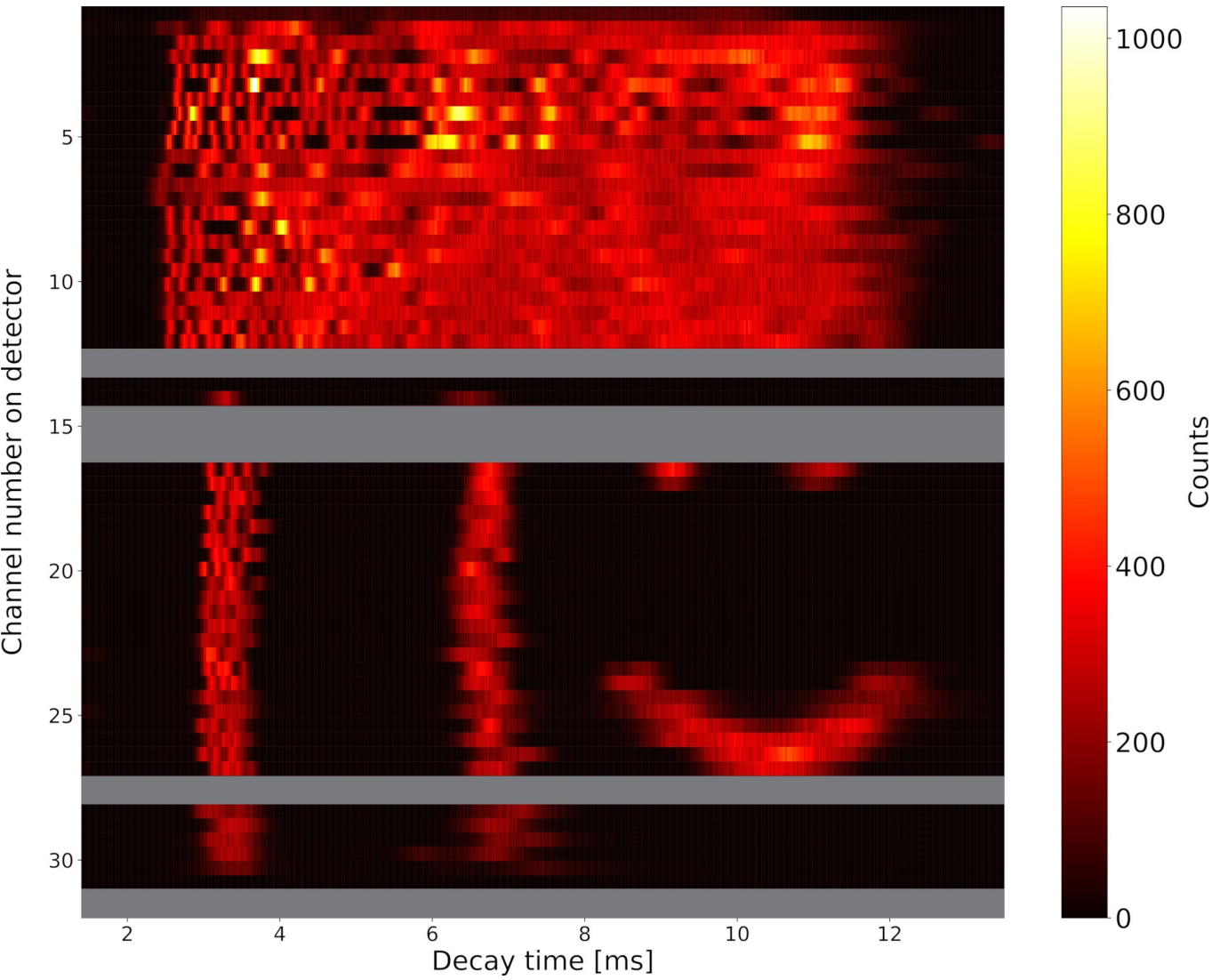
- Sensitive area:  $4.48 \text{ cm} \times 4.48 \text{ cm}$
- $64 \times 64$  pixel
- Pixel size:  $700 \mu\text{m} \times 700 \mu\text{m}$
- Readout by 32 two-stage SQUID channels

# MOCCA - First characterization

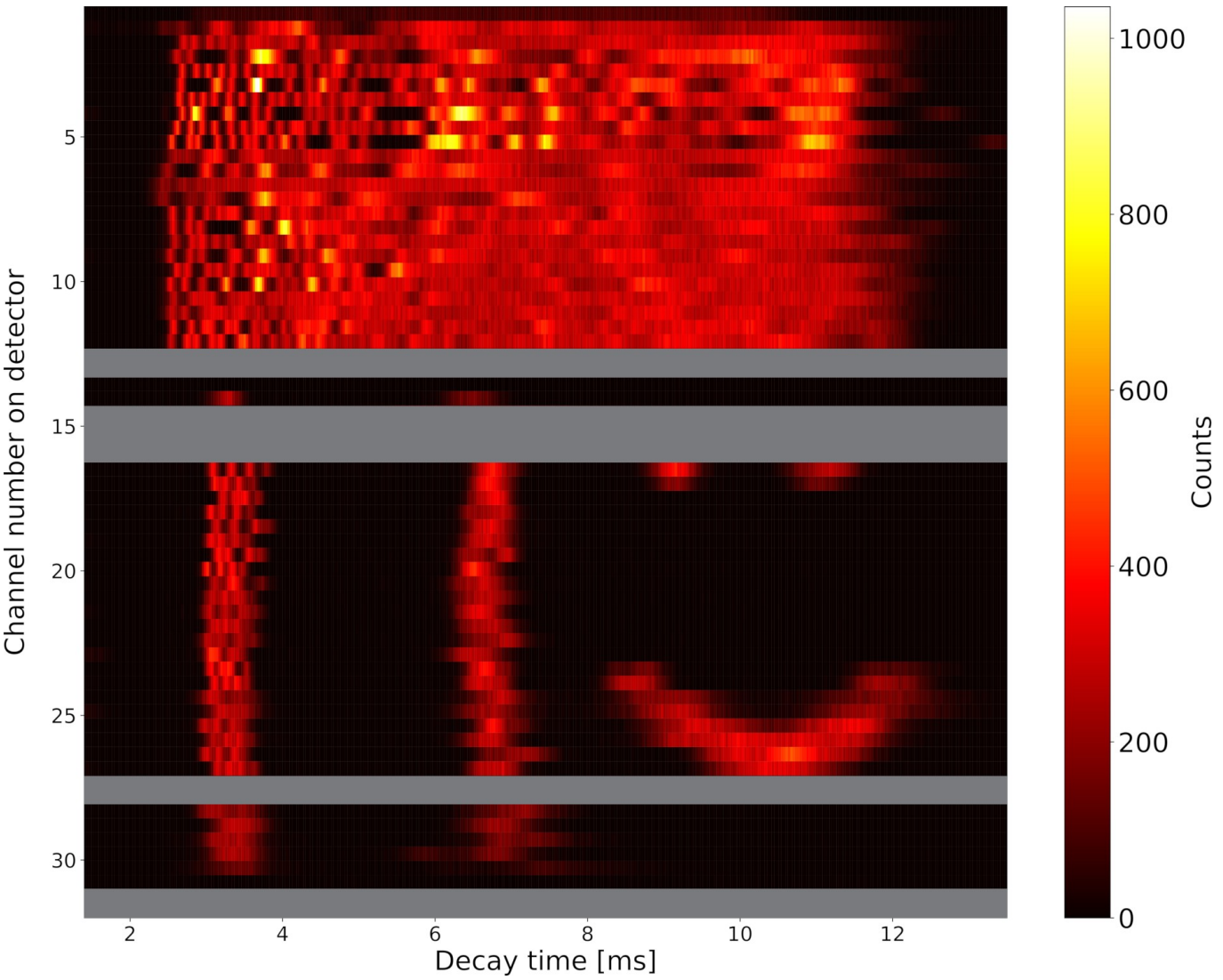
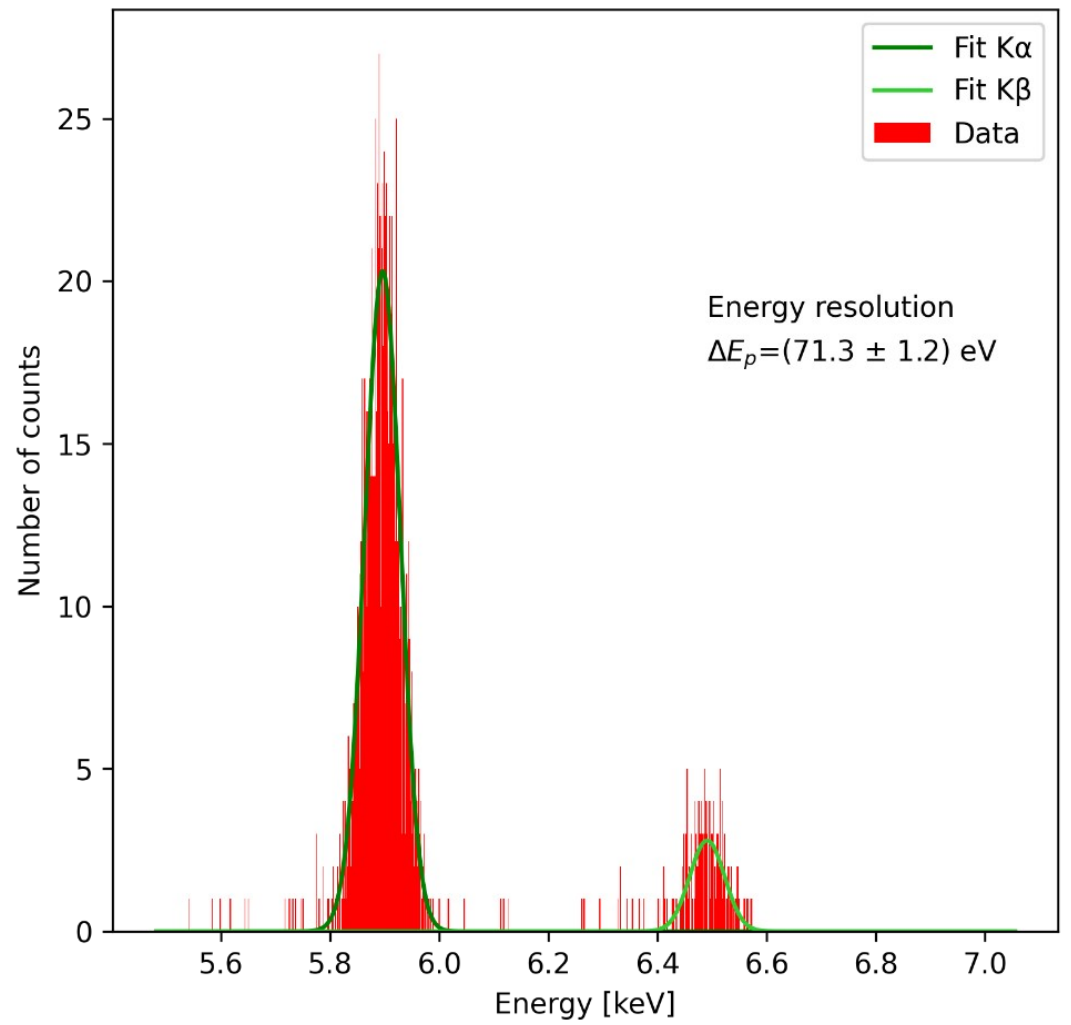
Mask



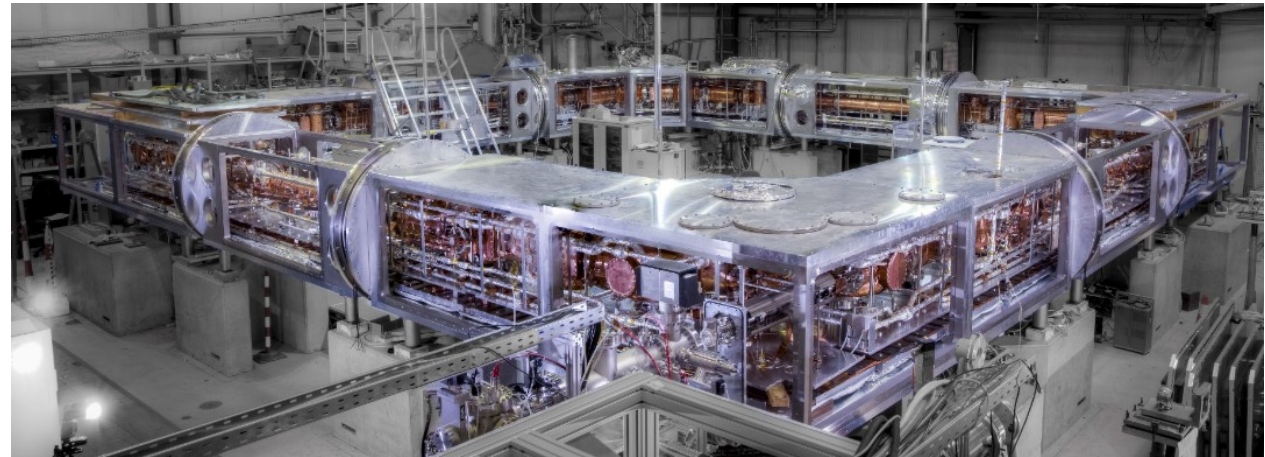
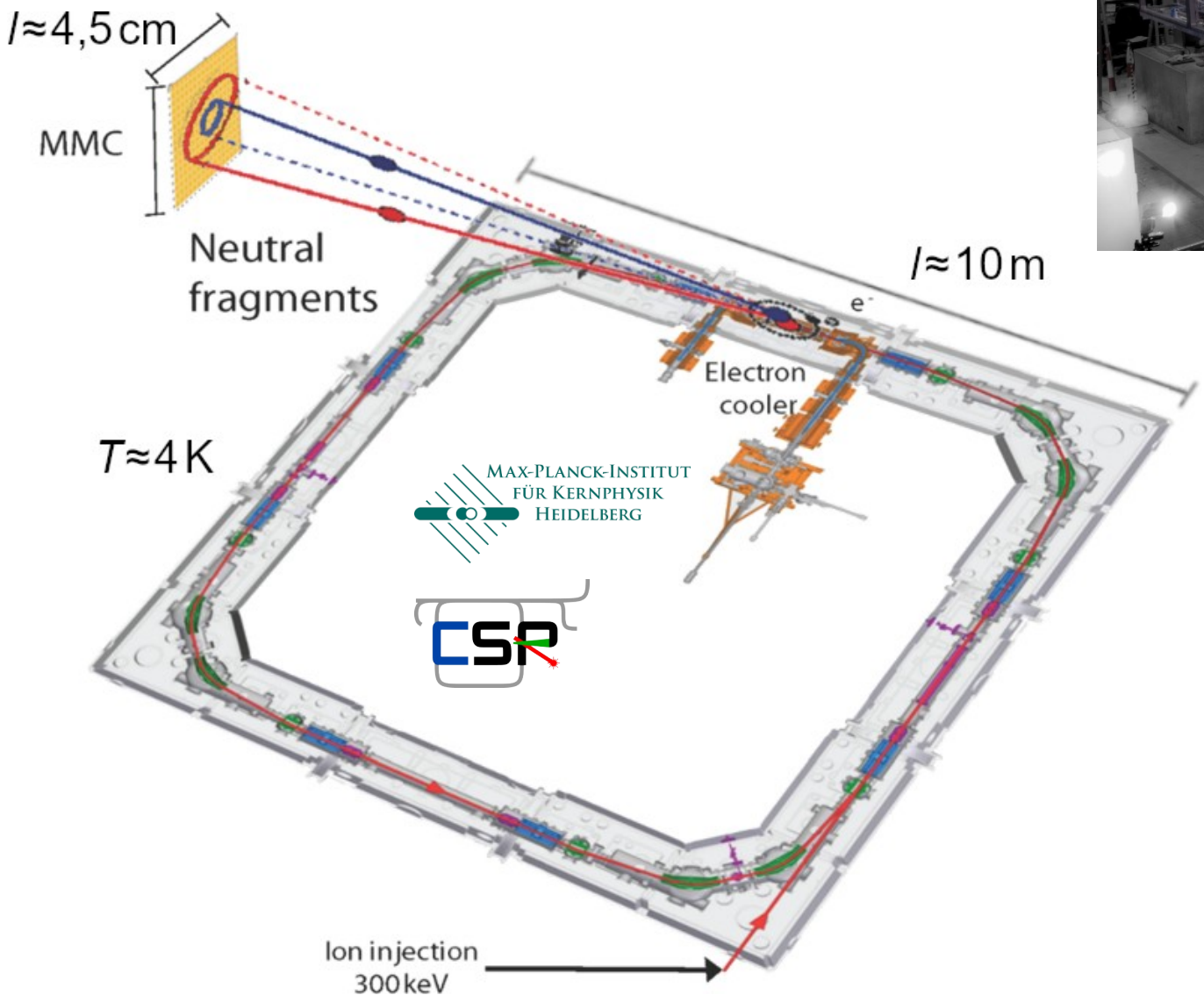
# MOCCA - First characterization



# MOCCA - First characterization



# MOCCA - Application



## Detector requirements:

- High energy resolution → fragment masses

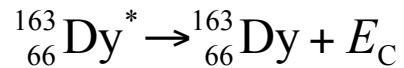
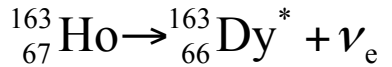
$$m_A \approx \frac{E_{\text{kin}, A}}{E_{\text{kin}, \text{ABC}}} m_{\text{ABC}} +$$

- Position sensitivity
- Large area
- Time resolution of a few ns
- No dead layer

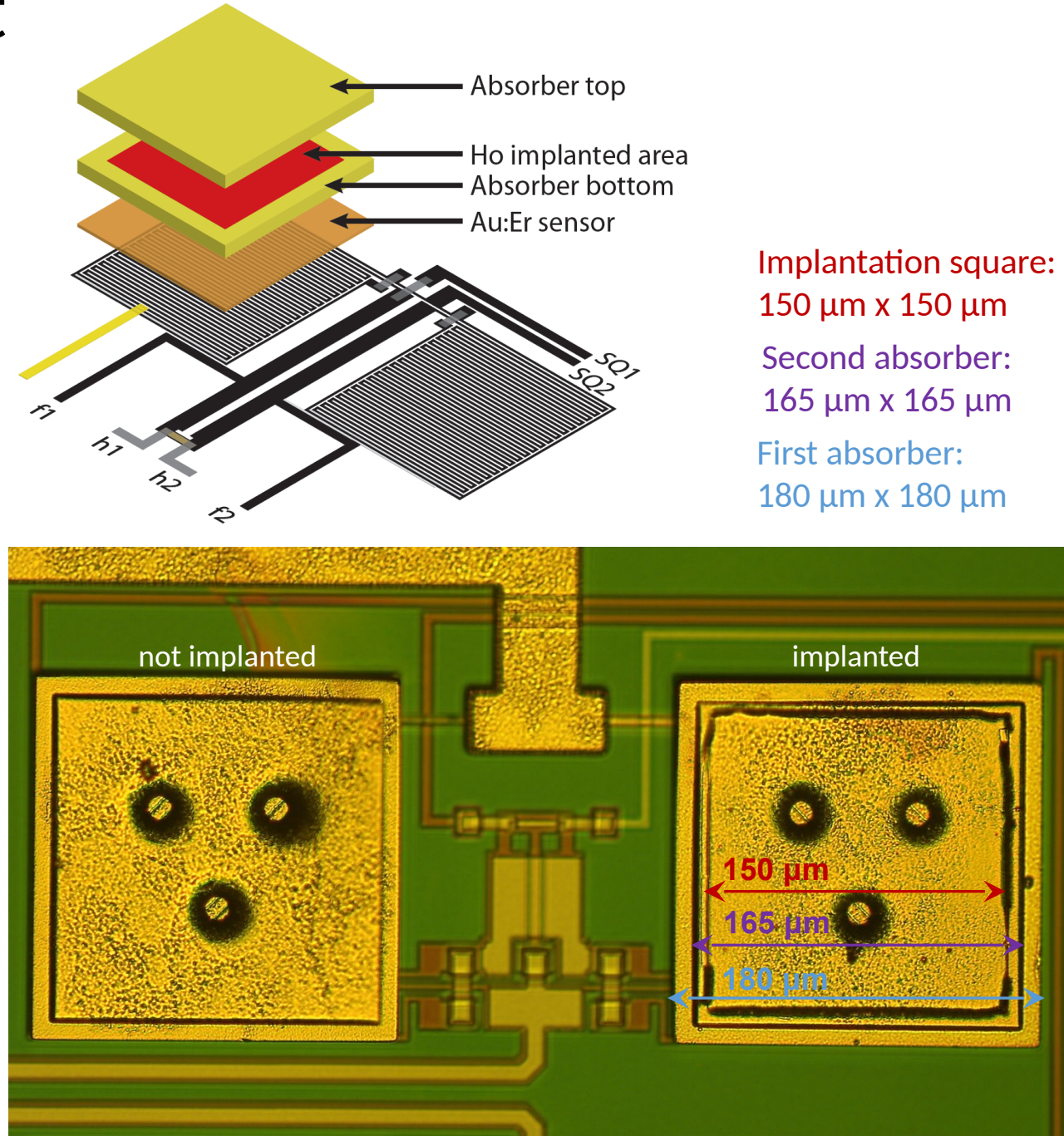
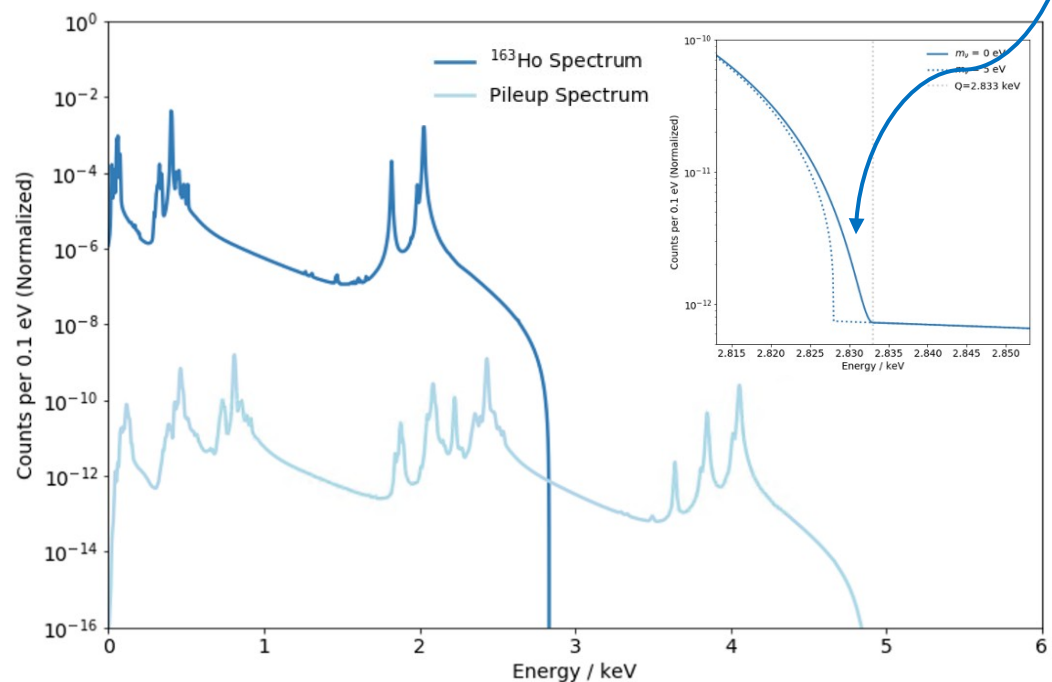
} 3D fragment imaging

# MMCs for the ECHo experiment

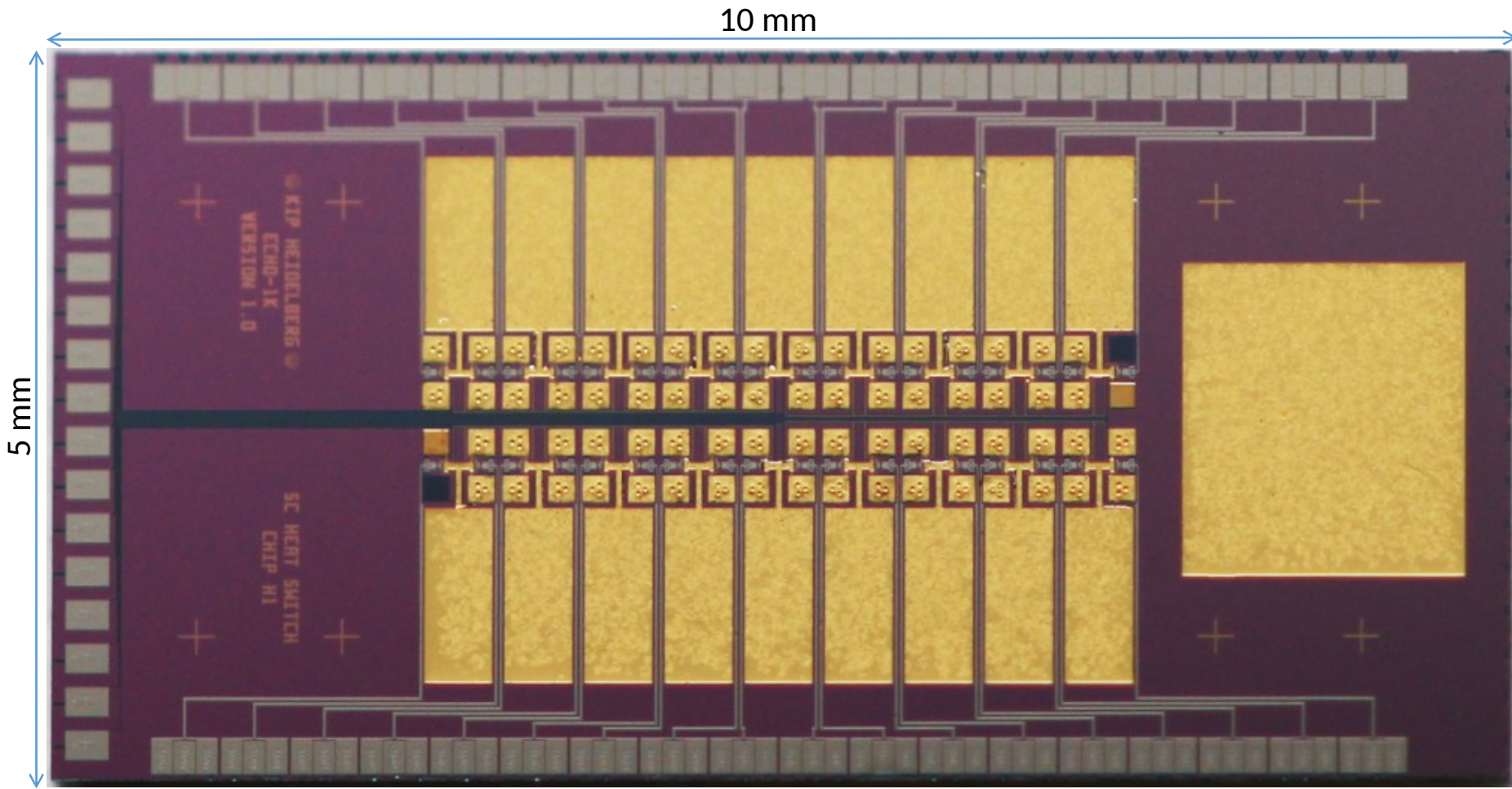
ECHO uses large arrays of MMCs with enclosed  $^{163}\text{Ho}$



Fraction of events  
in the last eV  $\sim 10^{-12}$



# ECHO-1k array



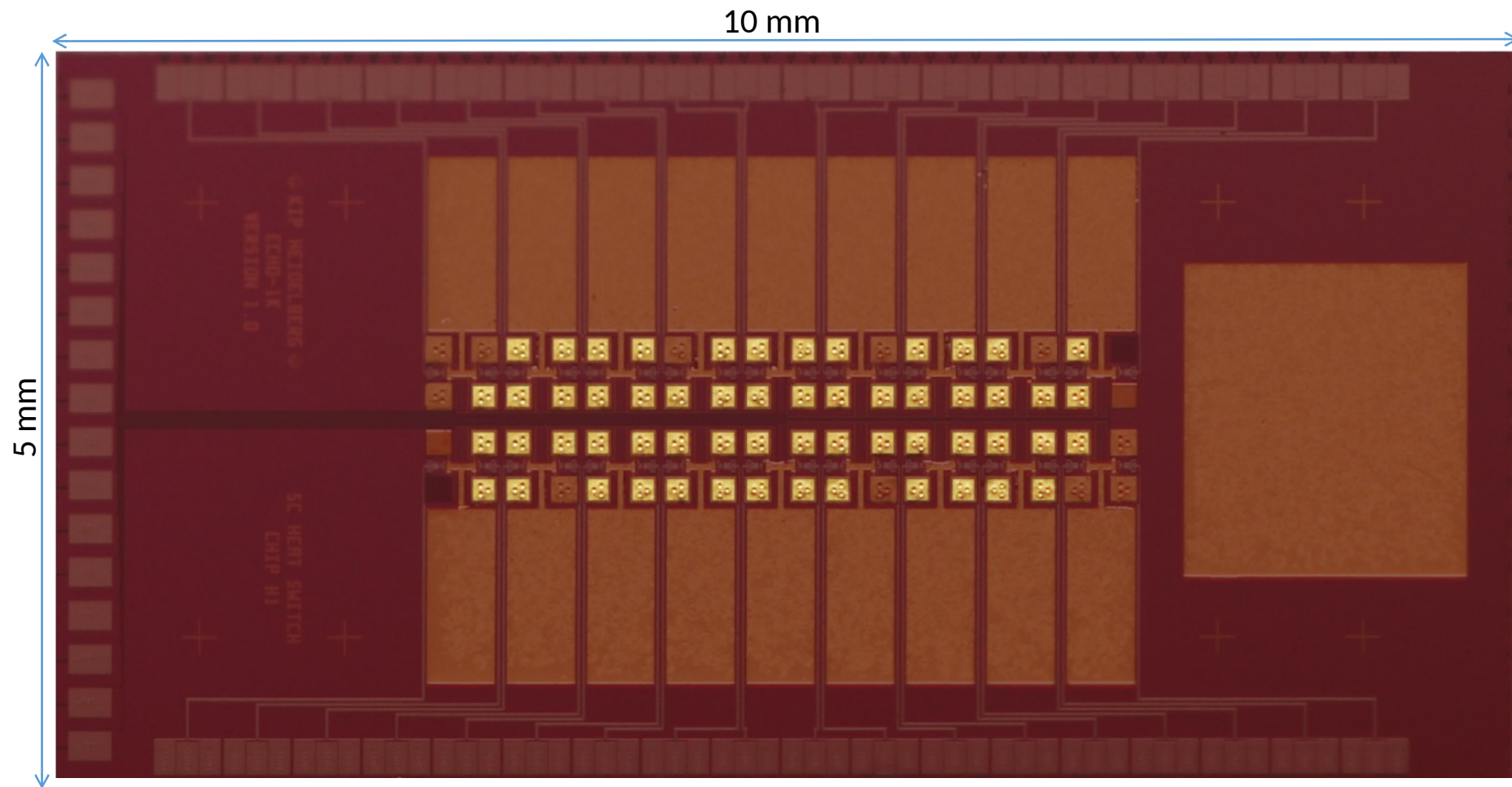
64 pixels can be loaded with  $^{163}\text{Ho}$   
+ 2 temperature pixels  
+ 2 detectors for diagnostics

Design performance:

$\Delta E_{\text{FWHM}} \sim 5 \text{ eV}$

$\tau_r \sim 90 \text{ ns}$  (single channel readout)

# ECHO-1k array



64 pixels can be loaded with  $^{163}\text{Ho}$   
+ 2 temperature pixels  
+ 2 detectors for diagnostics

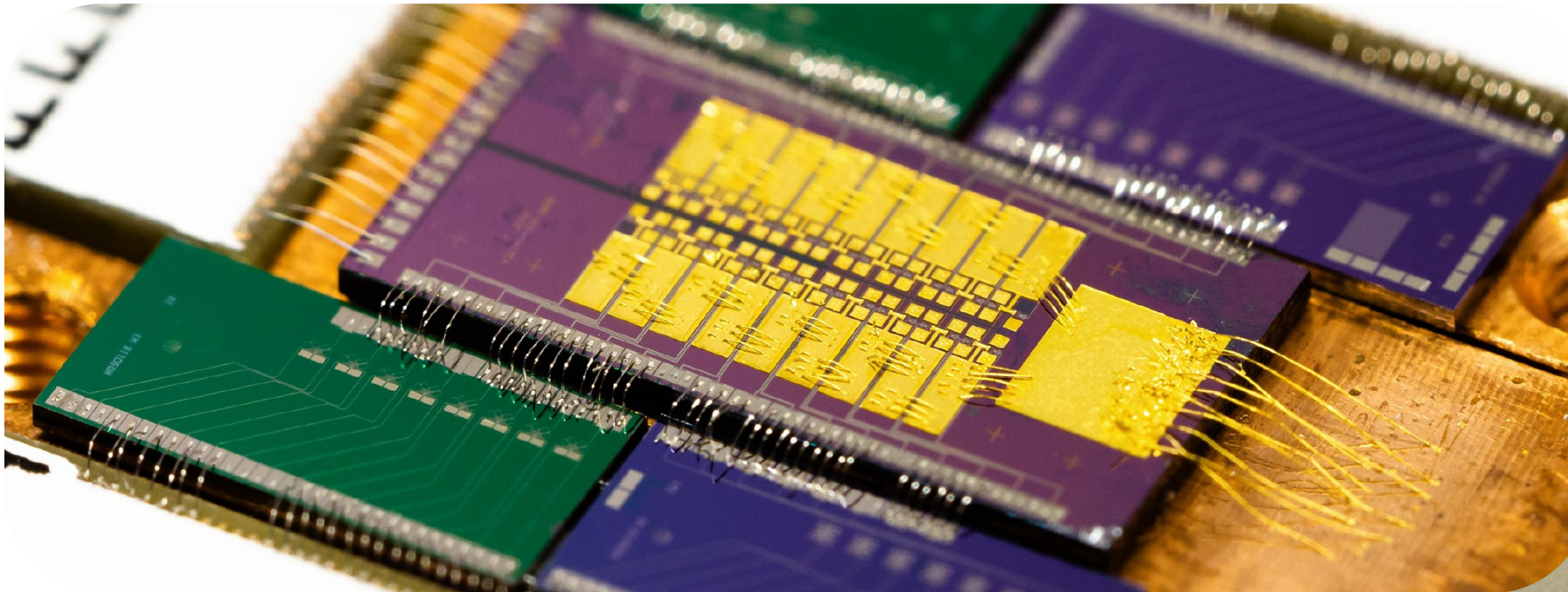
Design performance:

$\Delta E_{\text{FWHM}} \sim 5 \text{ eV}$

$\tau_r \sim 90 \text{ ns}$  (single channel readout)

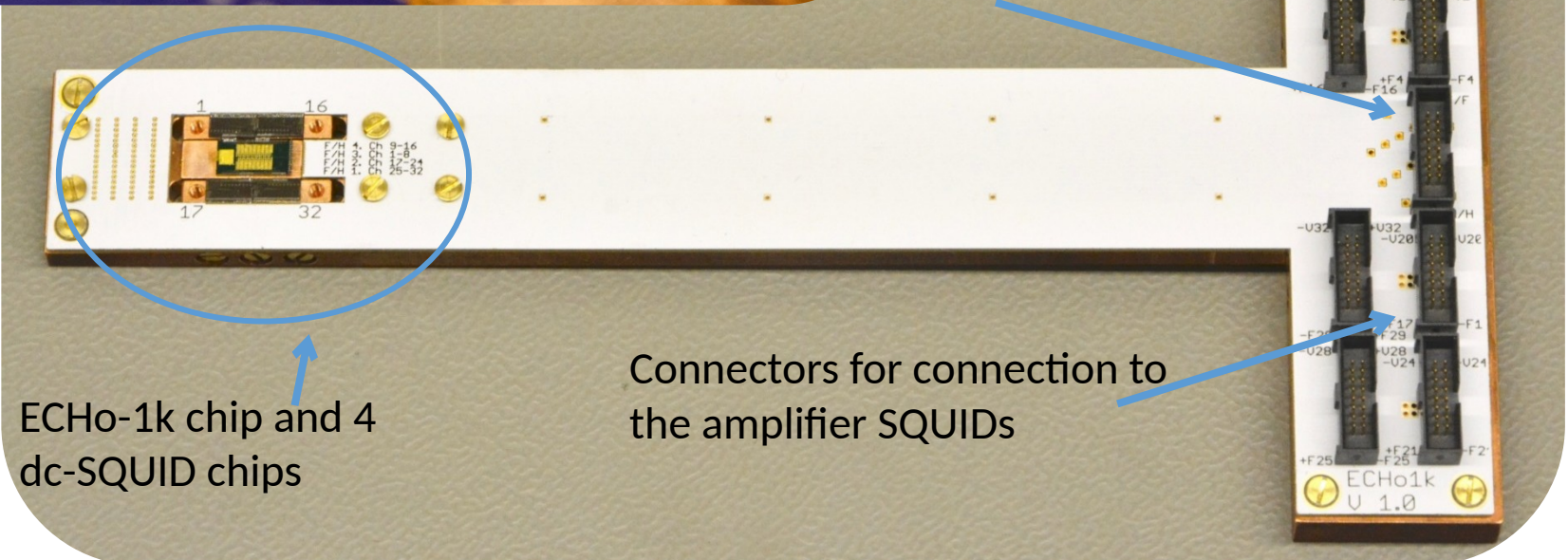
- ✓ presence of non-implanted chips for in-situ background determination

# ECHo-1k readout

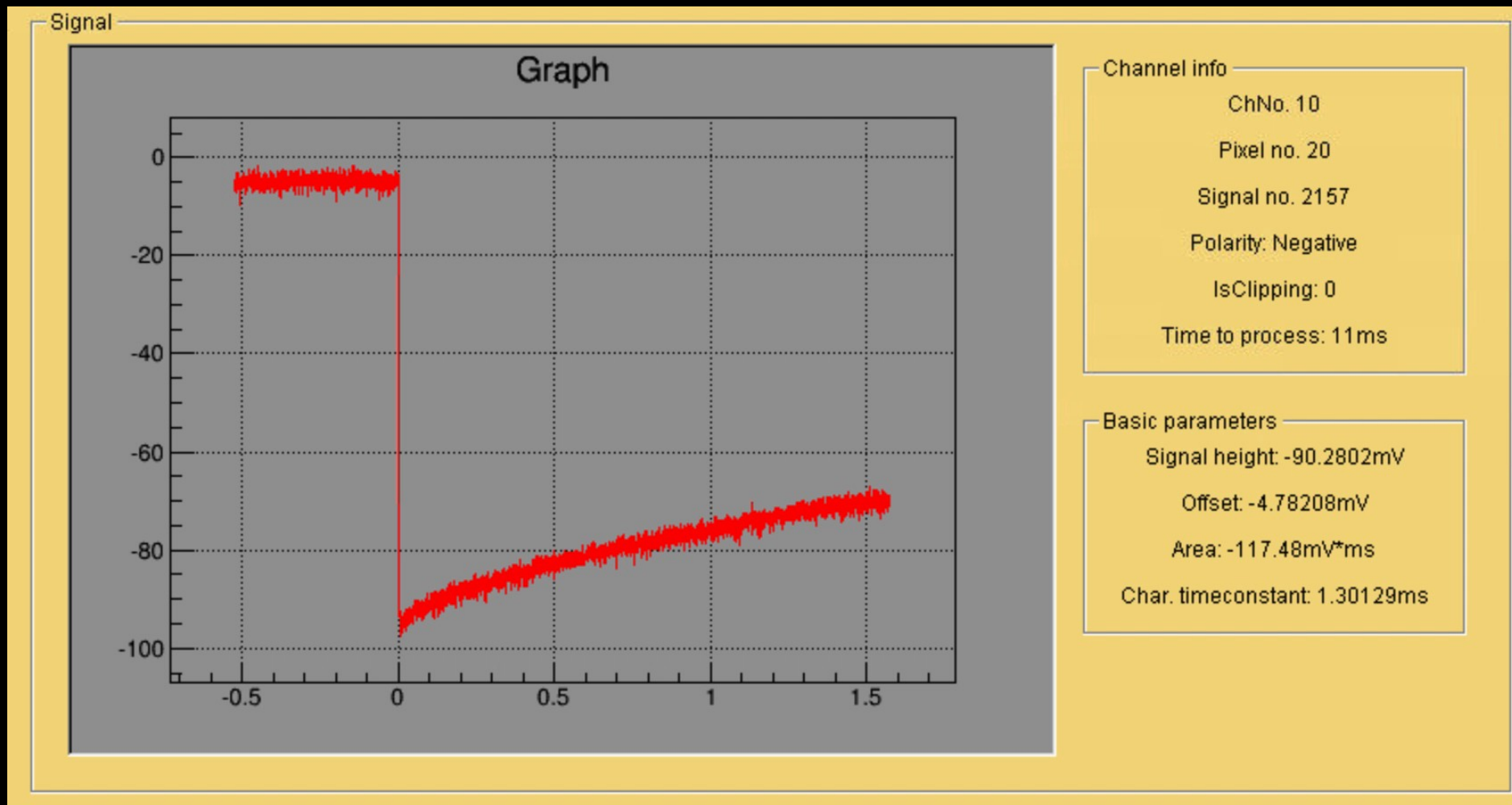


## ECHo-1k chip-Au implanted @RISIKO

- High purity  $^{163}\text{Ho}$  source  
→ activity per pixel  $a \approx 1 \text{ Bq}$
- 4 Front-end chips each with 8 dc-SQUIDs for parallel readout



# ECHO-1k data - Live!



# Conclusions

## metallic magnetic calorimeters

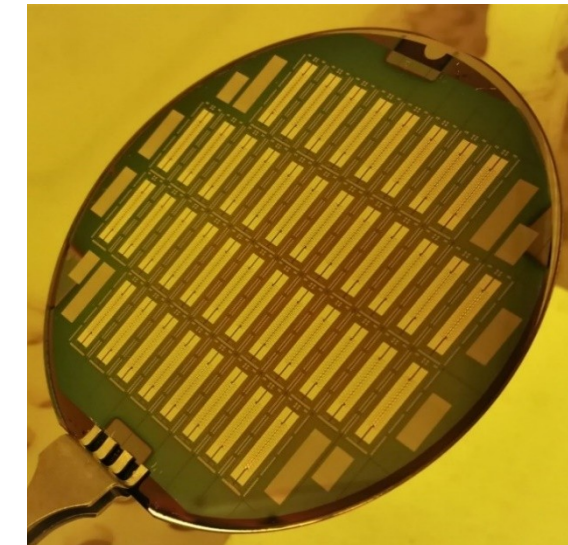
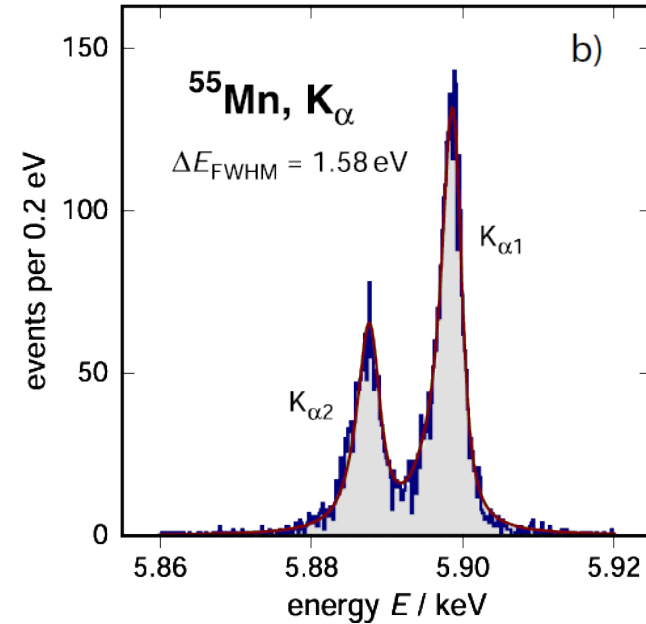
- are versatile low temperature detectors
- high resolution for all kinds of particles
- wide range of energies
- impressive resolving power

## micro-fabrication works

- detector arrays reliably fabricated
- designed performance is reached
- reproducibility of performance

## multiplexing

- demonstrated principles



# Conclusions

## metallic magnetic calorimeters

- are versatile low temperature detectors
- high resolution for all kinds of particles
- wide range of energies
- impressive resolving power

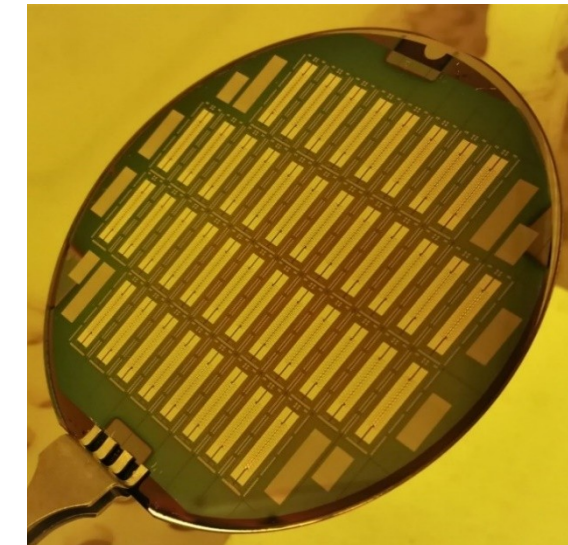
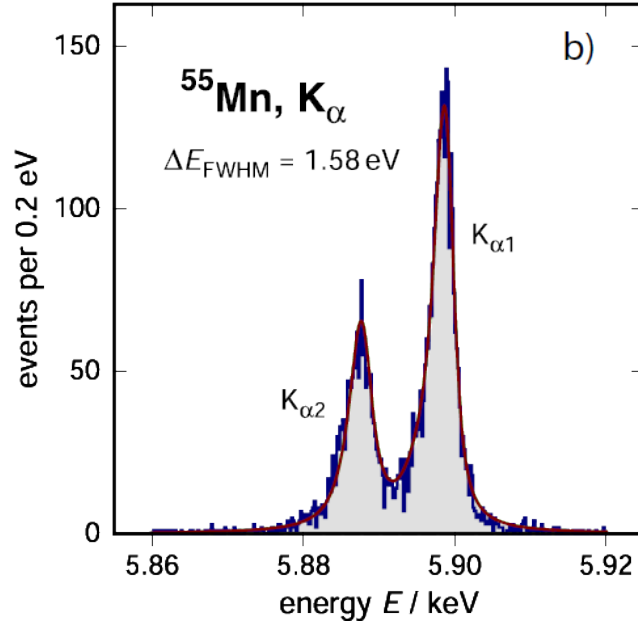
## micro-fabrication works

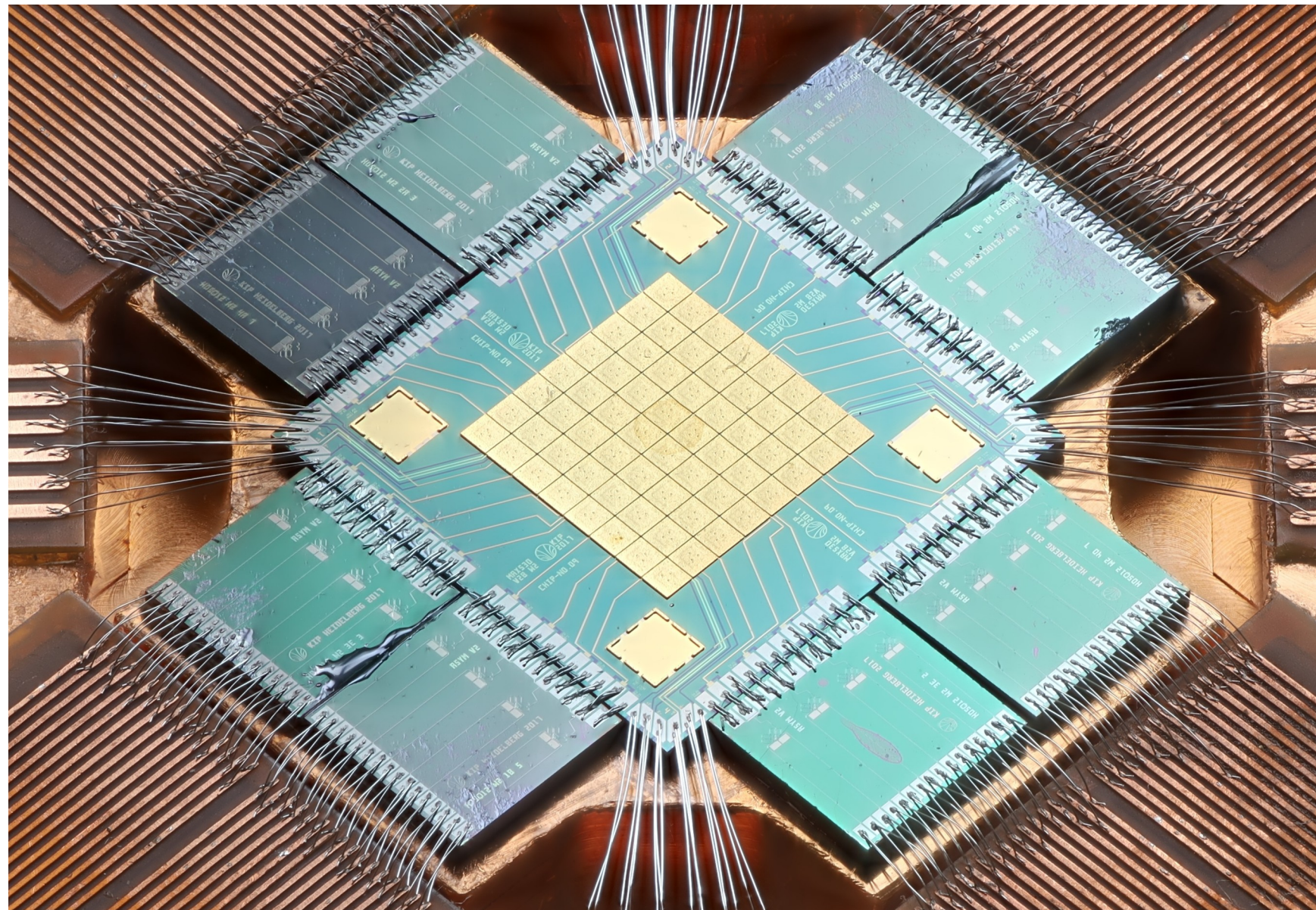
- detector arrays reliably fabricated
- designed performance is reached
- reproducibility of performance

## multiplexing

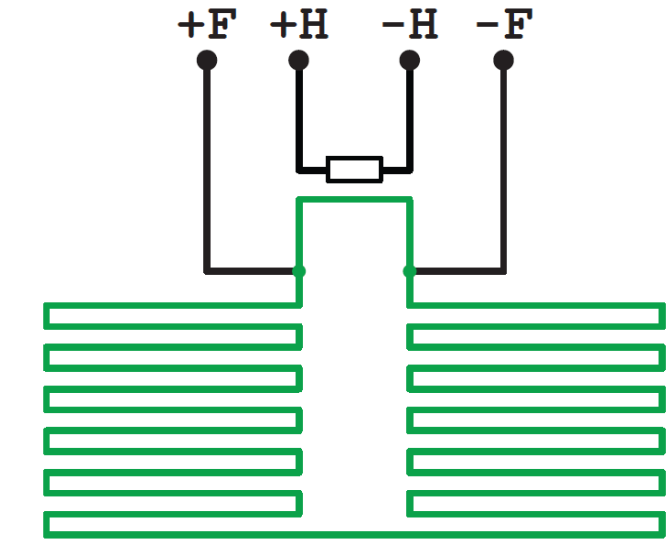
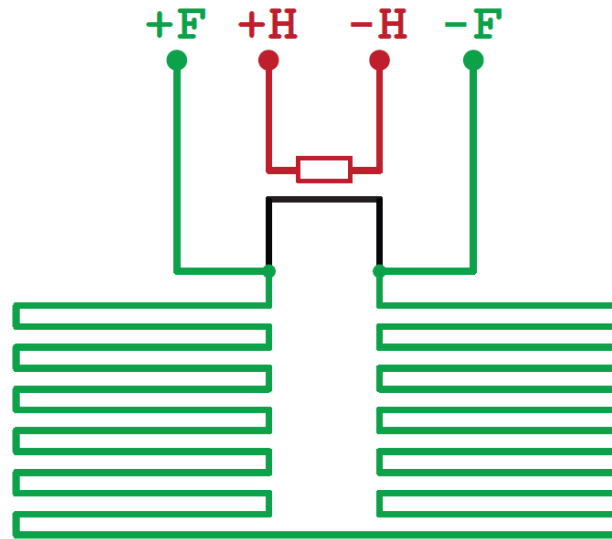
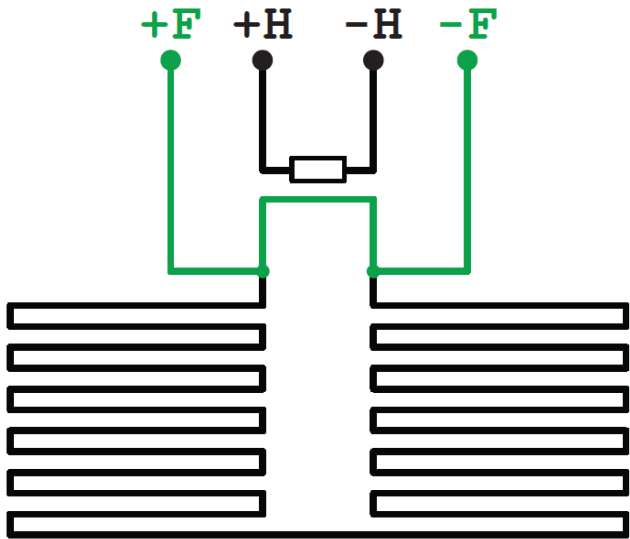
- demonstrated principles

Thank you for the  
questions!

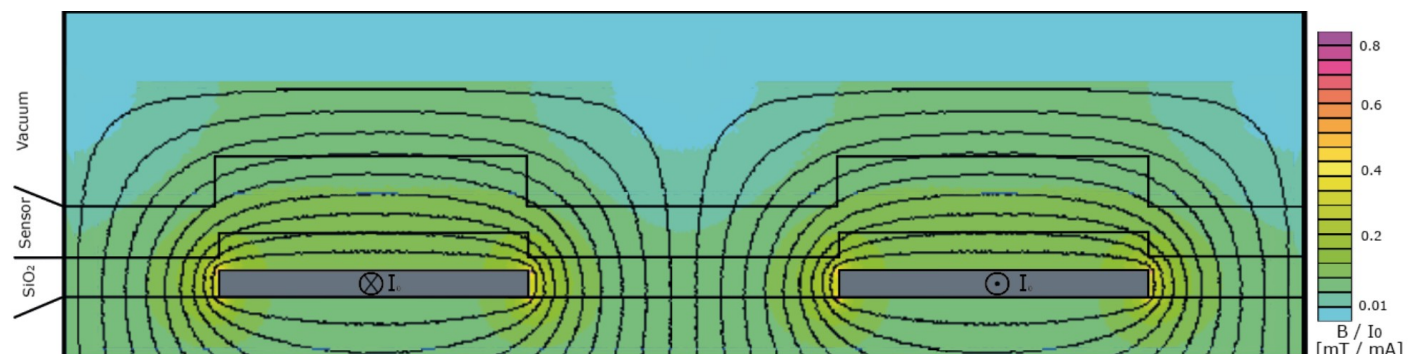




# Persistent current

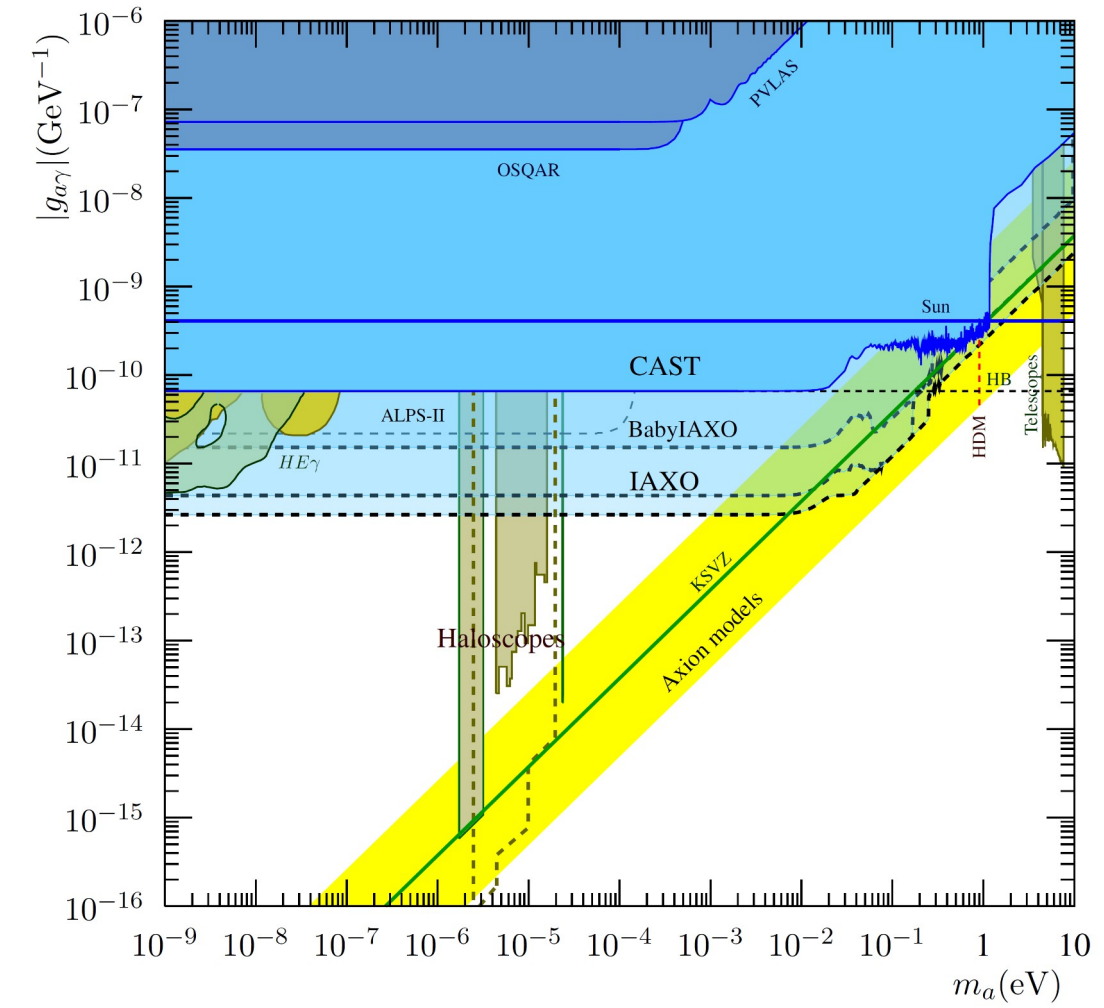
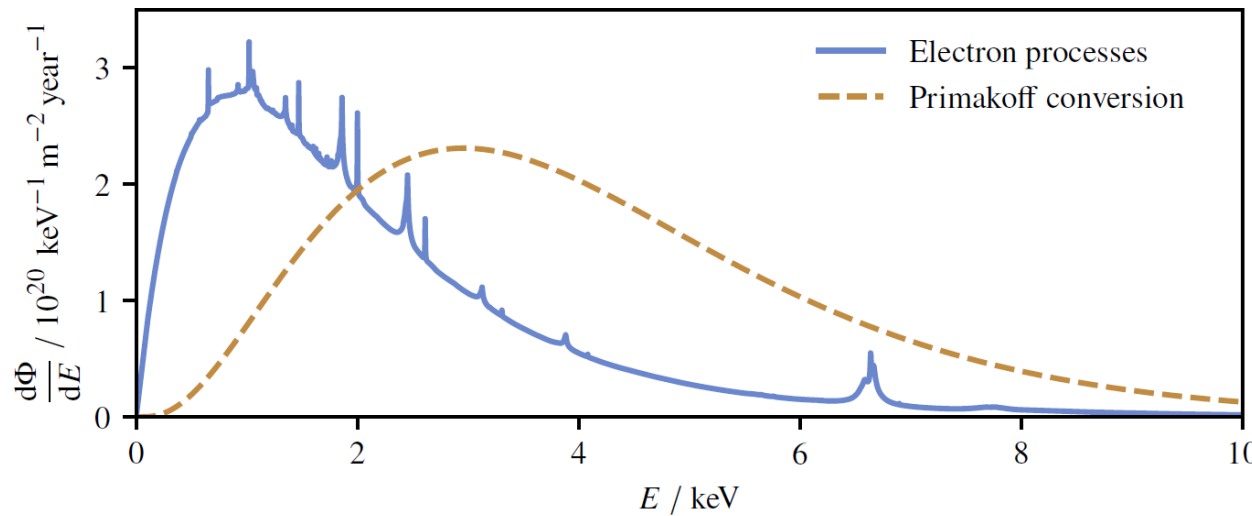
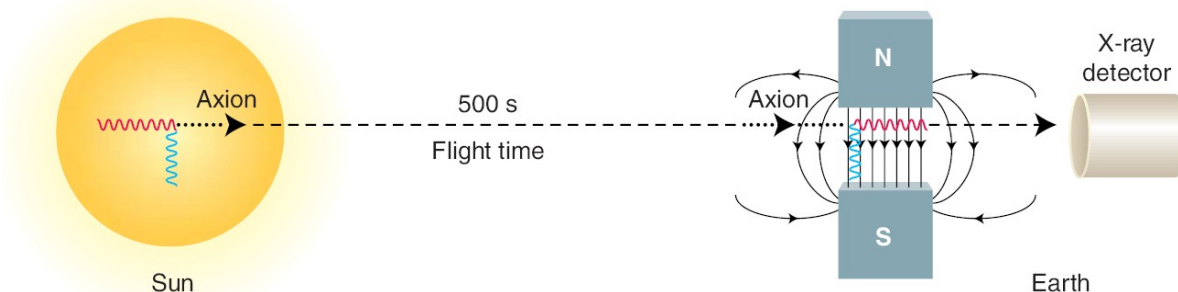


Reliable injection of a persistent current in the superconducting coil:  
Achievable critical current density:  $\sim 10 \text{ MA/cm}^2$



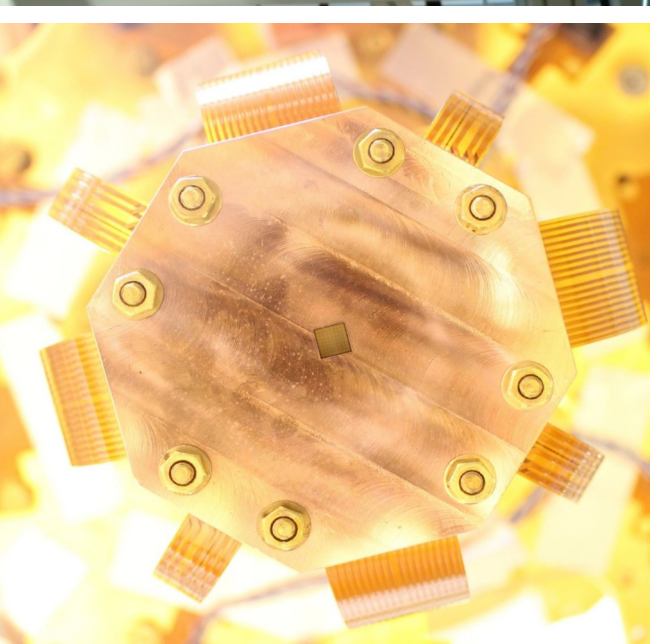
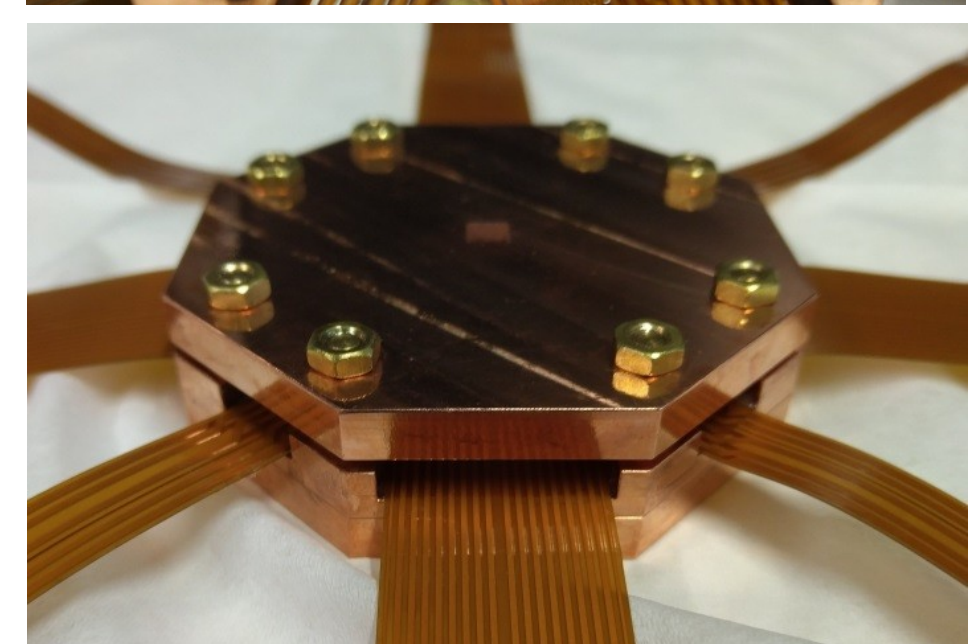
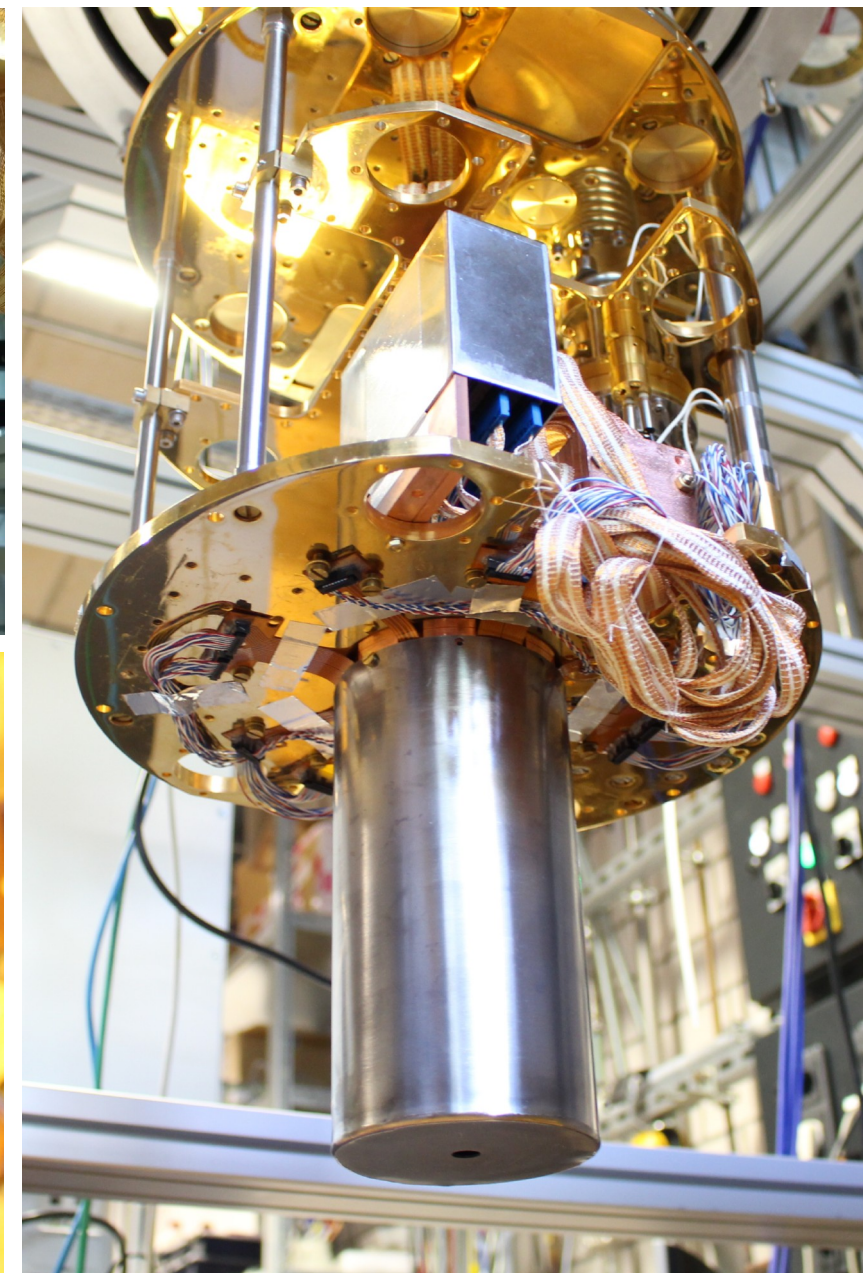
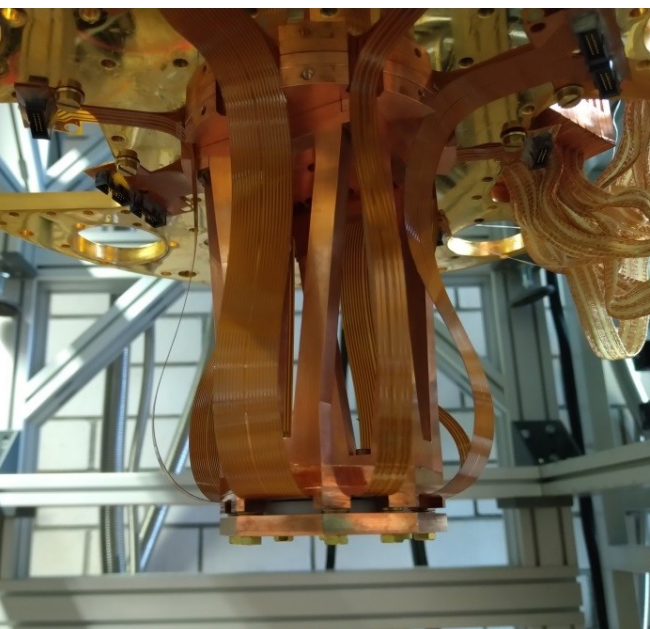
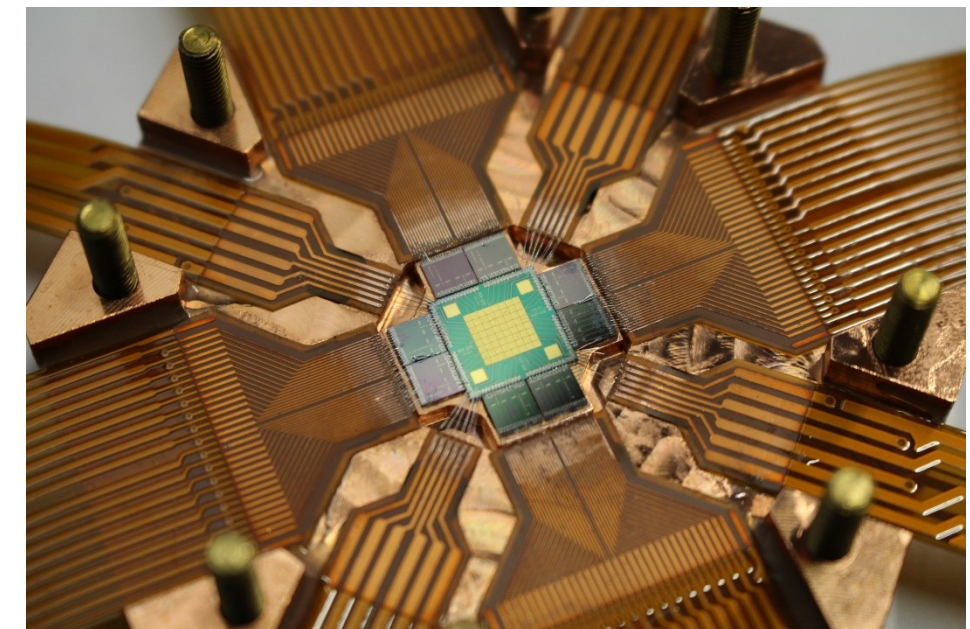
# maXs-30 set-up for IAXO

Search for an evidence for [solar axions](#)



Low background and high energy resolution  
(low threshold) x-ray detectors

# maXs-30 set-up for IAXO



# Towards ECHO-100k – Multiplexing

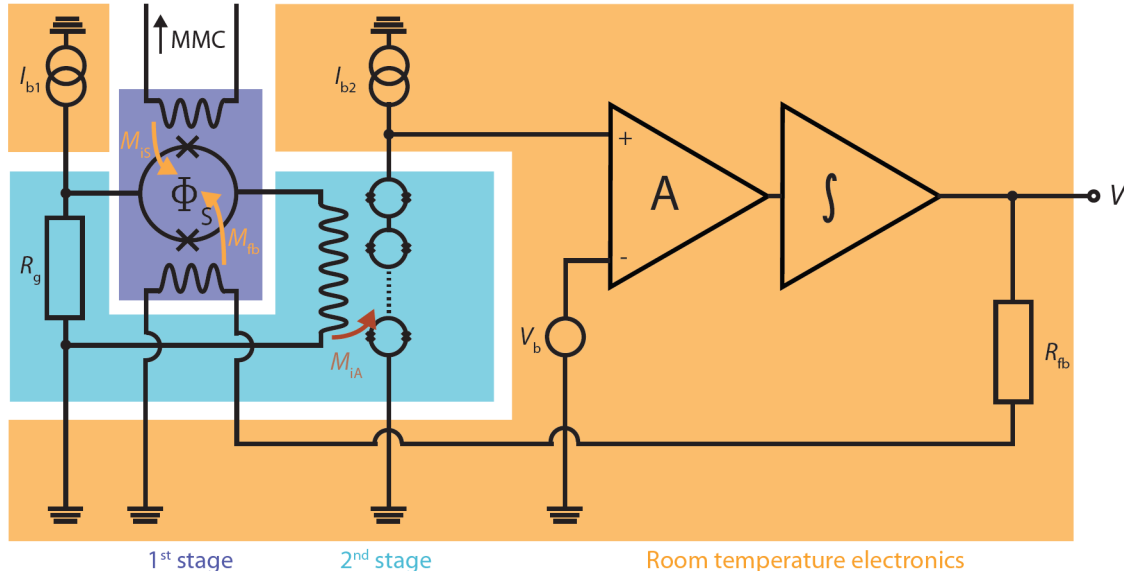
ECHO-1k:

~ 50 detectors



ECHO-100k:

> 5.000 detectors



Single channel readout – **two stage SQUID scheme:**

10 wires per channels

SQUID electronics

**Not scalable** →

{  
 parasitic heat load  
 number of wires  
 costs  
 complexity

$\sim N$

How to read out a large number of detectors ?

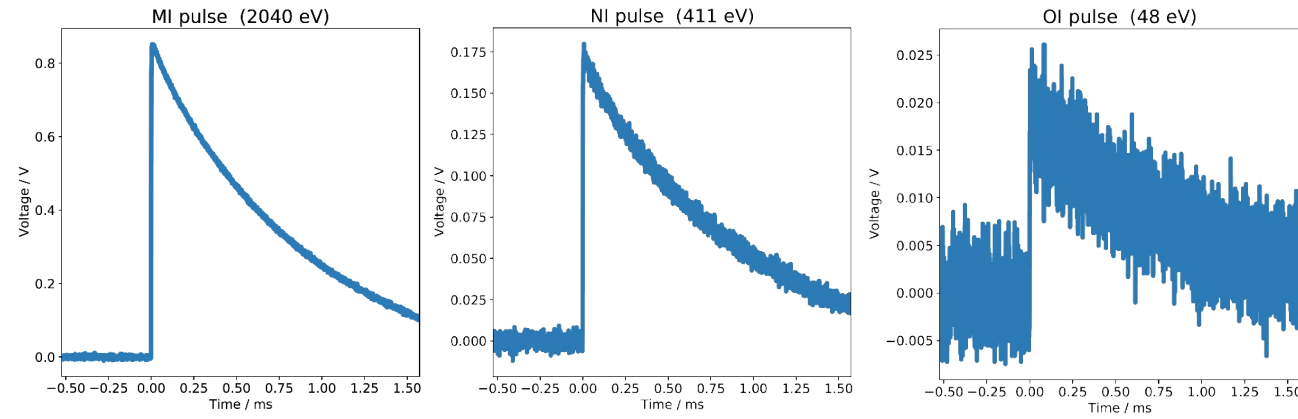
**Multiplexed readout:**

~ 1000 detectors per readout channel

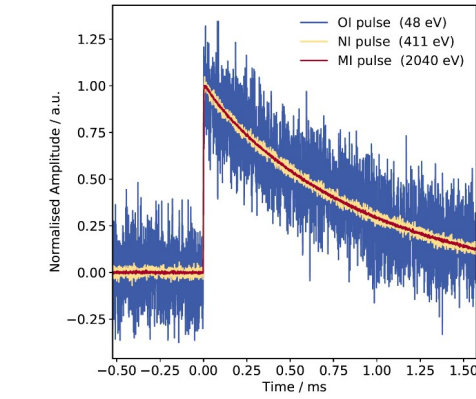
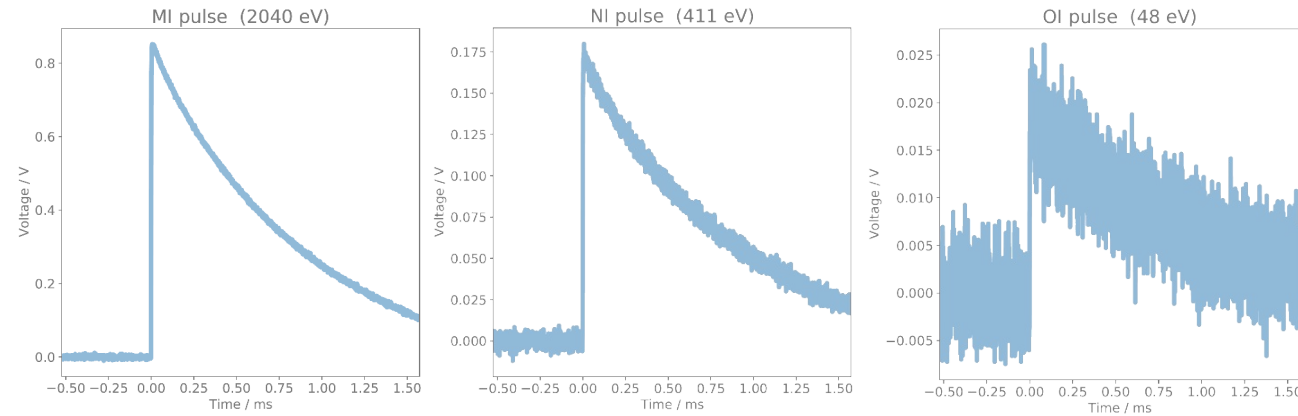
For ECHO → **Microwave SQUID multiplexing**

**Scalability**

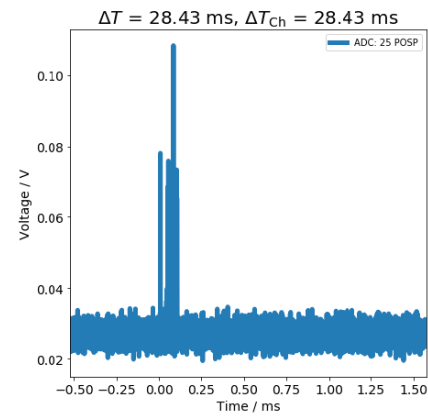
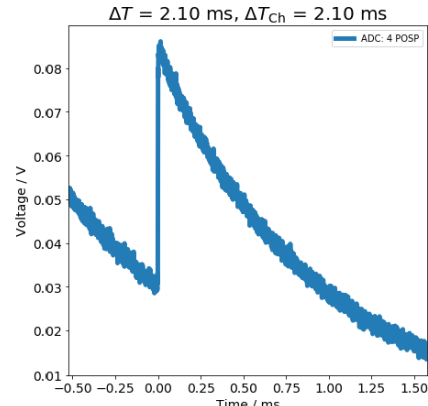
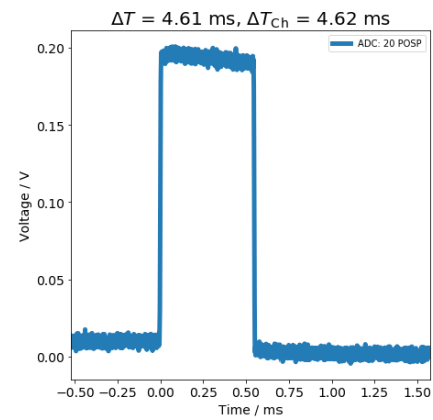
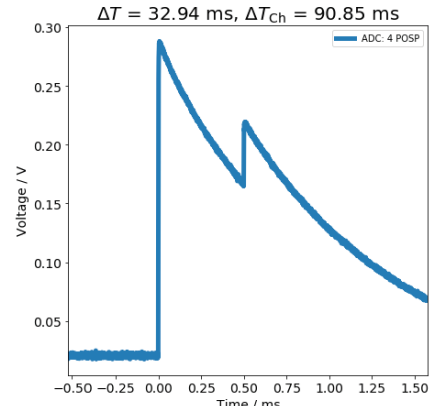
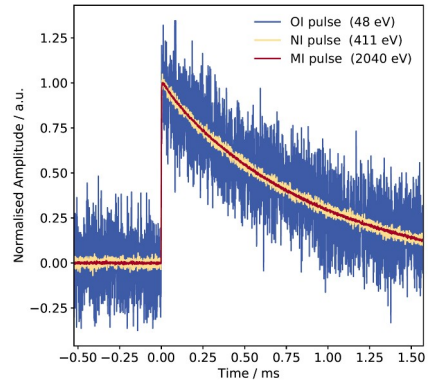
# Data reduction



# Data reduction



# Data reduction



$^{163}\text{Ho}$  events

Energy independent pulse shape

→ Pulse shape discrimination can be used to select  $^{163}\text{Ho}$  Pulses

$^{163}\text{Ho}$  pile-up events in time window

→ pulse shape discrimination

outside the time window  
→ trigger hold-off

Triggered noise

GSM signals

→ well-defined repetition time

electromagnetic signal coupled to readout

Muon related events + background events

# Data reduction - structure

- The acquisition of all channels is synchronized
- For each acquired trace, the trigger time is saved

→  $\Delta T_{\text{Ch}}$  Time difference to previous trace in a channel

→  $\Delta T$  Time difference to previous trace in any channel

## First Level: Time Information Filter

### Holdoff Filter

Discard traces with  $\Delta T_{\text{Ch}} < T_{\text{Holdoff}}$

### Burst Filter

Discard time intervals with abnormally high rate

### Coincidence Filter

Discard traces with  $\Delta T < T_{\text{Coincidence}}$

### GSM Filter

Discard traces with  $\Delta T$  associated to GSM pulse frequencies

## Second Level:

### Template Fit

- Create mean pulse from traces by cross-fitting traces in batches
- Fit traces to template to recover amplitude and  $\chi^2_{\text{red}}$

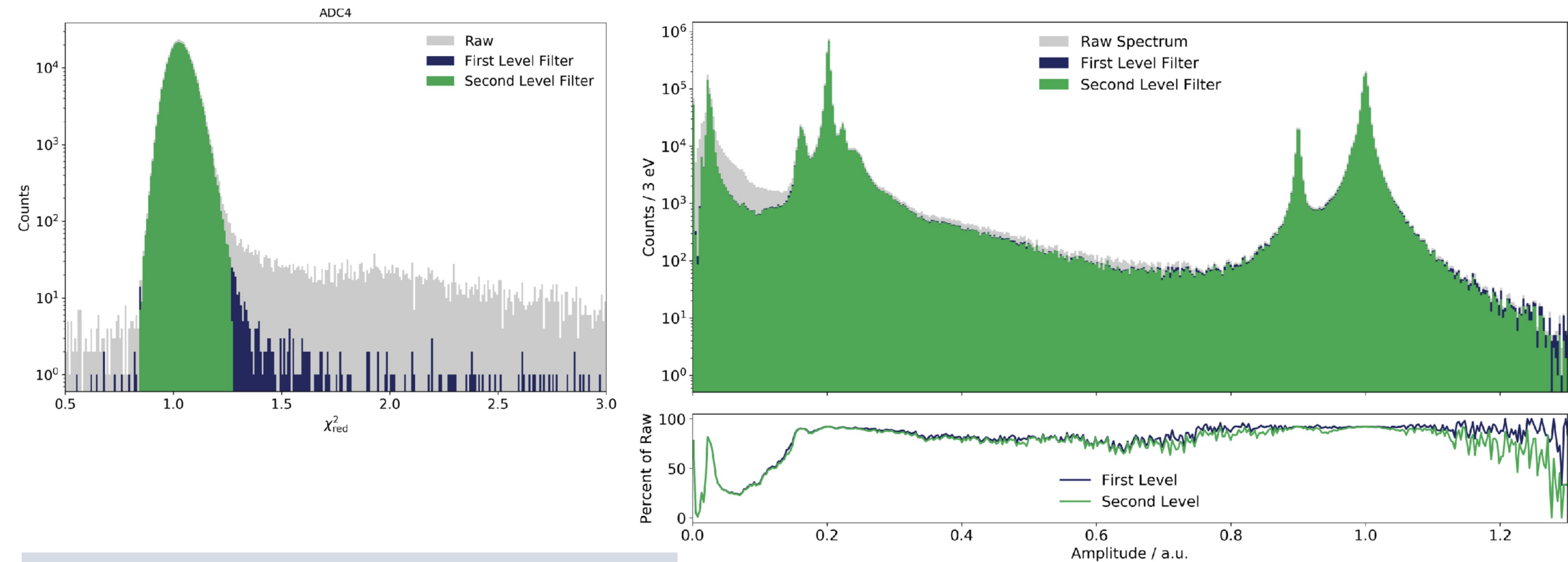
### Pulse Shape Filter

Discard traces with high deviation from template

Energy independent filter

tiny and predictable energy dependence

# Example



On-going:

- determination of efficiency for filters

# Combining many files

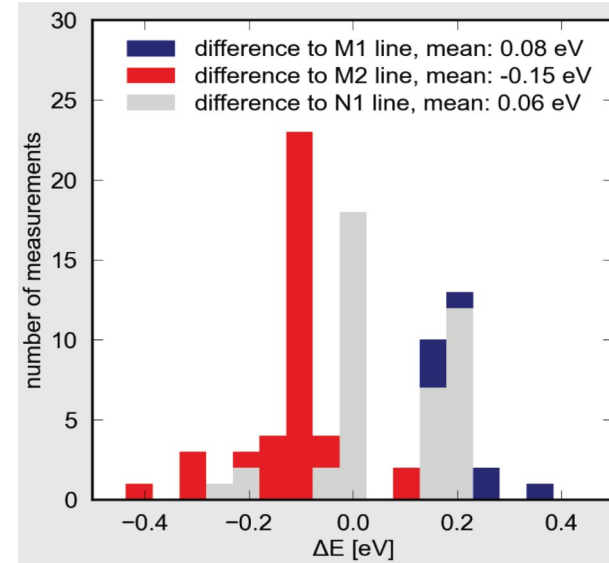
## Quality checks

### 1. level filter

Monitor fraction of removed events over time for a pixel

### 2. level filter

Monitor  $\chi^2$  distribution



## Energy calibration

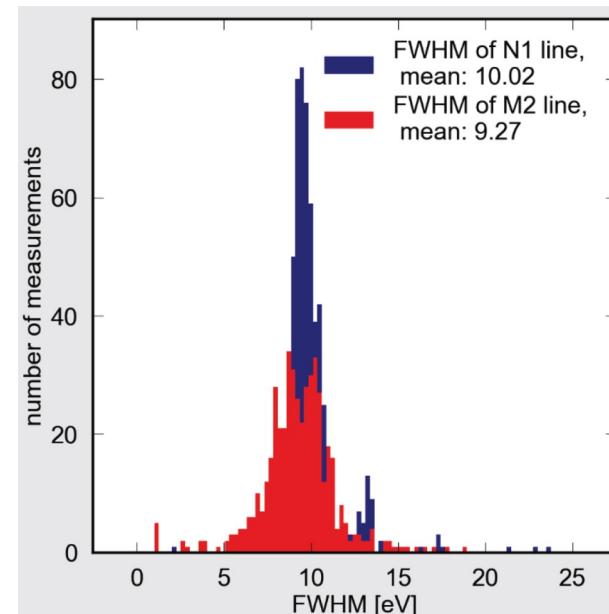
new calibration with  $^{55}\text{Fe}$  with a  $^{163}\text{Ho}$  high resolution spectrum

→ Alignment test

## Energy resolution

Extract “Pseudo-energy resolution” for each single histogram

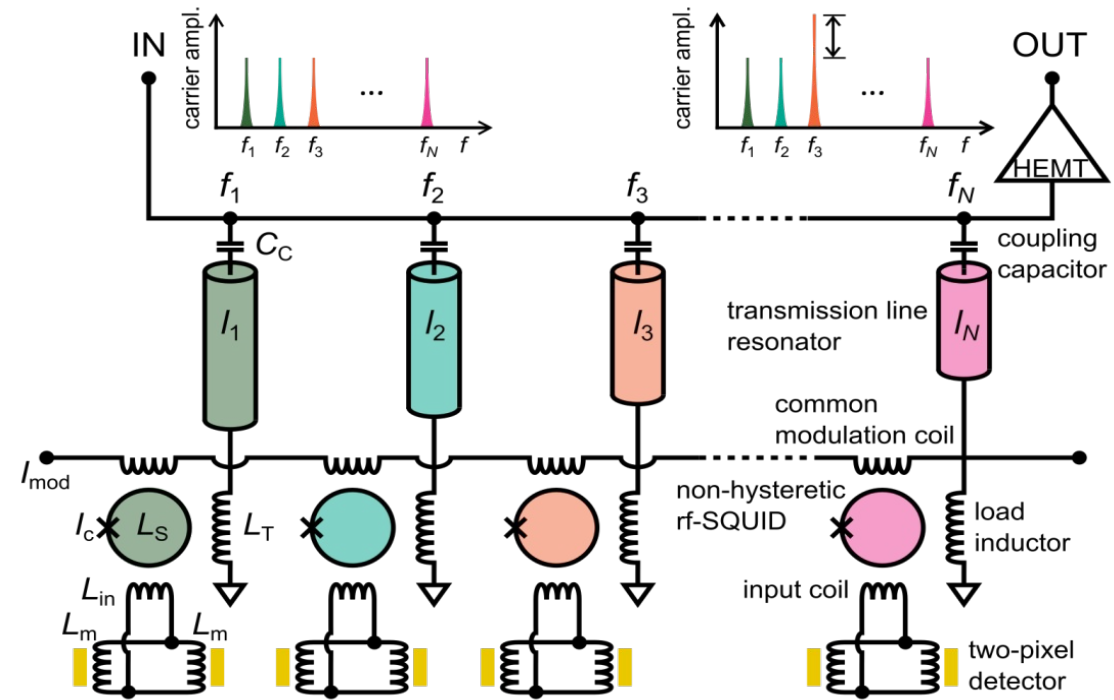
→ define acceptance range



# Towards ECHO-100k - Multiplexing

## Microwave SQUID multiplexing

Single HEMT amplifier and 2 coaxes  
to read out **100 - 1000** detectors

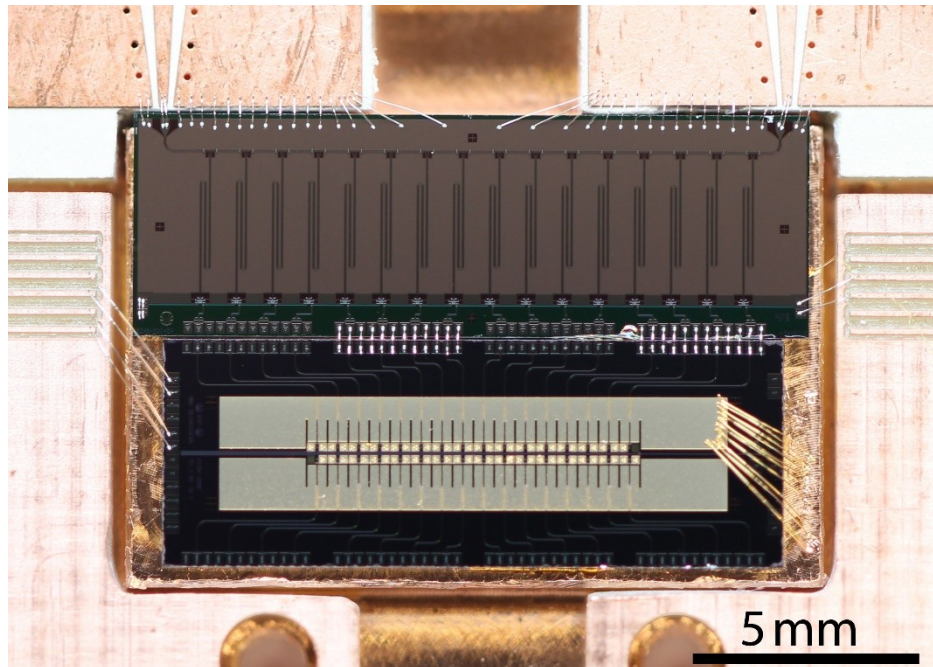


# Towards ECHO-100k - Multiplexing

## Microwave SQUID multiplexing

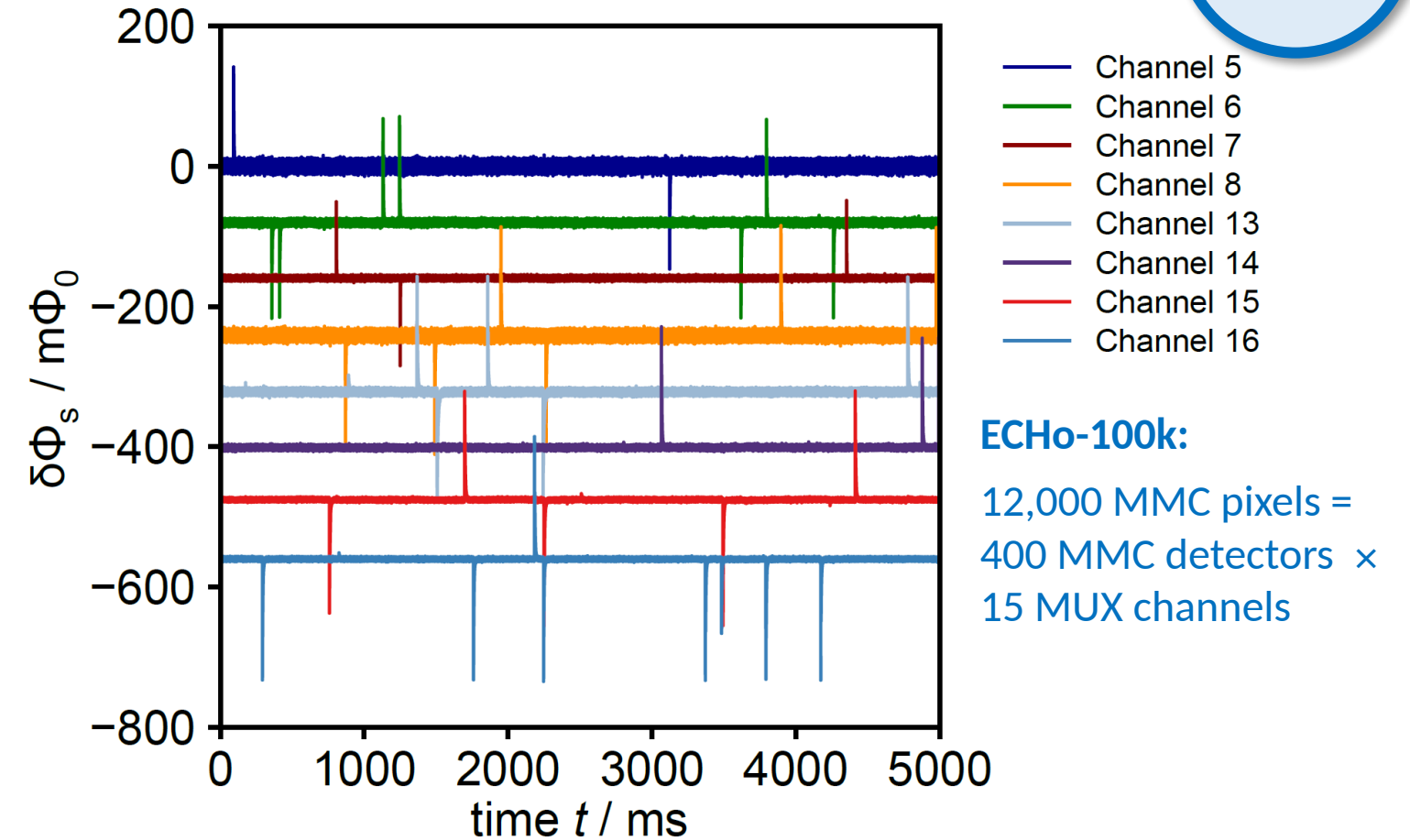
Single HEMT amplifier and 2 coaxes  
to read out **100 - 1000** detectors

- Successful characterization of first prototypes with external  $^{55}\text{Fe}$   
→ **Very promising results:**  
8 channels (16 pixels)



S.Kempf et al., J. Low. Temp. Phys. **175** (2014) 850-860

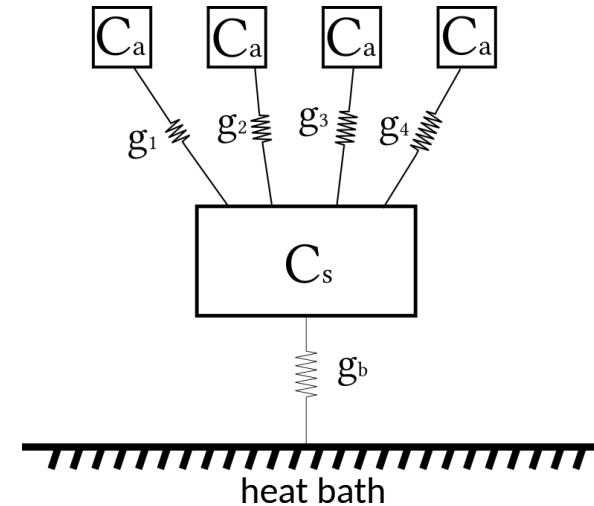
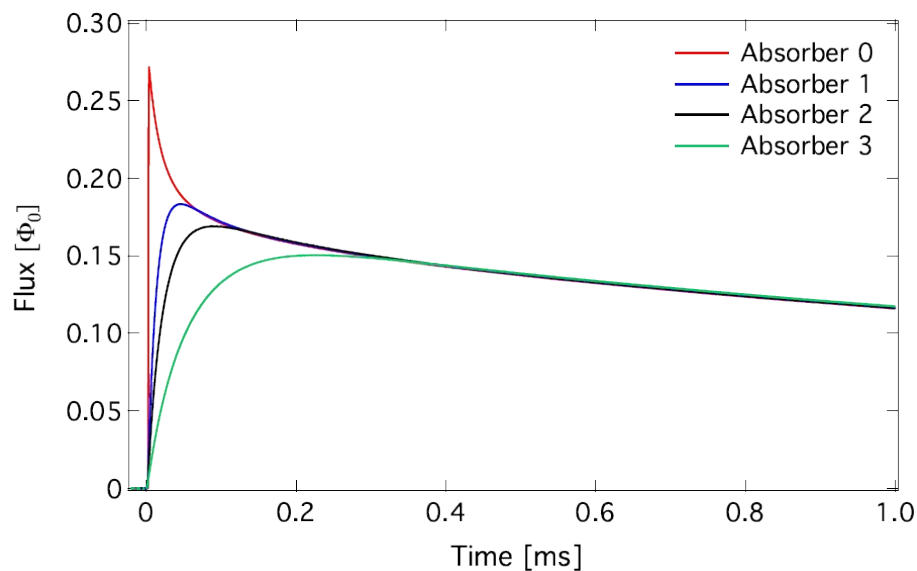
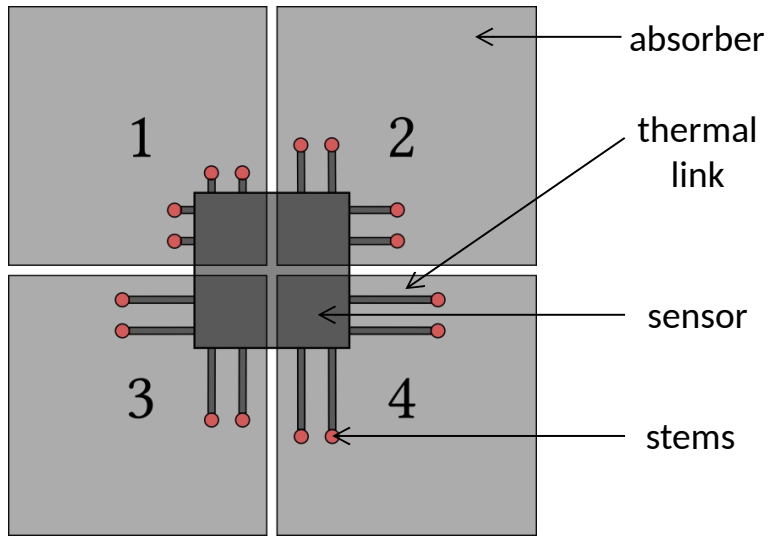
M. Wegner et al., J. Low Temp. Phys. **193**, 462 (2018)



Soon tests with  $^{163}\text{Ho}$  loaded MMC arrays

# 32 readout channels for 4000 pixels

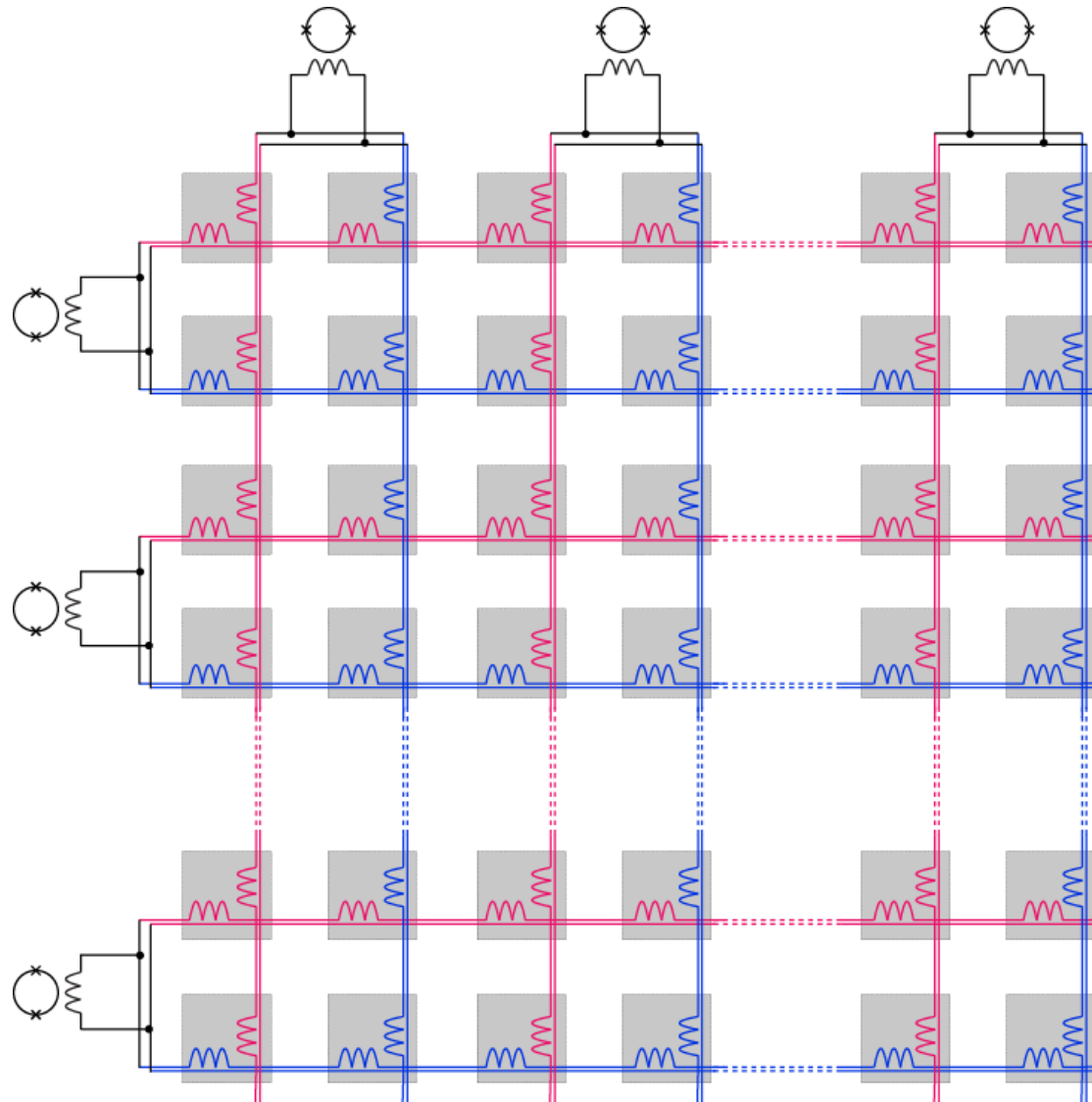
## 1) The Hydra principle



Pixel identification via rise-time  
of the detector signal

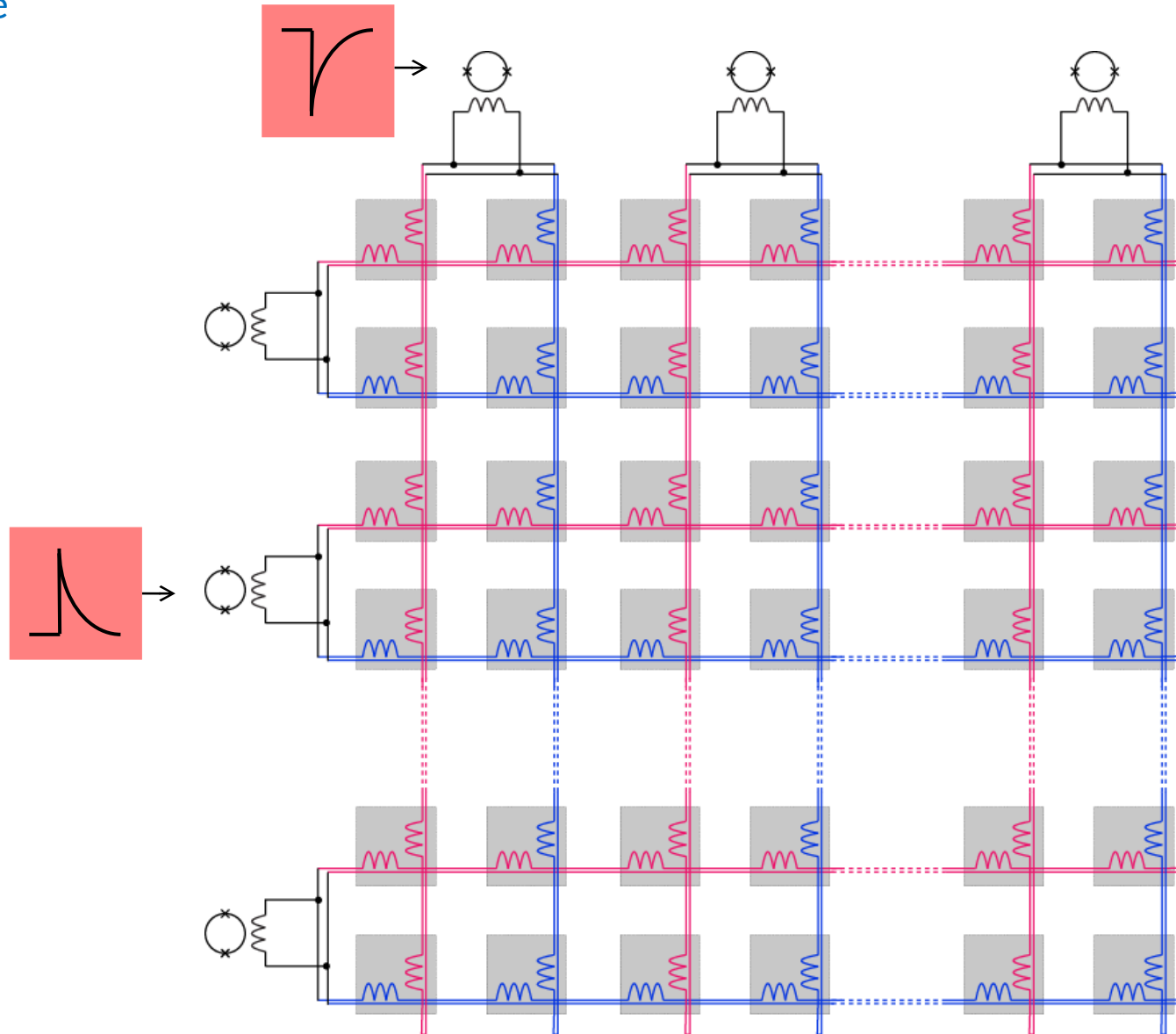
# 32 readout channels for 4000 pixels

- 1) The Hydra principle
- 2) Segmented sensor



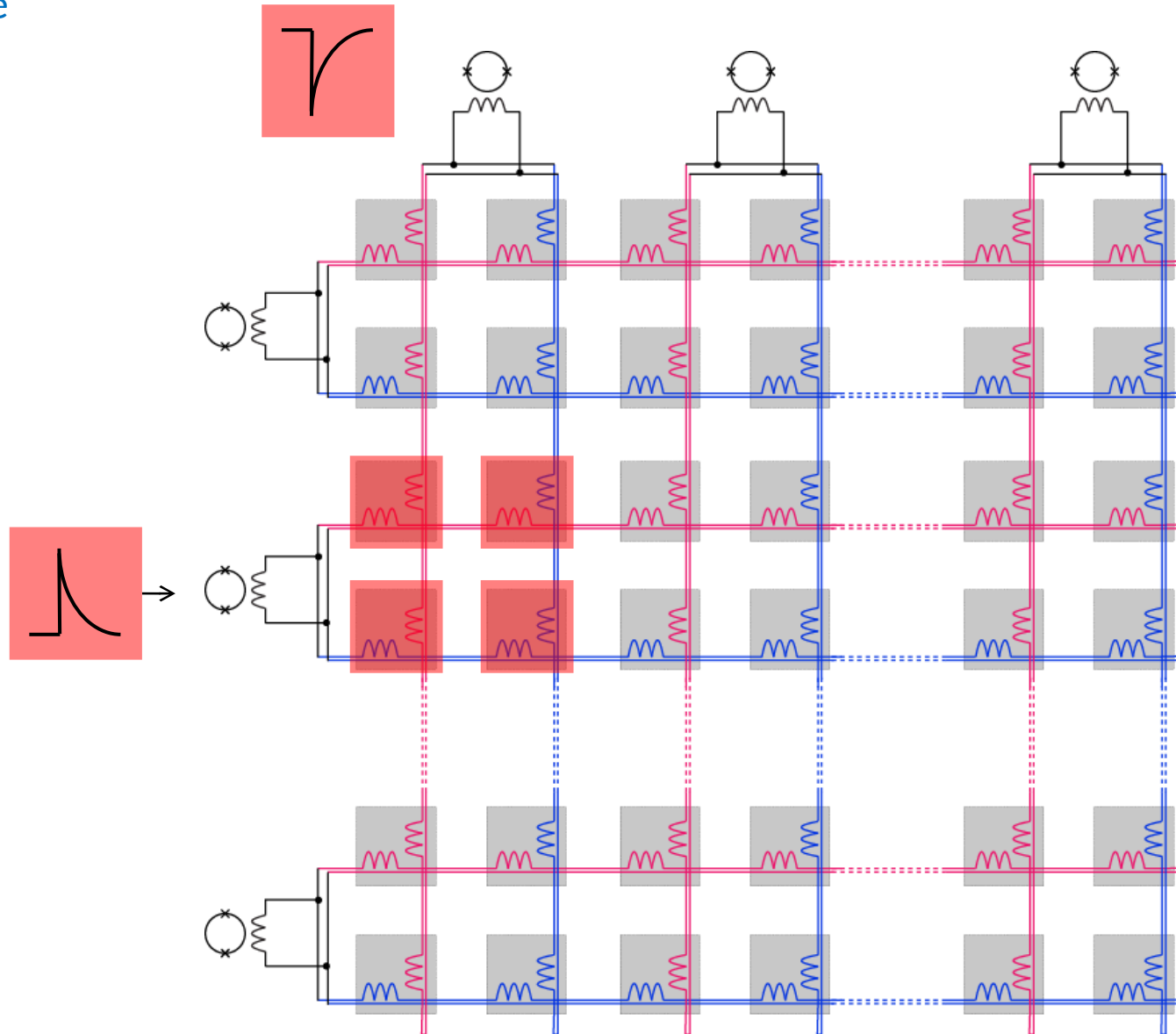
# 32 readout channels for 4000 pixels

- 1) The Hydra principle
- 2) Segmented sensor



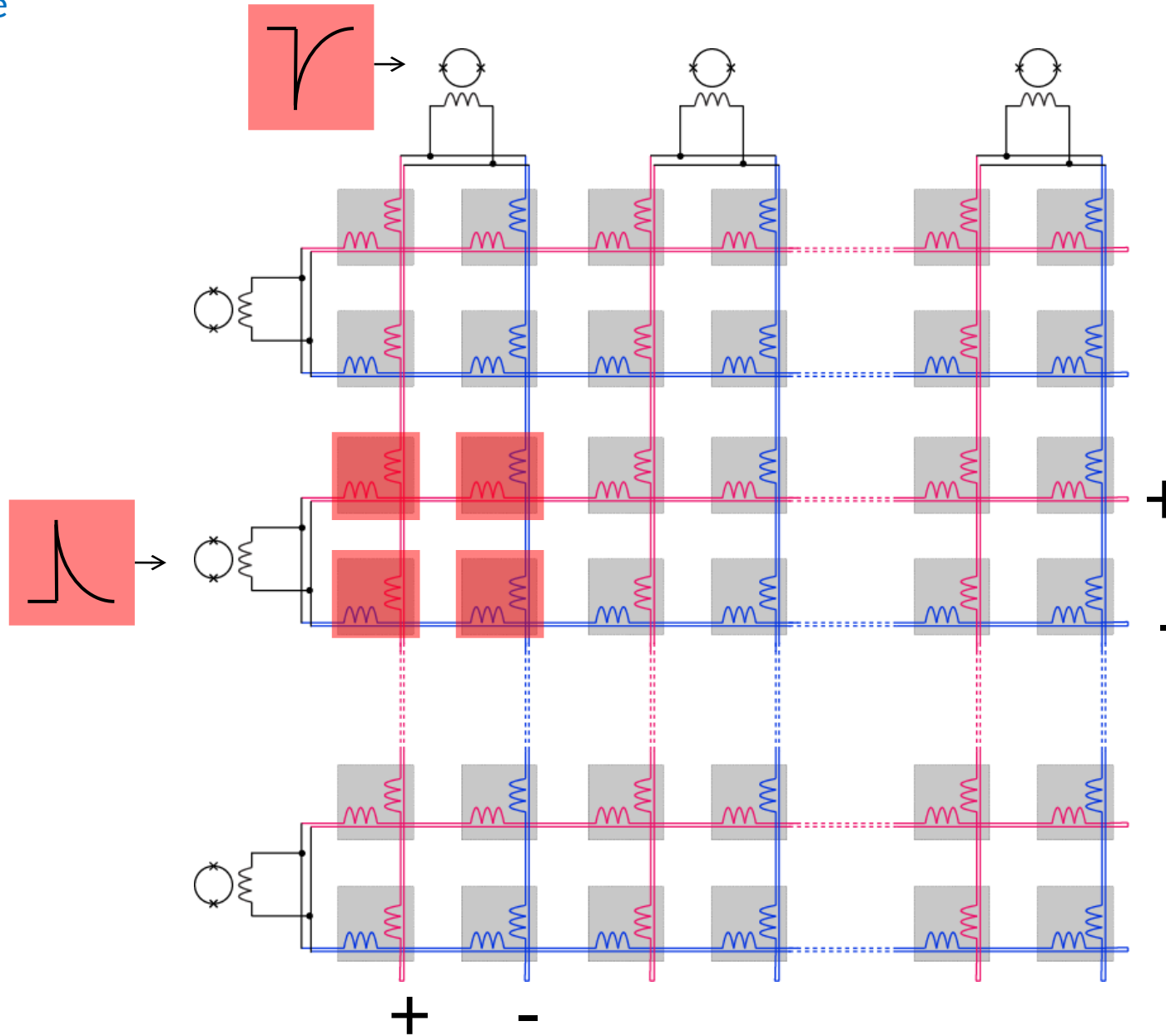
# 32 readout channels for 4000 pixels

- 1) The Hydra principle
- 2) Segmented sensor



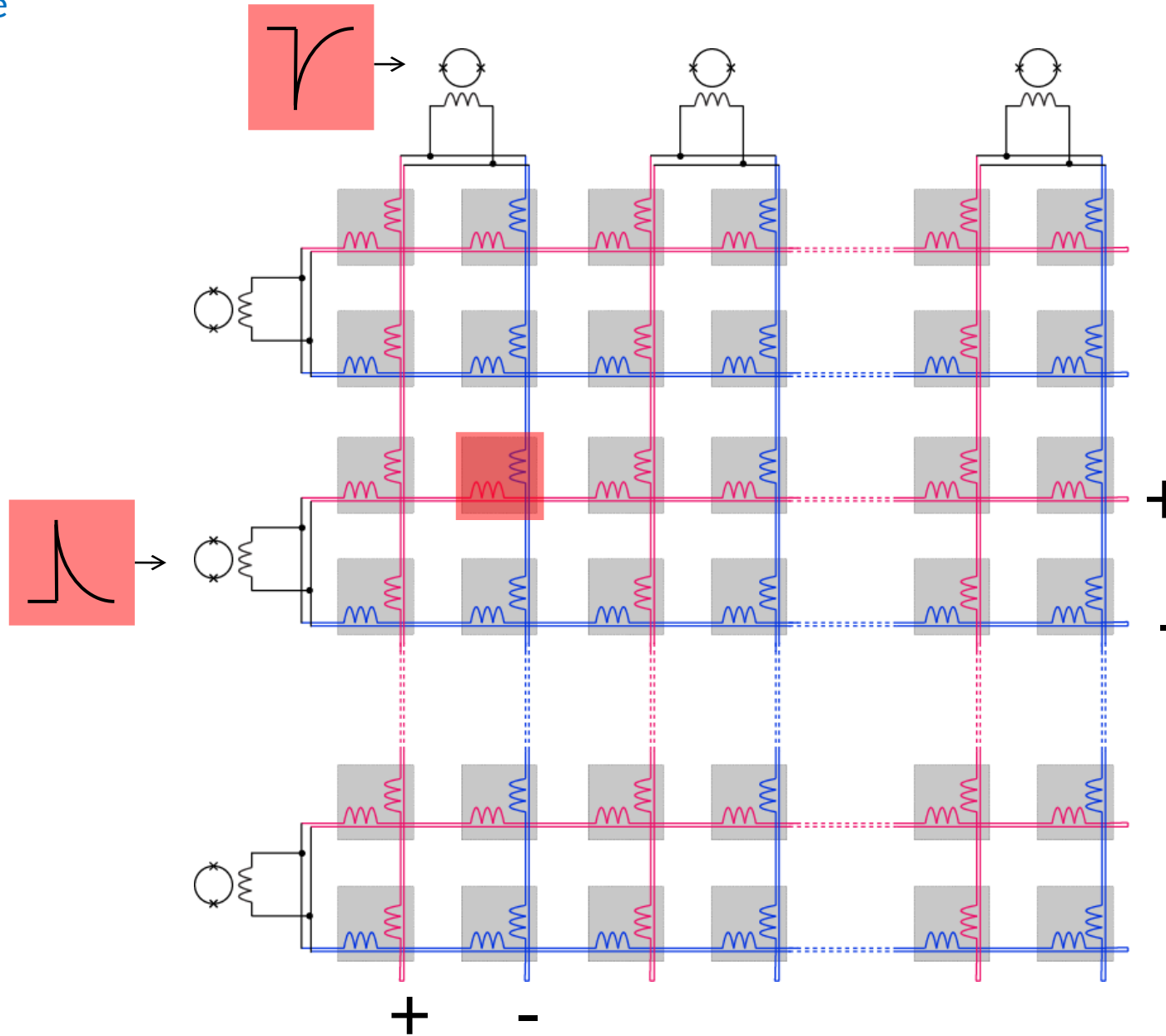
# 32 readout channels for 4000 pixels

- 1) The Hydra principle
- 2) Segmented sensor



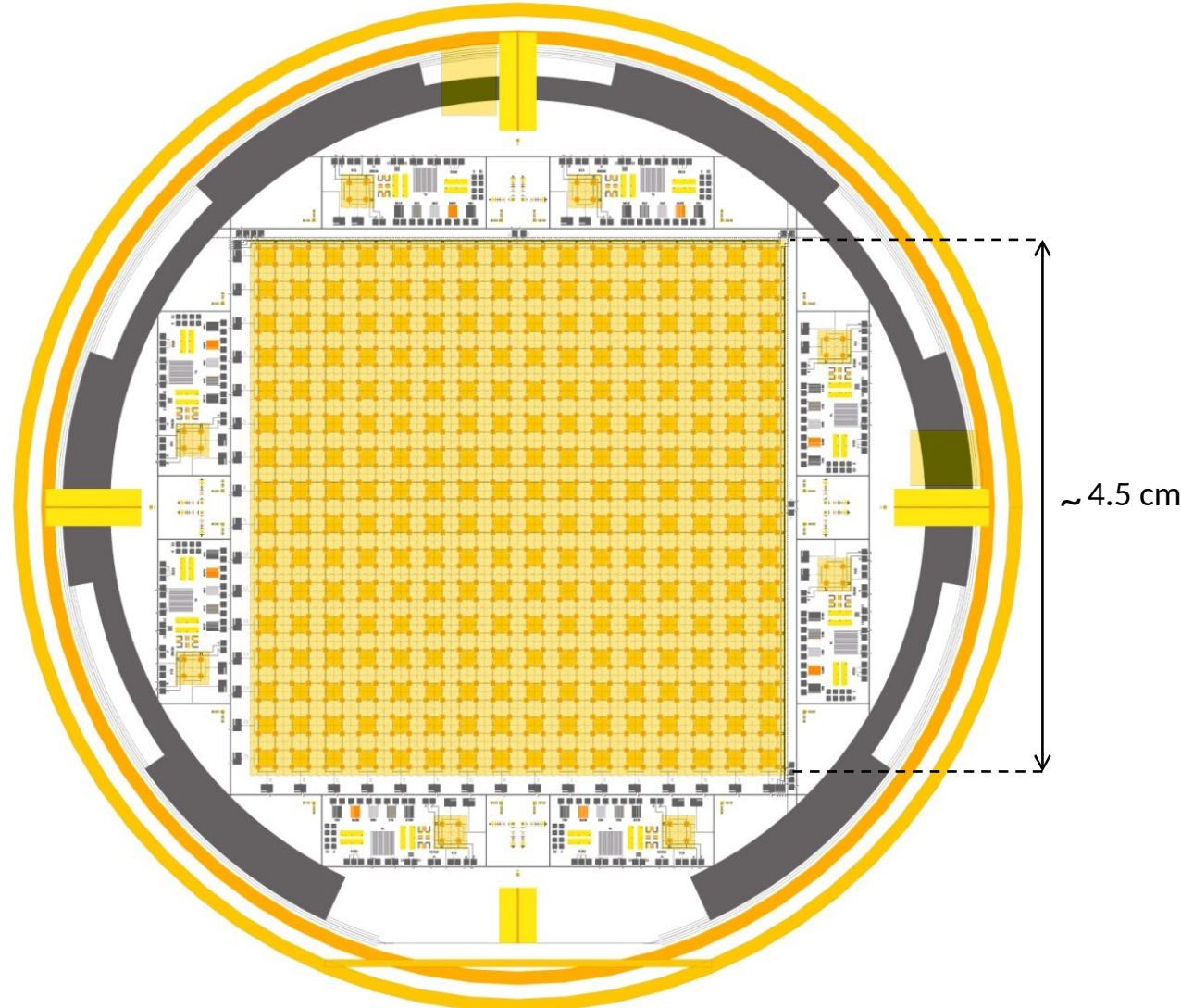
# 32 readout channels for 4000 pixels

- 1) The Hydra principle
- 2) Segmented sensor



# 32 readout channels for 4000 pixels - MOCCA

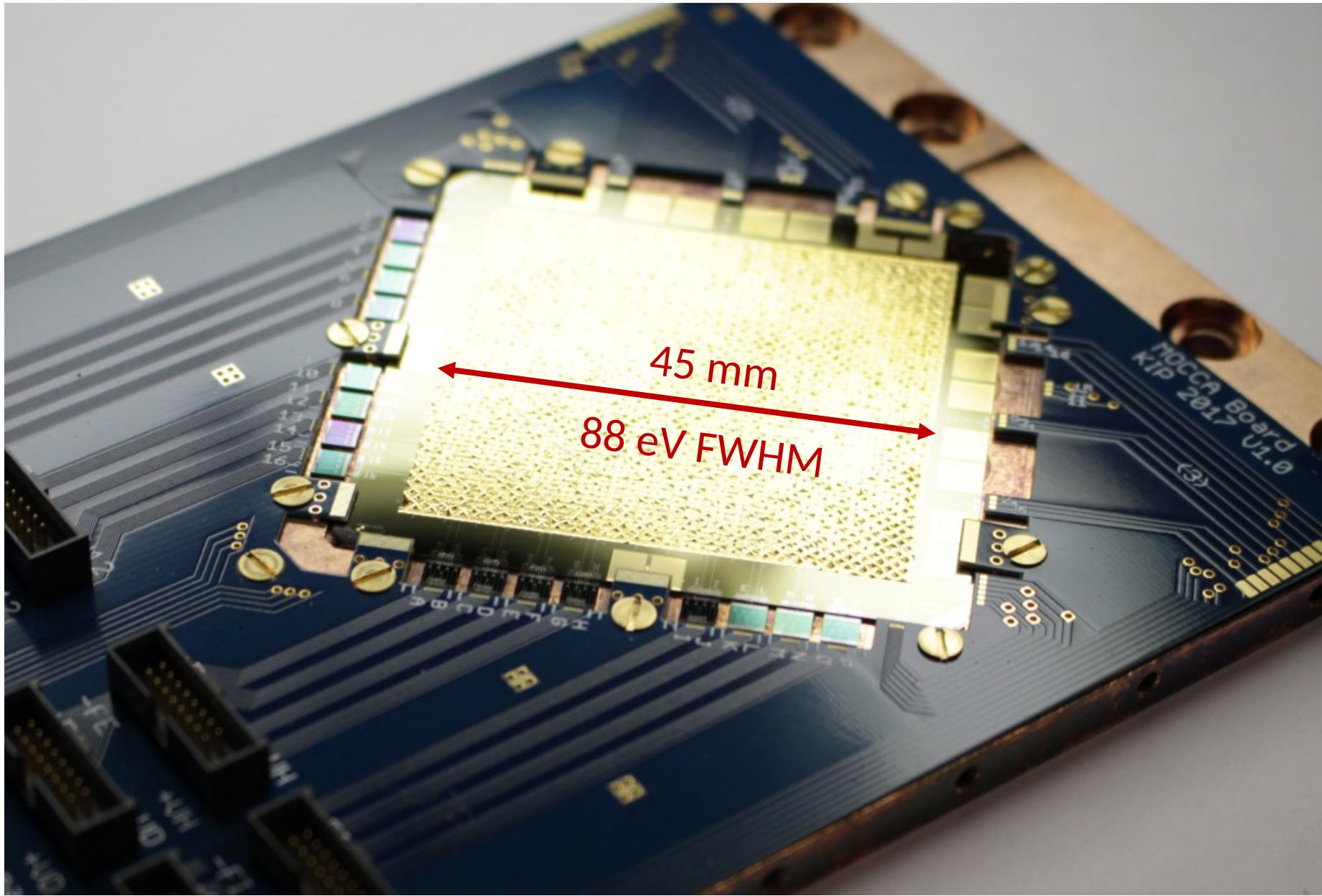
- 1) The Hydra principle
- 2) Segmented sensor



- $64 \times 64$  pixels
- $\sim 100$  eV (FWHM)
- $32 \times 32$  temperature sensors
- Read out by 16 + 16 SQUIDs

# 32 readout channels for 4000 pixels - MOCCA

- 1) The Hydra principle
- 2) Segmented sensor



- $64 \times 64$  pixels
- $\sim 100$  eV (FWHM)
- $32 \times 32$  temperature sensors
- Read out by 16 + 16 SQUIDs